Diversity, function and oxygen relationship of free-living and flagellate-associated *Opitutales* (phylum*Verrucomicrobiota)* in the termite gut

Dissertation

zur Erlangung des Grades eines

Doktors der Naturwissenschaften

(Dr. rer. nat.)

des Fachbereichs Biologie der Philipps-Universität Marburg

vorgelegt von

Christopher Feldewert

aus Soest

Marburg, 2022

Die vorliegende Dissertation wurde von Oktober 2018 bis Juni 2022 am Max-Planck-Institut für terrestrische Mikrobiologie in Marburg unter Leitung von Prof. Dr. Andreas Brune angefertigt.

Vom Fachbereich Biologie der Philipps-Universität Marburg
(Hochschulkennziffer 1180) als Dissertation angenommen am:

Erstgutachter: Prof. Dr. Andreas Brune

Zweitgutachter: Prof. Dr. Johann Heider

Tag der Disputation:

SUMMARY

The phylum *Verrucomicrobiota* is a relatively new bacterial lineage that belongs to the PVC superphylum. They are ubiquitous in soil and aquatic environments but can also be found in association with animal hosts. Especially the order *Opitutales* comprises members that are inhabiting the guts of ants, cockroaches and termites. During my doctoral studies, I investigated different aspects of *Verrucomicrobiota* in the termite gut.

While most members of the family *Opitutaceae* had been described without special attention to their oxygen relationship, recent studies suggested that at least host-associated species are potential microaerobes that are specifically adapted to their suboxic environments. Therefore, I investigated the oxygen relationship of three representative family members at the genomic, transcriptomic and physiological level. Functional genome analysis of the respiratory chains revealed that *Opitutaceae* have high-affinity oxidases (HATOx) that potentially allow them to respire low concentrations of oxygen. Transcriptional analysis showed that all terminal oxidases of *Opitutaceae* are constitutively expressed but can adapt to changing oxygen conditions. Using microelectrodes and the deoxygenation of myoglobin as a measure for oxygen concentration, I determined oxygen uptake rates and affinities of *Opitutaceae* under different oxygen concentrations. These experiments showed that *Opitutaceae* can take up oxygen at nanomolar concentrations and can respond to changes in the oxygen availability in their temporarily or permanently oxygen-limited environments.

A recent study that recovered metagenome-assembled genomes (MAGs) from termite gut metagenomes yielded 90 MAGs of uncultured *Verrucomicrobiota*, most of them in the order *Opitutales*. Building on these MAGs, I was able to show that they represent several deep-branching, termite-specific lineages with highly reduced genomes that are endosymbionts of termite gut flagellates. Fluorescence *in situ* hybridization experiments confirmed their endosymbiotic association with different flagellate species from lower termites. Functional genome analysis revealed a severe genome erosion that affected energy metabolism, central carbon metabolism, cofactor biosynthesis and amino acid biosynthesis. The acquisition of ATP/ADP translocases and sugar phosphate transporters via horizontal gene transfer underscores that the flagellate-associated *Opitutales* are obligately dependent on the provision of metabolites from the cytoplasm of their respective hosts and suggests a potentially parasitic nature of their relationship.

ZUSAMMENFASSUNG

Das Phylum *Verrucomicrobiota* ist eine verhältnismäßig neue bakterielle Gruppe, die zum PVC-Superphylum gehört. Sie kommen ubiquitär im Boden und aquatischen Umgebungen vor, aber auch assoziiert mit Tieren. Besonders die Ordnung *Opitutales* besteht aus vielen Spezies die den Darm von Ameisen, Termiten oder Schaben kolonisieren. Während meiner Doktorarbeit habe ich verschiedene Aspekte von *Verrucomicrobiota* im Termitendarm untersucht.

Während die meisten Mitglieder der Familie *Opitutaceae* ohne besonderen Fokus auf ihr Verhältnis gegenüber Sauerstoff beschrieben wurden, haben neue Studien gezeigt, dass besonders Darm-assoziierte *Opitutaceae* potentielle Mikroaerobier sind und sich den suboxischen Bedingungen in ihrer Umwelt angepasst haben. Daher habe ich in dieser Dissertation das Sauerstoffverhältnis von drei repräsentativen *Opitutaceae* auf genomischer, transkriptioneller und physiologischer Ebene untersucht. Die funktionelle Analyse der Genome zeigte, dass *Opitutaceae* verschiedene hoch-affine Oxidasen haben, durch die sie potentiell geringe Sauerstoff Mengen in ihrer Umwelt veratmen können. Transkriptionelle Analysen haben gezeigt, dass alle terminalen Oxidasen von *Opitutaceae* konstitutiv exprimiert sind und sich wechselnden Sauerstoffbedingungen anpassen können. Durch Mikroelektrodenmessungen und die Deoxygenierung von Myoglobin, konnte ich die Sauerstoffaufnahmeraten und Affinitäten der *Opitutaceae* zeigen. Diese Experimente haben gezeigt, dass sie Sauerstoff im nanomolaren Bereich aufnehmen können und sich den wechselnden Bedingungen in ihren temporär oder dauerhaft sauerstoffarmen Habitaten anpassen können.

In einer früheren Studie, in der Metagenom-assemblierte Genome (MAGs) aus Termitendärmen assembliert wurden, wurden auch 90 MAGs von unkultivierten *Verrucomicrobiota* gewonnen, die meisten in der Ordnung *Opitutales*. In weiterführenden Experimenten konnte ich zeigen, dass sie mehrere tief verzweigte, termitenspezifische Linien mit reduzierten Genomen bilden, die mit Flagellaten im Termitendarm assoziiert sind. Fluoreszenz *in situ* Hybridisierung bestätigte, dass die *Opitutales* mit verschiedenen Flagellaten im Darm von niederen Termiten assoziiert sind. Funktionelle Genomanalysen zeigten, dass *Opitutales* diverse Gene ihres zentralen Kohlenstoff- und Energiestoffwechsels, als auch ihrer Cofaktor- und Aminosäurebiosynthese verloren haben. Die horizontale Aufnahme von ATP- und Zuckerphosphat-transportern bekräftigt, dass Flagellaten-assoziierte *Opitutales* obligat abhängig von Nährstoffen aus dem Cytoplasma ihrer Wirte sind und suggeriert eine potentiell parasitische Natur ihrer Symbiose.

TABLE OF CONTENTS

1 INTRODUCTION

Members of the phylum *Verrucomicrobiota* are part of the microbial community in the gut of numerous termite species (Mikaelyan *et al.* 2015a; Mikaelyan *et al.* 2017a; Bourguignon *et al.* 2018; Arora *et al.* 2022). In the first part of this thesis, I will focus on the verrucomicrobial family *Opitutaceae* and their relationship to oxygen. In the second part, I will characterize several novel, deep-branching lineages of uncultured *Opitutales* that are associated with termite gut flagellates.

1.1 The phylum *Verrucomicrobiota*

Verrucomicrobia were first recognized as a bacterial division by Hedlund *et al*. (1997) who found that three previously described prosthecate bacteria (genus *Prosthecobacter*) are phylogenetically deep-branching and only distantly related to other prosthecate bacteria. Traditionally, all prosthecate bacteria had been placed in the proteobacterial order *Caulobacteriales* by early taxonomists (Henrici and Johnson 1935). Using phylogenetic analysis, Hedlund *et al.* also placed other species of uncertain taxonomy into the new phylum. These included the also prosthecated *Verrucomicrobium spinosum*, the earliest isolate of the phylum (Schlesner 1987), but also non-prosthecated isolates from terrestrial (Liesack and Stackebrandt 1992; Ueda *et al.* 1995) and aquatic environments (Fuhrman *et al*. 1993; Wise *et al.* 1996). During a recent unification of phylum names, the phylum was renamed as *Verrucomicrobiota* (Oren and Garrity 2021).

Phylogenetic studies revealed that *Verrucomicrobiota* form a deep-branching monophyletic group with the phyla *Planctomycetota* and *Chlamydiota* forming the PVC super-phylum (Wagner and Horn 2006). Features like the compartmentalization in *Planctomycetota*, *Lentisphaerota* and some *Verrucomicrobiota* or the lack of peptidoglycan in *Planctomycetota*, some *Chlamydiota* and some *Verrucomicrobiota* highlight the exceptional nature of the PVC super-phylum that differs from the classical definition of bacteria (Fuerst 2013). Cell compartmentalization is achieved by intracytoplasmatic membranes (ICM) creating an inner compartment (pirellulosome) that usually contains the nucleoid and the outer compartment (paryphoplasm). Within the PVC super-phylum, cell compartmentalization was probably lost in *Chlamydiota* and in the verrucomicrobial order *Opitutales* (Pinos *et al.* 2016). A study on the membrane proteins of the PVC-superphylum found similarities to the proteins of eukaryotes and suggests that PVC members contributed significantly to eukaryogenesis (Santarella-Mellwig *et al.* 2010).

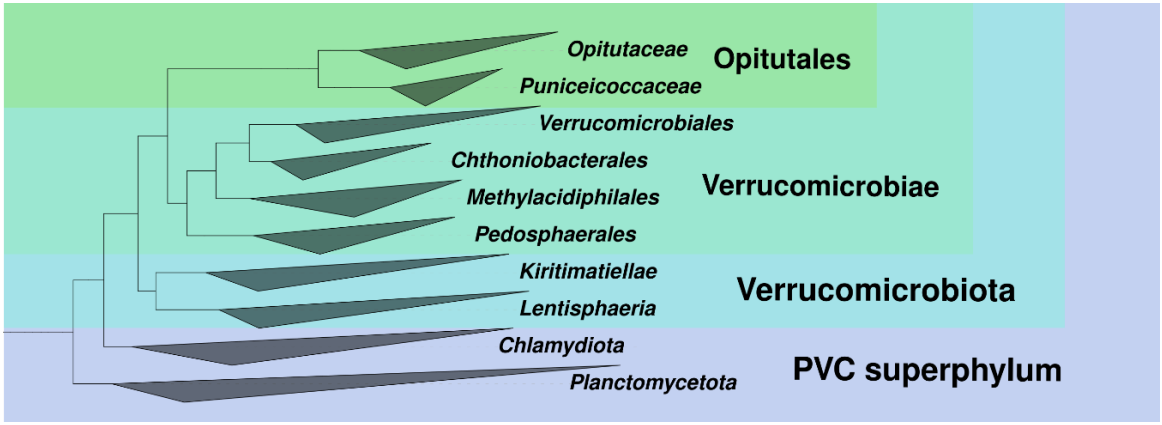

Figure 1: Taxonomy of the PVC superphylum. The tree is an adapted section of the bacterial tree of life downloaded from AnnoTree (Mendler *et al*. 2019) based on the phylogeny of the genome taxonomy database (GTDB, Parks *et al.* 2018). The phylum *Verrucomicrobiota*, the class *Verrucomicrobiae* and the order *Opitutales* are expanded. Only taxonomic groups that include cultivated members are shown.

Verrucomicrobiota comprise the classes *Lentisphaeria*, *Kiritimatiellae* and *Verrucomicrobiae* (Fig. 1). The class *Verrucomicrobiae* itself comprises the orders *Chthoniobacterales* (Sangwan *et al.* 2004), *Methylacidiphilales* (Hou *et al*. 2008), *Pedosphaerales* (Kant *et al.* 2011), *Verrucomicrobiales* (Ward-Rainey *et al.* 1996), *Opitutales* (Choo *et al.* 2007) and two order level lineages that are only represented by uncultivated members (Woodcroft *et al.* 2018, Alteio *et al*. 2020).

Chthonibacteriales include only a few cultivated species. *Chthoniobacter flavus* is an aerobic soil bacterium that lives on dead plant organic matter (Sangwan *et al.* 2004). Another soil inhabiting member of *Chthoniobacteriales*, *Terrimicrobium sacchariphilum*, is a strictly anerobic sugar fermenter in the rice paddy soil (Qui *et al.* 2014). Genome analysis of *Candidatus* Xiphinematobacter, an endosymbiont of plant-parasitic nematodes (genus *Xiphinema*), revealed that despite genome reduction (genome size: 917 kbp) the endosymbiont is still able to support its hosts diet with all essential amino acids and certain vitamins (Myers *et al.* 2021). The investigated members of *Chthoniobacteriales* seem to be very diverse, suggesting a large number of non-analyzed members within the order.

The order of *Methylacidiphilales* so far solely comprises of acidophilic, hyperthermophilic methane oxidizers that have been isolated from acidic hot springs and acidic hot soils around the world. So far about a dozen species representing three genera (*Methylacidiphilum, Methylacidimicrobium, Methlacidithermus)* with pH optima between 1 and 3 have been isolated (Schmitz *et al.* 2021; Picone *et al.* 2021). Other than methane, also methanol (Pol *et al*. 2007) and hydrogen (van Teeseling *et al.* 2014) can be used as substrates. Members of

the genus *Methylacidiphilum* can grow on C3 compounds like acetone by oxidation with a homolog of the particulate methane monooxygenase (Awala *et al*. 2021).

The order *Pedosphaerales* comprises several metagenome-assembled genomes from hyperthermal soil environments. So far, the isolate *Limisphaera ngatamarikiensis* and uncultured *Candidatus* Pedosphaera parvula are the only described representatives of the order (Kant *et al.* 2011; Anders *et al.* 2015).

A much larger number of described genera and species can be found in *Verrucomicrobiales*. Many of them are aerobes isolated from marine environments, sometimes in association with marine algae or sponges (Scheuermayer *et al.* 2006; Yoon *et al.* 2008a; Yoon *et al.* 2008b; Otsuka *et al.* 2013; Szuróczki *et al.* 2020). However, also *Akkermansia* spp., mucin-degrading bacteria that were isolated from human intestinal tracts as well as from chicken guts and python feces, are well investigated members of the order (Derrien *et al.* 2004; Ouwerkerk *et al.* 2016: Gilroy *et al.* 2021).

The order *Opitutales* comprises the families *Opitutaceae* and *Puniceicoccaceae* (former oder: *Puniceicoccales*, Parks *et al.* 2018) but also not yet named family-level lineages from aquatic environments that contain the genera *Cerasicoccus* (Yoon *et al.* 2007), *Ruficoccus* (Lin *et al.* 2017), and *Oceanipulchritudo* (Feng *et al.* 2020) that were previously ranked as *Puniceicoccaceae*. Members of the genus *Pelagicoccus,* previously classified as *Puniceicoccaceae*, were re-classified as *Opitutaceae* based on genome phylogeny. With exception of *Opitutaceae*, the 16S-based taxonomy of *Opitutales* was not very solid and improved drastically by genome-based approaches (Parks *et al*. 2018). The family *Opitutaceae* comprise a diverse group of mostly facultatively anaerobic, coccoid-shaped bacteria from limnic, terrestrial and also host-associated environments (Cho *et al.* 2015).

Verrucomicrobiota is a highly diverse bacterial phylum found in several fundamentally different environments. Compared to other major phyla, *Verrucomicrobiota* are clearly under-sampled and require numerous further investigations to understand their true diversity, physiology and ecology. *Opitutales* are members of the gut microbiota of numerous termite species, however they are often overlooked and need further attention. In this work, I investigate the respiratory potential of members of *Opitutaceae* and report several metagenome-assembled genomes, representing deep-branching lineages of uncultured *Opitutales* from the termite gut.

1.2 The oxygen relationship of *Opitutaceae*

1.2.1 Importance of oxygen

The rise of atmospheric oxygen levels, due to the development of oxygenic photosynthesis by *Cyanobacteria*, came along with major consequences for the so far anaerobic life on earth (Soo *et al.* 2017). Nowadays, oxygen is the second most abundant gas in the atmosphere of the earth and therefore an important player for several chemical and biological processes (Holland 2006, Falkowski *et al.* 2008). The most important biological way of oxygen reduction is aerobic respiration. The goal of aerobic respiration is to utilize energy-rich substrates to generate energy for all kinds of cellular processes. Metabolic pathways like glycolysis or Krebs-cycle are used to oxidize multi-carbon compounds like glucose to carbon dioxide. The surplus electrons accumulate as reducing equivalents like NADH or ferredoxin (Fuchs 2014). In the final step of aerobic respiration, these reducing equivalents are oxidized by the membrane-bound respiratory chain where the electrons are ultimately transferred onto oxygen. This process is called oxidative phosphorylation and happens at the inner mitochondrial membranes of eukaryotes and the inner cytoplasmic membrane of prokaryotes (Fuchs 2014).

1.2.2 Aerobic, respiratory electron transport chains

Typical bacterial and eukaryotic respiratory chains consist of five major protein complexes (Fig. 2). At least three different types of unrelated variants of complex I, the entry point of respiratory chains, have been identified in bacteria (Kaila and Wikström 2021). The most common one uses a chain of eight or nine iron-sulfur (Fe-S) clusters to tunnel electrons from NADH to the quinones (Verkhovskaya *et al.* 2008), while translocating 2 H+/e- and contributing to the electrochemical proton gradient. Other variants do not translocate any protons or translocate sodium ions instead (Bogachev *et al.* 1997; Melo *et al.* 2004). Complex II, the succinate dehydrogenase, is a membrane-bound protein complex that is part of the TCA cycle but also connected to the respiratory chain via a flavin-adenine-dinucleotide (FAD/FADH) carrier. The complex is not in contact with the outside of the membrane and not involved in proton translocation (Fig. 2, Yankovskaya *et al.* 2003). The quinone/quinole pool stores electrons by changing from oxidized quinones to reduced quinoles when electrons are available. Besides ubiquinone which is present in most eukaryotes, prokaryotes can also use the low-potential menaquinone as part of their respiratory chains (Kao and Hunte 2014). All eukaryotic respiratory chains as well as bacterial respiratory chains with cytochrome *c* oxidases use the cytochrome bc_1 complex

((ubi)-quinone:cytochrome *c* oxidoreductase, complex III) to utilize the electrons of the quinole pool for the reduction of cytochrome *c*. Complex III also contributes to the proton motif force, however, the mechanism differs from the other respiratory complexes. While the protons are channeled through the whole membrane in a charged state in complex I and complex IV, the protons are transferred using the Mitchellian redox-loop (Q-loop) mechanism, where the protons travel neutrally in the form of hydrogen (quinoles) and the electrical charge is transmitted by transmembrane electron transfer (Mitchell 1975, Crofts 2004, Kaila and Wikström 2021). The role of the bc_1 complex was shown to be fulfilled by an unrelated complex in several different bacteria. The alternative complex III (ACIII) is structurally not similar to the bc_1 complex (Refojo *et al.* 2012; Sousa *et al.* 2018).

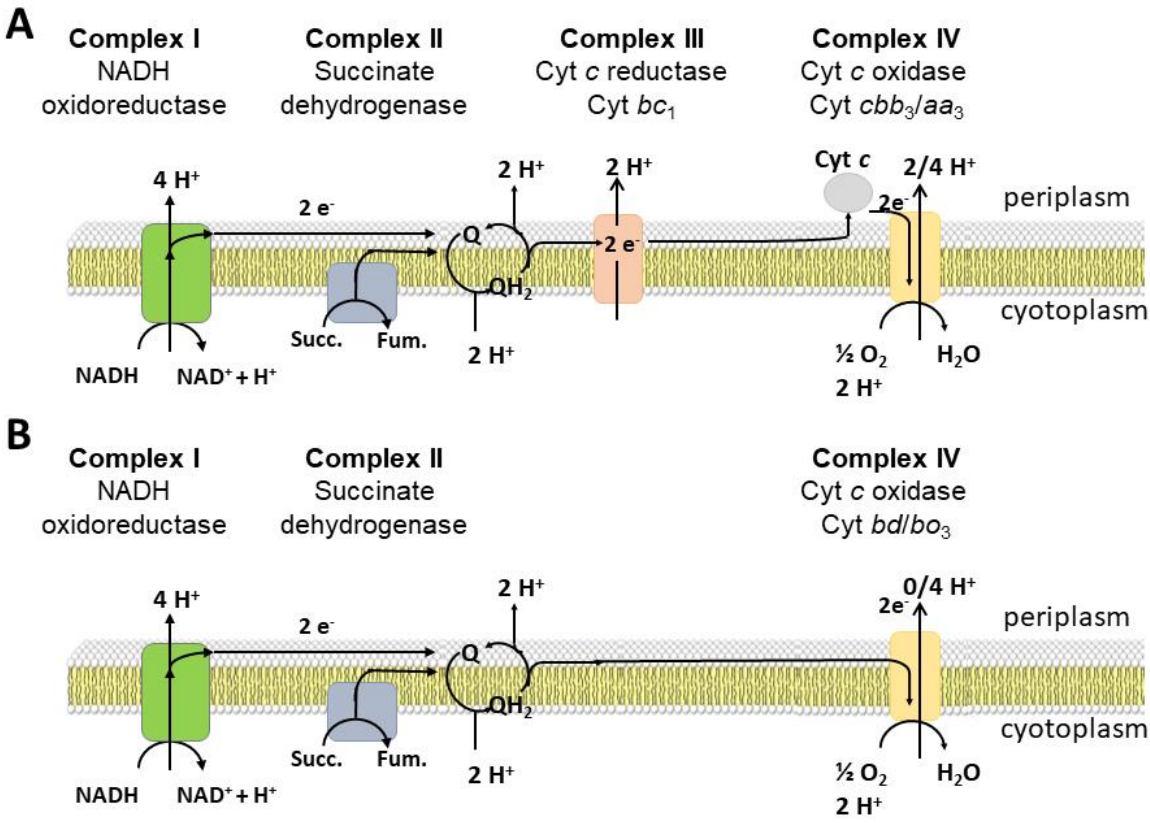

Figure 2: Simplified bacterial respiratory chains. Complex I (NADH oxidoreductase, green) and complex II (succinate dehydrogenase, blue) oxidize reducing equivalents and feed electrons into the quinole pool by reducing an oxidized quinone (Q) to a quinole (QH_2). A) In case of cytochrome *c* oxidases, the quinole pool gets oxidized by complex III (cytochrome *c* reductase, orange), which reduces cytochrome *c* at the periplasmatic side of the membrane. The reduced cytochrome *c* itself gets reduced at by the terminal oxidase (complex IV, yellow, cbb_3 and aa_3 oxidase) while the electrons are finally used to reduce oxygen. B**)** In case of quinole oxidases (bo_3 and *bd* oxidase), the quinole pool is oxidized by the terminal oxidases. Several processes release free energy which is used to translocate protons to the outside of the membrane. The numbers of protons translocated by the terminal oxidases differs dependent on the oxidase type.

1.2.3 Terminal oxidases (Complex IV)

The final part of respiratory electron transport chains are terminal oxidases. These multi-protein complexes oxidize a reduced electron carrier and ultimately reduce oxygen to water (Fig. 2). Some terminal oxidases use the free energy of this reaction to translocate protons, and thereby contribute to the electrochemical gradient (Morris and Schmidt 2013). Oxidases can be differentiated by (1) their metal content in the catalytic center, (2) by the substrate that is oxidized or (3) by their affinity to oxygen. The large group of Heme-Copper-Oxidases (HCOs) is characterized by a bimetallic center consisting of heme and copper. Based on structural and phylogenetic analysis, HCOs can be further divided into three classes, where A-type HCOs are low-affinity oxidases (LATOx), while B-type and C-type oxidases are mainly high-affinity oxidases (HATOx) (Pereira *et al.* 2001; Hemp *et al.* 2006). A-type HCOs usually have two channels for proton translocation (K-channel and D-channel) whereas B- and C-type HCOs only have one (K-channel), resulting in a differential efficiency in energy conservation (Hemp *et al.* 2007; Chang *et al.* 2009; Sharma and Wikström 2016). The second group of oxidases, the *bd*-oxidase family, mainly consists of high-affinity oxidases. In many bacteria, *bd* oxidases are mainly not used for energy conservation purposes but as a respiratory or non-respiratory defense mechanism against oxygen (Poole and Hill 1997; Lemos *et al.* 2001) or reactive oxygen species (Borisov *et al.* 2013). Members of the *bd* oxidase family exclusively oxidize reduced menaquinol or ubiquinol, while HCOs can either oxidize quinols or cytochrome *c*, depending on the particular enzyme (Fig. 2; Morris and Schmidt 2013). A homolog of the classical *bd* oxidase, the cyanide-insensitive oxidase (CioAB, cytochrome *bb*), is important for respiration and used in quorum sensing by *Pseudomonas* spp. (Cunningham *et al.* 1997; Yan *et al.* 2007). Further, low-affinity terminal oxidases (LATOx; K_S > 100 nM) can be differentiated from high-affinity terminal oxidase (HATOx; K_S in 3 – 7 nM) (D´mello *et al.* 1995; Preising *et al.* 1996) by their substrate affinity.

In this dissertation, the classification of oxidases follows the suggestion of Morris and Schmidt, in which anaerobes have no terminal oxidase, aerobes have low-affinity oxidases and microaerobes have at least one high-affinity oxidase in their genomes (Morris and Schmidt 2013). This concept improves the early concept of aerobes, microaerophiles and anaerobes, which is neglecting the microaerobic potential of aerobes that grow optimally at atmospheric oxygen conditions.

1.2.4 Adaptation to microoxic environments

Low affinity oxidases usually have much higher turnover rates than high affinity oxidases, however, whether or not a bacterium has access to a high affinity oxidase can be crucial for its competitive success in microoxic environments. Whenever the oxygen consumption outperforms the oxygen diffusion within a bacterial community at an oxic-anoxic interface, oxygen gradients with differential oxygen concentrations occur. Those environments include soils (Tiedje *et al.* 1984), marine sediments (Ploug 2001; Fenchel and Finlay 2008) and biofilms (Kühl *et al.* 2008), but also host-associated bacteria have to deal with fluctuating oxygen conditions and gradients. Rhizobia living in the root nodules of legumes have to use high-affinity oxidases to scavenge low concentrations of oxygen in the tissue because high oxygen concentrations would be inhibitory for nitrogen fixation in the nodules (Kuzma *et al.* 1993). Bacteria in the gastro-intestinal tracts of animals have to deal with oxygen fluxes from the gut epithelium towards the gut center (Brune *et al*. 1995; Charrier and Brune 2003; Marteyn *et al.* 2010).

1.2.5 Distribution of terminal oxidases in different environments

An excessive search by Morris and Schmidt (2013) revealed the number of terminal oxidases found in genomes from different environments (Fig. 3). Genomes from marine environments, that are constantly saturated with oxygen contain mainly low-affinity oxidases, while genomes from environments with changing oxygen levels like soil contain both, high- and low-affinity oxidases. Genomes from host-associated environments encode for a high number of high-affinity oxidases, and particularly low number of low-affinity oxidases. The analysis of genomic and metagenomic data revealed, that the same trend can be also found in the higher termite gut microbiome (Carsten Dietrich and Andreas Brune, unpublished data) The dominance of HATOx in host-associated environments was also reported in humans, where mutualists but also pathogens possess HATOx to compete for the limited oxygen that is available (Shi *et al.* 2005, Weingarten *et al.* 2008).

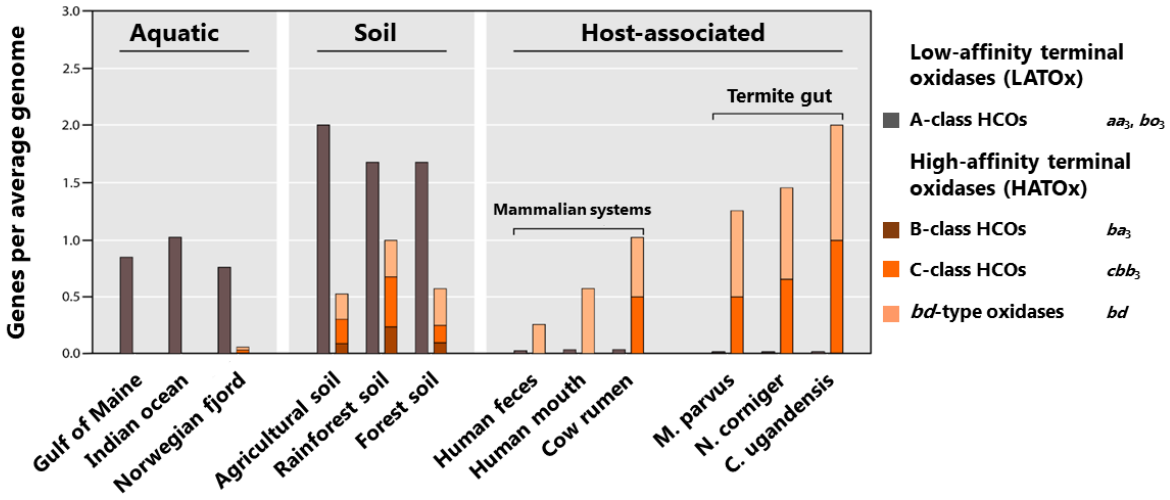

Figure 3: Distribution of HATOx and LATOx in different environments. The figure is adapted from Morris and Schmidt 2013 and was extended for termite gut data (Carsten Dietrich and Andreas Brune, unpublished results). The bar graphs show the average number of genes for low-affinity oxidases (LATOx, grey) and high-affinity oxidases (HATOx, different shades of orange) per genome in the respective environment.

1.2.6 Oxygen reduction in the termite gut

Microsensor experiments identified termite guts as oxygen sinks by revealing a steep gradient of oxygen from the gut wall to the gut center. However, about half of the gut volume remains anoxic to promote important anoxic processes in the termite gut (Brune *et al.* 1995) which are crucial for the anaerobic production of acetate, the major carbon source for the termites (Tholen and Brune 2000). In the gut of lower termites, flagellates are considered the main players in oxygen reduction (Wertz and Breznak 2007a). Besides that, also microorganisms like *Stenoxybacter acetivorans*, *Geminisphaera colitermitum* and *Ereboglobus luteus* have been shown to respire oxygen in the guts of lower termites and cockroaches (Wertz and Breznak 2007a; 2007b; Tegtmeier *et al*. 2018; Wertz *et al*. 2018). The situation in higher termite guts is rather unclear since flagellates are absent. A study on the functional compartmentation of two *Nasutitermes* species suggests a few taxa, including members of *Actinobacteriota* and *Bacteroidota*, that are likely to be associated with the gut wall, making them good candidates for oxygen reduction in the guts of higher termite guts (Köhler *et al.* 2012). Oxygen reduction in termite guts is not restricted to aerobic respiration but can also be acquired by other processes. *Sporotalea propionica*, a firmicute isolated from the gut of the soil-feeding termite *Thoracotermes macrothorax*, is a propionic acid bacterium that is capable of oxygen reduction with lactate, glucose, glycerol or hydrogen as electron donors (Boga *et al.* 2007). Sulfate-reducing *Desulfovibrio* species in the gut of *Reticulitermes santonensis* can reduce sulfur compounds with oxygen (Kuhnigk *et al.* 1996).

Even some strictly anaerobic methanogens have been shown to reduce oxygen with hydrogen (Tholen *et al.* 2007). Termites and their symbionts also have to deal with reactive oxygen species (ROS) like hydrogen peroxide and superoxide. Besides the well-known defense mechanisms of prokaryotes (Krumova and Cosa 2016; Lu and Imlay 2021), also the termites themselves contribute to the removal of ROS. Termites were shown to accumulate uric acid, which is in important antioxidant and likely contributes to the longevity of termite individuals (Tasaki *et al*. 2017). Overall, oxygen reduction should be considered an important task in the termite gut because it allows the strictly anaerobic processes in the gut center to occur. Therefore, it is important to identify the players and investigate their oxygen reducing machinery.

1.2.7 Diversity of *Opitutaceae*

Compared to other verrucomicrobial lineages, the family *Opitutaceae* contains a great number of isolated and well-characterized species and genera. *Opitutaceae* comprise bacteria isolated from fresh-water environments like *Rariglobus hedericola* (Pitt *et al.* 2020), *Lacunisphaera* spp. (Rast *et al.* 2017), *Alterococcus agarolyticus* (Shieh and Jean 1998) and *Nibricoccus aquaticus* (Baek *et al.* 2019), but also isolates from soil like *Opitutus terrae* (Chin *et al.* 2001) have been isolated. Additionally, an exceptionally high number of host-associated *Opitutaceae* have been described. These include isolates from the termite gut like *Verrucomicrobia* sp. TSB47 (Fang *et al.* 2015) and *Geminisphaera colitermitum* and related strains (Wertz *et al.* 2018), however, also species from the cockroach gut (*Ereboglobus luteus*, Tegtmeier *et al.* 2018), the gut of ants (*Cephaloticoccus spp*., Lin *et al.* 2016) as well as a symbiont of tunicates (*Candidatus* Didemnitus mandela, Lopera *et al.* 2017) have been described. Interestingly, all species seem to have a peptidoglycan-containing cell wall, despite most *Verrucomicrobiota* and related *Planctomycetota* lacking it (Fuerst 2013). Functionally, *Opitutaceae* comprise simple sugar fermenters but also organisms that are potential microaerobes. *E. luteus* and *G. colitermitum* were suggested to be involved in oxygen reduction in their respective gut habitats (Tegtmeier *et al.* 2018), but also other host-associated and free-living *Opitutaceae* reveal differential range of oxygen reducing potential (Rast *et al.* 2017; Lin *et al*. 2016; Baek *et al.* 2018; Rochman *et al.* 2018).

This study is built on the work of Tegtmeier *et al.* 2018, who measured the growth parameters and showed metabolic balances of *Ereboglobus luteus*, *Geminisphaera colitermitum* and *Opitutus terrae* and also reported the presence of high-affinity oxidases in their genomes. In this study, these three *Opitutaceae* strains were chosen as a model. Genomic, transcriptomic and physiological methods were used to study the differential response to changing oxygen regimen. The various different habitats and genomic equipment of *Opitutaceae* make them an ideal model to compare results and to investigate their functional role and importance in their respective environments.

1.3 Flagellate-associated *Opitutale*s in termite guts

1.3.1 Association of termites with gut flagellates

Termites are eusocial insects that can be found globally but are present in greater numbers and species richness in the tropics (Bignell and Eggleton 2000; Jones and Eggleton 2010). They are of profound ecological importance for several biogeochemical cycles including the decomposition of dead plant material (Wood and Sands 1978; Davies *et al.* 2003), as food source for animals and humans (Figueirêdeo *et al*. 2015), but also as structural pest species for agriculture (Mitchell 2002) and buildings (Gaju-Ricart *et al*. 2002). First fossil traces of termites date back to 195 million years ago (Xing *et al.* 2013). Other than previously accepted, termites (Isoptera) are not an individual insect order but are a monophyletic group of eusocial cockroaches within the order Blattodea (Fig. 4; Inward *et al*. 2007; Lo *et al.* 2007; Chouvenc *et al.* 2021).

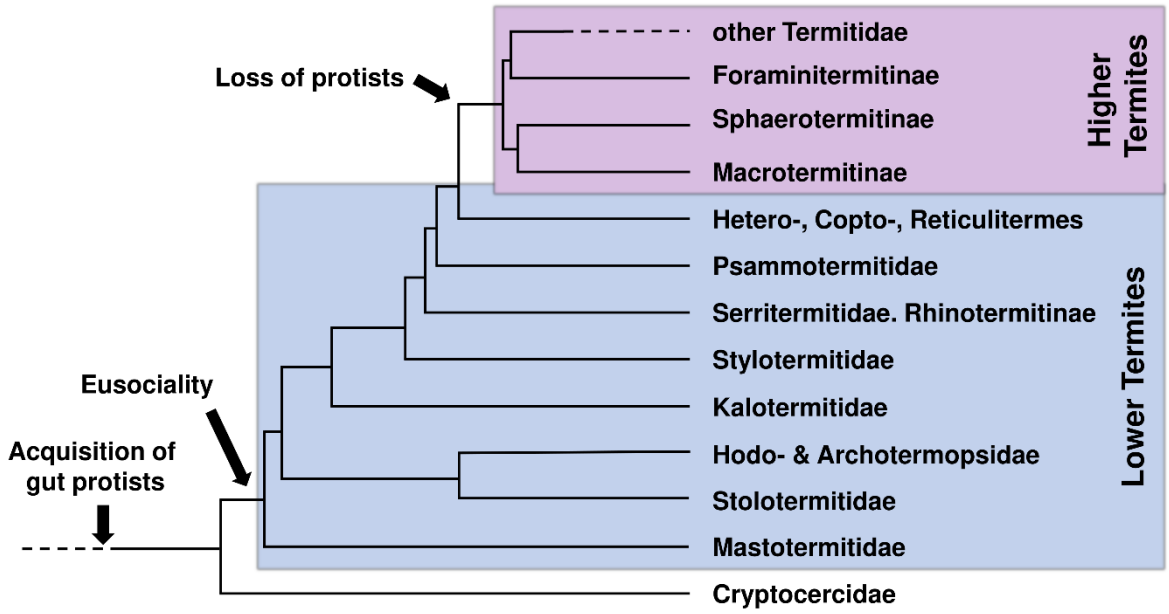

Figure 4: Major events during the evolution of termites. The tree is simplified and based on the phylogeny of Buček *et al.* 2019. The acquisition of gut protists already happened in the cockroach ancestor of termites (Cryptocercidae) and the development of eusociality marked the beginning of termites. The youngest termite family, Termitidae, lost the gut protists.

Termites are among the few animals that manage break down lignocellulose and are therefore able to feed on wood. Although termites produce several cellulolytic enzymes such as β-glucosidases and endo-β-1,4-glucanases in their salivary glands (Tokuda *et al.* 2004), the main load of the enzymatic lignocellulose degradation is contributed by the termites´ gut microbiota (Engel and Moran 2013; Brune 2014). In lower termites, this job is mainly

fulfilled by cellulolytic flagellates, which are typically specific for their respective host (Yamin 1979; Breznak and Brune 1994). Defaunation experiments have shown that the flagellates are crucial for the survival of the termites (Cleveland 1924; Veivers *et al.* 1983). The flagellates were already present in *Cryptocercus* spp. (wood-feeding cockroaches, Fig. 4), the common ancestor of termites, and have been transmitted since then (Brune and Dietrich 2015). Phylogenetically, termite gut flagellates belong to the eukaryotic phyla of Parabasalia or Oxymonadida (Ohkuma 2008). Detailed physiological data on the flagellates´ metabolism is rare due to the little number of cultivation-based studies (Breznak 2000). Major events in the evolution of termites often coincided with a major shift in the termite gut community structure (Dietrich *et al.* 2014). The loss of flagellate symbionts in the family Termitidae (higher termites, Fig. 4) led to the acquisition of new bacterial and fungal symbionts, a diversification in diet and a greater species richness in this family (Brune 2014). Termitidae comprise 70% of all termite species described today and feed on wood, soil, leaf litter, gras and fungus (Chouvenc *et al.* 2021).

1.3.2 Symbiotic processes in the termite gut

The guts of termites are often highly compartmentalized allowing different biochemical processes to happen at different physiological conditions. Microelectrode experiments revealed major changes in pH, redox potential, hydrogen- and oxygen partial pressures in the different gut compartments and also when comparing different feeding groups (Brune *et al*. 1995; Brune and Kühl 1996; Ebert and Brune 1997; Kappler und Brune 2002). Besides the breakdown of complex polymers like lignocellulose, the nutritional role of the gut microbiota also includes the supply with scarce nitrogen compounds (Tayasu *et al.* 1997; Hongoh 2011) and the production of acetate which is absorbed as the major carbon source for the termite (O´Brien and Breznak 1984; Brune 2014). Another important process in the termite gut is methanogenesis (Brune 2018). Termites emit significant amounts of methane with studies estimating the contribution to the total global natural methane emission to 5–20% (Bignell 2010). The knowledge about the function of the vast majority of the termite gut community is limited by the little number of cultured and culturable microorganisms (Tyson and Banfield 2005), especially in gut environments. However, recent genomic and metagenomic studies revealed the diversity and roles of more and more symbionts.

1.3.3 Prokaryotic symbionts of termite gut flagellates

It is long known that the termite gut flagellates themselves are associated with a number of ecto- and endosymbionts (Kirby 1941; Dolan 2001). These include diverse prokaryotic groups like methanogenic archaea (Tokura *et al*. 2000), *Spirochaetota* (Breznak and Leadbetter 2002), *Bacteroidota* (Noda *et al.* 2005*), Desulfobacterota* (Sato *et al*. 2009), *Endomicrobia* (Stingl *et al.* 2005) and *Actinobacteriota* (Strassert *et al.* 2012).

Ectosymbiotic partners of flagellates can fulfil different roles. Nitrogen fixation in the guts of dry-wood termites is shaped by the symbionts of their specific flagellate population and dominated by ectosymbiotic *Bacteroidales* (phylum: *Bacteroidota*, Desai and Brune 2012). Another *Bacteriodales* ectosymbiont of *Dinenympha spp*., *Candidatus* Symbiothrix dinenymphae, likely ferments lignocellulose-derived monosaccharides to acetate and provide it as an energy source for the termite (Yuki *et al*. 2015). Genomic and metagenomic studies revealed that even putatively acetogenic spirochaetes attached to termite gut flagellates (Iida *et al*. 2000; Song *et al.* 2021) have further bacteria (Candidate phylum: Margulisbacteriota) attached to them that probably exploit them as hydrogen sinks (Utami *et al.* 2019).

Endosymbionts of termite gut flagellates are not in direct contact to the gut lumen and are therefore most likely exclusively in symbiosis with the flagellate host and potentially other endosymbionts. *Candidatus* Desulfovibrio trichonymphae (phylum: *Desulfobacterota*) was found in *Trichonympha agilis* cells in the gut of *Reticulitermes speratus,* spacially separated from *Endomicrobia* (phylum: *Elusimicrobiota*) endosymbionts in the same cell. *Candidatus* Desulfovibrio trichonymphae has the genetic potential for sulfate reduction and is likely a sink for hydrogen produced by the flagellate or the *Endomicrobia* endosymbionts (Stingl *et al.* 2005; Ohkuma *et al.* 2007; Sato *et al.* 2009). *Endomicrobia* contain both endosymbiotic and free-living species and were shown to have adapted in the process of becoming an endosymbiont. They underwent massive genome reduction and acquired new genes that allow to fulfil certain niches and may provide the host cells with important metabolites (Zheng *et al*. 2017). Next to endosymbiotic *Endomicrobia*, the endosymbiotic *Candidatus* Ancillula trichonymphae (phylum: *Actinobacteriota*) also underwent a similar process of genome reduction and newly gained genetic potential. The genes for amino acid biosynthesis were preserved, suggesting a supply of essential amino acids to the host. Additionally, both groups lost and gained similar sets of enzymes like sugar phosphate transporters to adapt to the new environments. These findings suggest that multiple lineages of termite gut flagellate

endosymbionts fulfil similar ecological niches and have convergently evolved (Strassert *et al.* 2016; Mikaelyan *et al.* 2017b).

Although some flagellates are inhabited by more than one prokaryotic endosymbiont, the association of flagellates and their specific endosymbionts is highly specific and mostly characterized by a co-evolution between symbiont and host (Noda *et al*. 2008; Ikeda-Ohtsubo and Brune 2009). The knowledge about the functional role of the vast majority of the termite gut community remains limited by the little number of cultured and culturable microorganisms in the gut. However, recent advances in genomic and metagenomic techniques led to a rising number of studies that revealed the roles of more and more symbionts.

1.3.4 Flagellate-associated *Verrucomicrobiota* in termite guts

Members of the order *Opitutales* (phylum: *Verrucomicrobiota*) have been shown to be a part of the termite gut microbiota. Besides isolates (Wertz *et al.* 2012) and their appearances in studies covering the diversity of the microbial termite gut community (Hongoh *et al.* 2003; Nakajima *et al.* 2005), *Opitutales* can also be associated with termite gut flagellates (Yang *et al*. 2005; Strassert *et al*. 2012). Fluorescence *in-situ* hybridization (FISH) experiments also revealed two intranuclear symbionts of *Trichonympha agilis* within the gut of *Reticulitermes speratus*. (Sato *et al.* 2014). These symbionts form monophyletic groups and are mostly only distantly related to cultivated members of the families *Opitutaceae* and *Puniceicoccaceae* (Sato *et al.* 2014). Because genomic data and isolates are missing, the functional role of these flagellate-associated *Opitutales* remains unclear.

This study investigates 90 metagenome-assembled genomes (MAGs) that were recovered from 21 different termite metagenomes and classified as *Verrucomicrobiota*. The MAGs were assembled, curated and classified in a previous study in our group (Vincent Hervé, Andreas Brune, Max Planck Institute for Terrestrial Microbiology, Marburg, in preparation) and were provided for this study.

1.4 Goal of the thesis

This thesis aimed to investigate two aspects of *Verrucomicrobiota* in host-associated environments, especially in the termite gut. Although the number of described *Verrucomicrobiota* is rising, the true diversity of the phylum is hidden behind the cultivation bottleneck. Especially the order *Opitutales* comprises several isolates and clones from free-living and host-associated environments. The role of host-associated *Opitutales* is often speculative and requires further investigation. However, in order to shed light on the true taxonomic and functional diversity of *Opitutales*, it requires the application of both cultivation-based and cultivation-independent experiments.

The first part of this dissertation focuses on *Opitutaceae*, a verrucomicrobial lineage that is characterized by a widespread potential for microaerobic respiration. This study aimed to apply genomic, transcriptomic and physiological methods to investigate the oxygen relationship of *Opitutaceae* under differential oxygen regimens. The second part focused on uncultured *Opitutales*, represented by MAGs recovered from termite gut metagenomes. The goal was to apply functional genome analysis to get insights into the metabolism and the general biology of these uncultured lineages. Furthermore, microscopy methods aimed to investigate the nature of the symbiosis of *Opitutales* and their hosts.

2 MATERIAL AND METHODS

2.1 The oxygen relationship of *Opitutaceae*

2.1.1 Investigated strains

Three members of *Opitutaceae*, representing all existing combinations of terminal oxidases, found in the family, were chosen for physiological and transcriptomic experiments (Tab. 1).

Table 1: Investigated strains

Strain	DSMZ* Acc. Number	IMG** Genome ID	Publication
Opitutus terrae	DSM: 11249	641522643	Chin *et al.* 2001
Geminisphaera colitermitum	DSM: 25453	2517572100	Wertz *et al.* 2018
Ereboglobus luteus	DSM: 102184	2687453771	Tegtmeier *et al.* 2018

* German collection of microorganisms and cell cultures
** Integrated Microbial Genome server

2.1.2 Cultivation

All strains were routinely grown in AM5 medium (Tegtmeier *et al*. 2016) supplemented with (final concentration) glucose (10 mM), yeast extract (0.1%, Roth, Karlsruhe, Germany) and casaminoacids (0.1%, Roth, Karlsruhe, Germany). The headspace of the bicarbonate buffered medium was flushed with a mixture of nitrogen (80%) and carbon dioxide (20%). All strains were incubated at 30 °C. For certain experiments, the cells were constantly bubbled with gas mixtures that contained either 10%, 1%, 0.1% or 0.01% oxygen and 20% carbon dioxide in nitrogen. Gas tanks were purchased from Westfalen (Münster, Germany). Growth was routinely monitored using a tube spectrophotometer measuring OD_{578}.

2.1.3 Genome analysis

The genome analysis of the *Opitutaceae* was performed based on publicly available and automatically annotated genomes on the Integrated Microbial Genome server (IMG/mer, Chen *et al*. 2019, Tab. 1) of the Joint Genome Institute (JGI, Walnut Creek, USA). The respiratory chains were analyzed based on their KEGG annotation in IMG and additional searches using PFAM models (e-value cutoff = 0.0001). The completeness of the respiratory chains was checked based on the annotations on IMG/mer. The sequences of the terminal oxidases of *E. luteus*, *G. colitermitum* and *O. terrae* were extracted from IMG/mer and saved as fasta files for further analysis.

Publicly available genomes of *Opitutaceae* members were downloaded from NCBI or IMG/mer. A phylogenomic analysis was performed in the framework of the Genome Taxonomy Database (GTDB, release 202) utilizing the GTDB toolkit (GTDBtk, version 1.3.0, standard settings, Chaumeil *et al.* 2019) with kind assistance of Dr. Vincent Hervé. The resulting maximum-likelihood tree based on a concatenated alignment of 120 bacterial single copy marker genes (list of all genes in Parks *et al.* 2018) was created using IQ-TREE (version 1.6.11, best-fitting model determined by ModelFinder, Nguyen *et al.* 2015) containing branch support estimation by ultra-fast bootstrap approximation (1000 replicates, Minh *et al*. 2013). The taxonomic levels of the respective groups were estimated using FastANI (version 1.3, boundaries: species = 95%, genus = 83%, Jain *et al.* 2018) also considering relative evolutionary distances (RED values).

2.1.4 Phylogenetic analysis of the terminal oxidases

Amino acid sequences of terminal oxidase genes of *Opitutaceae* were downloaded from IMG/mer and added to an existing oxidase database (Dr. Penfei Liu, Prof. Dr. Andreas Brune, unpublished data) for heme copper oxidases and *bd* oxidases in ARB (version 6.0.6, Ludwig *et al.* 2004). The databases consisted of one representative oxidase of each type per prokaryotic genus available on NCBI. The original global alignments were generated with MAFFT (Version 7, Katoh and Stanley 2013). Maximum-likelihood trees were build using ARB utilizing the RAxML algorithm (Stamatakis 2014). The additional *Opitutaceae* sequences were manually added to the databases in ARB and adapted to the existing alignment. Phylogenetic trees were produced by highlighting the relevant groups that include *Opitutaceae* sequences and collapsing major groups that consist solely of oxidases from certain taxonomic groups.

2.1.5 Analysis of the oxidase transcription levels with qPCR experiments

Cells grown under different oxygen conditions were harvested by centrifugation and stored in RNA-Later until extraction. Resuspended cells were mechanically broken using a homogenizer (6.5 m/s, 45 s, FastPrep®, MP Biomedicals, Eschwege, Germany) after addition of TRIzol® (1ml TRIzol per 100 µl homogenate, ThermoFisher Scientific, Waltham, USA). RNA was subsequently purified by phase separations steps (chloroform, chloroform/isoamyl alcohol 1/1, isopropanole/3M sodium acetate 100/1). The RNA samples were digested with DNAse (RNase free DNase Set (50), Qiagen, Venlo, The Netherlands) and further purified using an RNA clean up kit (RNeasy MinElute CleanUp Kit (50), Qiagen, Venlo, The Netherlands). The purified RNA was used as template (1 µl) for a reverse

transcription reaction (Superscript IV-Kit, Thermo Fisher Scientific, Waltham, USA). The qPCR cycle parameters are summarized in Table 2. The cDNA samples were diluted and stored at -20°C.

Table 2: Protocol of the qPCR cycler

qPCR step	Temperature	Duration	
Initial denaturation	95 °C	300s	
Denaturation	95 °C	30 s	50 cycles
Primer annealing	57 °C	45 s	
Amplification	72 °C	45 s	
Fluorescence quantification			
Final amplification	72 °C	600 s	

Primers for qPCR experiments were designed for each oxidase of each investigated *Opitutaceae* strain (20 bp each, 150–250 bp amplicon, T_m = 59 °C, Tab. S2) using the NCBI Primer Blast tool (Ye *et al.* 2012). A second primer pair per investigated gene was designed which is flanking the qPCR primers. These flanking regions were amplified from gDNA using PCR and diluted to a concentration of 10^9 copies/µl. These solutions were the start of a decadal dilution series that was used as standard for qPCR. The resulting standard curve was also used to determine the primer efficiencies (Fig. S4).

The qPCR experiments were performed in 96-well plates using a SYBR-Green kit (SYBR® Green Jumpstart, Sigma-Aldrich, St. Louis, USA) and a qPCR cycler (CFX Connect, Bio-Rad, Hercules, USA). In order to evaluate the data, the cq values of the cDNA samples were converted into absolute copy numbers based on the standard curves (Fig. S4). The copy numbers were normalized to the original RNA concentration of the samples. In a second step, the copy numbers were set into perspective to two internal standard genes. In this study, the standard genes were *rpoA* (RNA-polymerase subunit 1) and the 16S rRNA gene (small ribosomal subunit). The stability of the copynumber of the standard genes under different oxygen conditions was observed (Fig. S5). The reliability of the qPCR experiments was ensured by observing melting curves (Fig. S3) and determination of the primer efficiency (Fig. S4). Only experiments with efficiencies between 90% and 105% were evaluated.

2.1.6 Microsensor measurements

For the microsensor measurements 50 ml cultures of the strains were grown in Müller-Krempel bottles under different oxygen concentrations. The cells were harvested by centrifugation at 4500 x g at 4 °C for 30 minutes. The centrifugation was repeated twice after the cells were resuspended in anoxic MOPS buffer (50 mM). The oxygen microsensors (Ox-10, tip diameter: 10 µm; Unisense, Aarhus, Denmark) were polarized for 1-2 hours and calibrated with dithionite-reduced water and oxygen saturated, bubbled water to achieve a two-point-calibration. The oxygen concentration was monitored over time using the *Rate* software (Unisense, Aarhus, Denmark) (five points per second). Washed cells were added to a final OD_{578} of about 1. After some time, glucose was added to a final concentration of 1 mM to trigger respiration of the cells. The oxygen reduction rate was determined using the slope of the oxygen decrease. The decreasing rates at lower oxygen conditions were used to analyze the kinetics of the oxygen uptake. The measurement was performed for cells that were precultured under anoxic conditions and under 1% oxygen.

2.1.7 Deoxygenation of globins as a measure for the oxygen uptake physiology

Preparation of deoxygenated myoglobin

Commercially available horse skeletal myoglobin (Sigma-Aldrich, St. Louis, USA) was solved in 25 µM sodium phosphate buffer to a final concentration of 5 mM. The solution was stored in a rubber stoppered glass bottle (V = 15 ml) and reduced by adding an extensive amount of sodium dithionite. After transfer to an anoxic tent, the solution was desalted using Zebra Spin desalting columns (Thermo Fisher, Waltham, USA). The resulting solution was still buffered with 25 µM sodium phosphate buffer. The myoglobin solution was stored in the anoxic tent until further handled.

Spectrophotometric measurements

Quartz cuvettes (V = 1 ml) were filled with 1 ml of the myoglobin solution within the tent and closed with custom fit rubber stoppers. The spectrophotometric experiments were carried out using a Speccord multi-wavelength spectrophotometer (Speecord S600, Analyticon, Jena). A full spectrum (λ = 300 – 700 nm) of the deoxygenated myoglobin solution was measured in the beginning. Afterwards, 20 µl of the solution were replaced by an oxic glucose solution (0.5 M) in order to oxygenate the myoglobin. After measuring a spectrum of the oxygenated myoglobin solution, cells, prepared as previously described (2.1.6 Microsensor measurement), were added to a final OD_{600} of 0.5–1. The following measurement recorded one spectrum every 10 s for a duration of 30–120 min. After the

spectra were stable and not changing, a few drops of a saturated sodium dithionite solution were added to ensure complete deoxygenation. Afterwards, a final spectrum was measured as a reference.

Data analysis

The spectra were analyzed using MS Excel software. The absorption of at 581 nm and 560 nm was copied and saved for further analysis. Oxygen concentrations at every given time point were calculated as described before (Bergersen and Turner 1979). The fractional oxygenation of the myoglobin was determined using the following formula (F1),

$$(F1) \qquad Y = \frac{\Delta\mathrm{A(t)} - \Delta\mathrm{A(deoxy)}}{\Delta\mathrm{A(oxy)} - \Delta\mathrm{A(deoxy)}}$$

where ΔA(t) is the ration of A581 to A560 at the given time, ΔA(deoxy) the ratio in the dithionite-reduced control and ΔA(oxy) is the ratio after full oxygenation. The free oxygen concentration at the given time was calculated with the following formula (F2).

$$(F2) \qquad Oxygen\ (M) = \frac{\mathrm{Y\ x\ ks\ (myoglobin)}}{1 - \mathrm{Y}}$$

Oxygen uptake rates were visualized by plotting the oxygen concentrations over time. The datasets were trimmed to reduce the dataset to the important areas before analyzing oxygen uptake affinities. The oxygen uptake rates (nmol × min^{-1} × g^{-1}) at every point was determined and normalized by the cell density in the cuvettes (OD_{600}). The usage of OD_{600} opposed to OD_{578} that was used in the microsensor experiments was inevitable because the absorption of myoglobin at 578 nm would interfere with the cell density measurement. Spectrophotometric measurements of a *Opitutaceae* cell suspensions made sure that the difference between OD_{600} and OD_{578} was neglectable (Fig. S1). The dry weight of *E. luteus* (390 mg/l at OD = 1, Tegtmeier *et al.* 2018) was used for all three investigated strains, assuming similar dry weights for similarly shaped and sized bacteria. The oxygen uptake rates were plotted against the corresponding oxygen concentration in order to visualize Michaelis-Menten kinetics. Using sum of squares regression with the SOLVER function in MS Excel, the best fitting regression, following Michaelis-Menten kinetics was calculated, yielding K_S and V_{max} values.

Leghemoglobin preparation

Since leghemoglobin is not commercially available, it had to be prepared from a natural source. Faba beans (*Vicia faba*, spp. faba, var. Bioro; Bingenheimer Saatgut, Echzell, Germany) were purchased from a commercial source. Plastic pots (V = 50 l) were filled with a 1+1 mixture of plant soil (Anzuchterde, Obi) and planting granula (Seramis ®, Mogendorf, Germany) and covered with a thin layer of planting granula. A total of 24 pots were planted with 6 seeds each and kept in a greenhouse. After watering, the pots and especially spots of the seed were inoculated with 20 ml of a solution (OD_{578} = 0.05) of *Rhizobium leguminosum* (*bv. vicae* vf398, supplied by T. Kabdullayeva, RG Becker, Universität Marburg) in Fahräeus medium (Tab. S6). The plats were regularly watered and kept for 8–10 weeks. The plants were harvested shortly before flowering started and after a few days of non-watering. The main body of the plants were cut off and the roots were carefully harvested and collected. Root nodules were carefully collected using a forceps, frozen in liquid nitrogen in a 2 ml reaction tube and stored at -70°C until further usage.

When needed, the nodules were washed in a sieve in order to get rid of residual soil at the nodules. Afterwards, the nodules were frozen in liquid nitrogen and immediately crushed with a mortar. The nodule fragments were further crushed with a homogenizer (4500/s, 30 s FastPrep®, MP Biomedicals, Eschwege, Germany). Residual cell fragments were removed by centrifugation. The resulting protein solution was treated with DNAse (DNAse kit, Qiagen, Hilden, Germany) to get rid of all DNA in the preparation. The protein concentration in the preparations were determined using the spectrophotometric Bradford assay using bovine serum albumin as standard. Afterwards the composition of the preparation was tested by separating the proteins using a SDS page. Since the preparations did not seem to contain any leghemoglobin, the usage of leghemoglobin was not further pursued.

2.2 Flagellate-associated *Opitutales* in termite guts

2.2.1 MAGs used in this study

A total number 2312 bacterial and archaeal metagenome-assembled genomes (MAGs) were reconstructed from 43 different metagenomes from 21 higher termites and 22 lower termite species. The reconstruction and curation of the MAGs was described previously (Hervé *et al.* 2020). The quality of all MAGs was determined using CheckM (Version 1.1.1, Parks *et al.* 2015). The MAGs were classified using the GTDB toolkit (GTDBtk, Chaumeil *et al.* 2019). The assembly, curation and initial classification of the MAGs was done by Vincent Hervé. A dataset consisting of all MAGs classified as *Verrucomicrobiota*, and representative genomes of every genus level taxon of *Verrucomicrobiota* was created. Analysis with GTDBtk (version 1.3.0, standard settings) also resulted in a concatenated alignment of 120 single copy marker genes of all the genomes (list of all marker genes in Parks *et al.* 2018). A maximum-likelihood tree based on the alignment was created using IQ-TREE (version 1.6.11, best-fitting model determined by ModelFinder, Nguyen *et al.* 2015) containing branch support estimation by ultra-fast bootstrap approximation (1000 replicates, Minh *et al.* 2013). The taxonomic levels of the respective groups were estimated using FastANI (version 1.3, boundaries: species = 95%, genus = 83%, Jain *et al.* 2018) also considering relative evolutionary distances (RED values).

2.2.2 Genome annotation and functional analysis

Open reading frames (ORFs) were predicted using Prokka (version 1.14.5, increment 1, minimum contig length 200, e-value 1e-06, Seemann 2014) or Prodigal (version 2.6.3, Hyatt *et al*. 2010). All genomes were investigated by Hidden-Markov Model (HMM) searches performed in HMMER (version 3.3, Eddy 2011). The genomes were searched against different databases including PFAM (version 33.1, e-value cutoff = 0.0001, El-Gebali *et al.* 2019), TIGR (version 15.0, e-value cutoff = 0.0001, Haft *et al.* 2003) and PANTHER (version 16.0, e-value cutoff = 0.0001, Mi *et al.* 2005). If necessary, the results of the HMM searches were proven by BLASTp (version 2.6, Altschul *et al.* 1997). A complete list of all used HMMs is located in the supplementary materials (Tab. S9). Presence/absence maps of the investigated genes were visualized using iTOL (version 4, Letunic and Bork 2019).

2.2.3 Phylogenetic analysis of hydrogenases and transporters

Open reading frames that were found with HMMs specific for hydrogenases were saved as fasta files. All classified hydrogenases from the hydrogenase database (Søndergaard *et al.* 2016, 3265 entries) were downloaded as one fasta file. A global aligment of all hydrogenases

was produced with MAFFT (Version 7, Katoh and Stanley 2013). IQTREE (version 1.6.11, best-fitting model determined by ModelFinder, Nguyen *et al.* 2015) was used to build a phylogenetic tree including branch support estimation by ultra-fast bootstrap approximation (1000 replicates, Minh *et al.* 2013). The tree was further handled and edited using iTOL (Letunic and Bork 2021). The phylogenetic analysis of different transporters was done identically.

2.2.4 Fluorescence in-situ hybridization

Probe choice and design.

The general Bacteria probes EUBI (Amann *et al*. 1990) and EUBIII (Daims *et al.* 1999) or a mixture of both labeled with fluorescein were used to visualize the location of Bacteria. EUBIII was necessary because EUBI does not cover some bacterial groups including some groups of *Verrucomicrobiota*. A custom *Opitutales* specific probe (Verr_CF: 5´-CGACCTATCCCCAACTTA-3´) was designed based on a previously describes probe (V-RsD37-130, Sato *et al.* 2014) and labeled with Cy3. The probes were designed and tested for suitability using the probe design function of the ARB software package (version 6.0.6, Ludwig *et al.* 2004).

Sample preparation and fixation

Living termite samples were obtained from Jan Šobotník (Czech University of Life Sciences, Prague), David Sillam-Dussès (Université Sorbonne Paris Nord) and Vincent Hervé (Université de Tours). The termites were either dissected directly or set on a cellulose powder diet for 1-2 weeks in order to get rid of remaining wood particles in the termite guts. The hindguts of 3-7 termites (depending on the species) were dissected and pooled into 1 ml 1×PBS solution in an hour glass. The guts were disrupted and washed out within the PBS solution. Afterwards, remaining gut wall fraction were removed from the solution. The remaining gut lumen fraction was then transferred into a reaction tube and spun down with a centrifuge (50 × g; 3 min). The supernatant was then replaced with a 4% formamide solution. The solution was incubated at 4°C for 3-5 h for fixation. Afterwards the samples were washed using 1 × PBS by replacing the supernatant after centrifugation for three times. In a final step, the supernatant was replaced with 96% ethanol (ice cold) and stored at -20°C until further experiments were done.

Sample hybridization and microscopy

When needed, 5 µl of a carefully inverted sample were transferred onto a poly-lysin-coated adhesion slide (Polysine ®, Carl Roth, Karlsruhe, Germany) and dried. Afterwards, the spot

that contained the sample was covered with a 5% agarose solution and dried. Hybridization was performed at 48°C for 3–5 h or overnight at formamide concentrations between 0% and 50%. 16 out of 1000 µl of the hybridization buffer, prepared as described in Daims *et al.* 2004 (Tab. 3) depending on the formamide concentration, was transferred onto the sample spot followed by 2 µl of each probe. The remaining volume of the hybridization buffer was transferred into a 50 ml reaction tube that was filled with some tissue paper. The reaction tube was then closed after the slide was placed inside and transferred to an oven set to 48°C. After 3–5 hours, the slide was removed from the reaction tube and transferred to another 50 ml reaction tube containing 50 ml washing buffer at 48°C for 15 minutes (Tab. 3). Afterwards, the slide was held into ice-cold water for 2–3 seconds and immediately dried using compressed air. A few drops of DAPI solution were transferred to the sample spot and removed by dripping ice-cold ethanol, followed by immediate drying. The visualization was carried out using the Axiophot fluorescence microscope (Zeiss, Oberkochen, Germany). Image editing and analysis was carried out in Fiji (Schindelin *et al.* 2012).

Table 3: Hybridization buffer and washing buffer as described by Daims *et al*. 2005

Hybridization buffer											
Formamide %	0%	5%	10%	15%	20%	25%	30%	35%	40%	45%	50%
5 M NaCl (µL)	180	180	180	180	180	180	180	180	180	180	180
1 M Tris-HCl (µL)	20	20	20	20	20	20	20	20	20	20	20
ddH_2O (µl)	799	749	699	649	599	549	499	449	399	349	299
Formamide (µl)	0	50	100	150	200	250	300	350	400	450	500
10% SDS (µl)	1	1	1	1	1	1	1	1	1	1	1
Washing buffer											
Formamide %	0%	5%	10%	15%	20%	25%	30%	35%	40%	45%	50%
5 M NaCl (mL)	9.0	6.3	4.5	3.18	2.15	1.49	1.02	0.70	0.46	0.30	0.18
1 M Tris-HCl (ml)	1	1	1	1	1	1	1	1	1	1	1
0.5 M EDTA	0	0	0	0	0.5	0.5	0.5	0.5	0.5	0.5	0.5
ddH_20	add to 50 ml										

3 RESULTS

3.1 The oxygen relationship of *Opitutaceae*

3.1.1 Phylogenomic analysis of *Opitutaceae*

The phylogenomic tree reveals the close relationship of the strains that were isolated from termites and cockroaches, namely *Geminisphaera colitermitum*, the other TAV-strains, strain TSB47 and *Ereboglobus luteus* (Fig. 5). Genomes of strains isolated from aquatic environments (*Lacunisphaera* spp., *Nibricoccus aquaticus*, *Oleiharenicola alkalitolerans*), soil (*Opitutus* spp.), but also ants (*Cephaloticoccus* spp.) are more distantly related. The outgroups for this tree were other *Verrucomicrobiota* as well as other members of the PVC superphylum. ANI analysis and consideration of relative evolutionary distance (RED-value) suggest that the group of the two *Cephaloticoccus spp*. and *Opitutus sp*. are likely members of the same genus. Additionally, all TAV strains belong to the same genus (*Geminisphaera*) with TAV3 and TAV4, as well as TAV1 and TAV5 likely representing the same species. The undescribed termite gut isolate *Opitutaceae* bacterium TSB47 is closest related to *E. luteus* and likely represents a second species from the genus *Ereboglobus*.

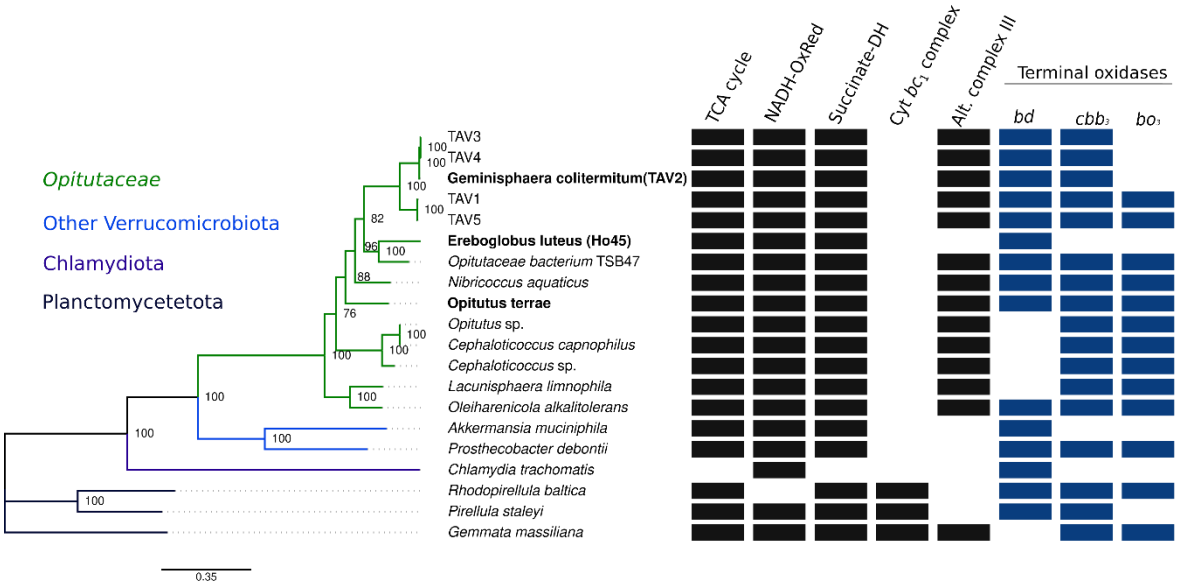

Figure 5: Phylogenomic maximum-likelihood tree of *Opitutaceae* genomes and their respiratory equipment. The tree was produced using the GTDB toolkit (GTDBtk, Chaumeil *et al.* 2019) applying standard settings. Branches of *Opitutaceae* are labeled in green while outgroups from other verrucomicrobial lineages and the PVC superphylum are labeled in shades of blue. The species that were focused in this study are highlighted. The presence and absence of the TCA cycle, NADH oxidoreductase, succinate dehydrogenase, cytochrome *c* reductase, alternative complex III (black) as well as the terminal oxidases (blue) are mapped.

3.1.2 Functional analysis of respiratory chains

The analysis of *Opitutaceae* genomes revealed three oxidases to be present in different variants of sets. These comprise of a low-affinity bo_3 oxidase (A-type HCO), a high-affinity cbb_3 type oxidase (C-type HCO) and a high-affinity *bd* oxidase (Fig. 5).

Several strains, including *Opitutus terrae* and *Opitutaceae* strain TSB47 have all three oxidases present in their genomes. *Geminisphaera colitermitum* lacks a complete bo_3 oxidase and therefore only encodes for high-affinity oxidases. *Ereboglobus luteus* lacks all HCOs and has only one *bd* oxidase present in the genome, however, it was still shown to be capable of aerobic respiration (Tegtmeier *et al.* 2018). Another variation, found in *Lacunisphaera limnophila* and *Cephaloticoccus capnophilus*, lacks the *bd* oxidase but has both HCOs present in the genome. Furthermore, the mentioned strains have all shown to be facultative anaerobes in the routine strain maintenance in the lab. However, this is in disagreement with the original description of *Opitutus terrae* (Chin *et al*. 2001). The detailed analysis of the respiratory chain proteins also revealed that *Geminisphaera colitermitum*, although encoding for the catalytic subunit of the bo_3 oxidase, is most likely not possessing the oxidase since three out of five subunits are absent and the two subunits that could be found are not in direct gene neighborhood.

Furthermore, most strains have genes for the remaining respiratory complexes, including a NADH oxidoreductase (complex I), a succinate dehydrogenase (complex II) and a cytochrome *c* reductase (complex III) (Fig. 5). However, the bc_1 complex was replaced by an alternative complex III (AC3).

3.1.3 Phylogenetic analysis of terminal oxidases

The phylogenetic analysis of the oxidase genes of *Opitutaceae* results in two different trees, since *bd* oxidases and HCOs are not related (Morris and Schmidt 2013). HCOs are phylogenetically related to each other and can therefore be analyzed together. The initial oxidase databases were created earlier in our group (Fengfei Liu and Andreas Brune, unpublished results).

The phylogenetic tree of *bd* oxidases (*cydA* gene) includes two different unrelated groups of *Opitutaceae*, suggesting the *bd* oxidases were acquired at least twice in *Opitutaceae* (Fig. 6). The *bd* oxidases of the strains from termites and cockroaches are closely related to *bd* oxidases from *Bacteroidota* and were therefore most likely horizontally transferred, while the genes of *Opitutus terrae* and other *Opitutaceae* from soil and fresh water environments

were most likely passed on vertically from other *Verrucomicrobiota* and further members of the PVC superphylum.

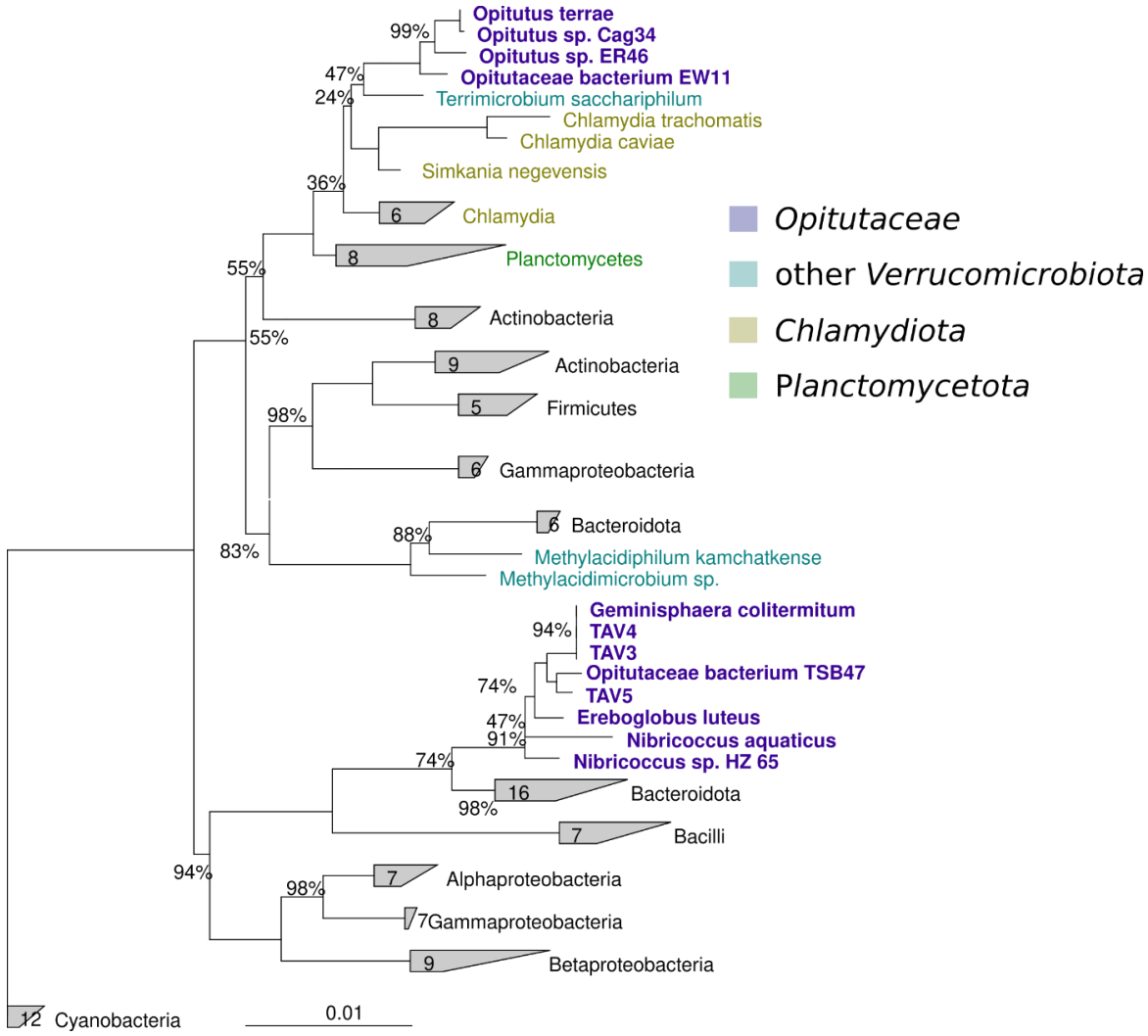

Figure 6: Phylogenetic maximum-likelihood tree of the *cydA* gene. The tree is based on an oxidase database that was built by Pengfei Liu (Pengfei Liu and Andreas Brune, unpublished results) The position of *Opitutaceae* and other members of the PVC superphylum is highlighted in different colors. All relevant groups are represented by 5–10 species. Non-*Opitutaceae* groups are collapsed while the number of genes in the collapsed groups is indicated. Genes of *Opitutaceae* cluster in two different, only distantly related groups.

The phylogenetic tree of heme copper oxidases (HCOs) includes all major groups of HCOs, including A1, A2, B, and C-type HCOs as well as nitric oxide reductases (NOR) as outgroup. The bo_3 oxidases that were identified in the genomic analysis of the respiratory chains of *Opitutaceae* belong to the A1 type and are closely related to oxidases of *Planctomycetota* (Fig. 7). The tree also includes a bo_3 oxidase of *Geminisphaera colitermitum*, however the functional analysis revealed that the oxidase is most likely not complete. A second group of

verrucomicrobial HCOs is found in another subtype of A-type HCOs but it does not include any oxidases from *Opitutales*. Within in the C-type HCOs, two groups consisting of oxidases from *Opitutaceae* were found. C-type oxidases are mainly represented by cbb_3 oxidases. Both groups are most closely related to either other *Verrucomicrobiota* and/or *Planctomycetota*. The investigated cbb_3 oxidases of *Geminisphaera colitermitum* and *Opitutus terrae* were only found in one of the groups. Neither A2- and B-type HCOs, nor nitric oxide reductases (NOR) were found to be represented by *Opitutaceae* or other *Verrucomicrobiota.*

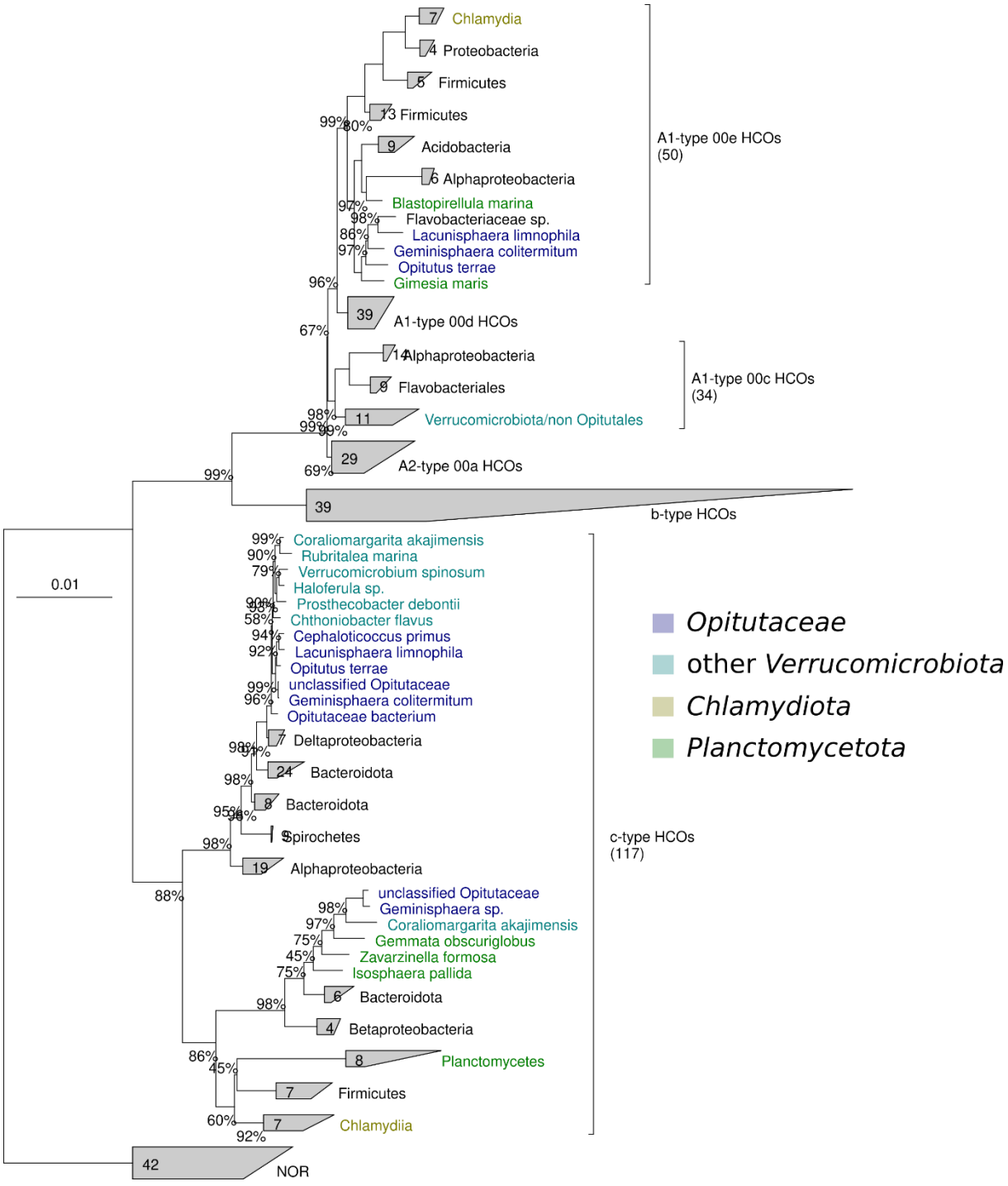

Figure 7: Phylogenetic maximum-likelihood tree of heme copper oxidases (HCOs) and the position of *Opitutaceae*. The tree is based on an initial HCO database produced by Pengfei Liu (Pengfei Liu and Andreas Brune, unpublished results). The maximum likelihood tree includes the four big groups of heme copper oxidases including A-type, B-type and C-type HCOs as well as the distantly related nitric oxide reductases (NOR) as outgroup. Nitric oxide reductases, B-type HCOs and A2-type HCOs are collapsed since they are not represented by any *Opitutaceae* members. *Opitutaceae* and other members of the PVC superphylum are highlighted by coloring.

3.1.4 Transcription level of *Opitutaceae* terminal oxidases

The quantification data from the qPCR experiments was used to calculate absolute copy numbers of the oxidase gene transcripts, present in the samples. The primer efficiency of all qPCR reactions was between 90% and 105% which ensured a reliable standard curve to calculate the absolute copy numbers (example Fig. S4) Additionally, the analysis of the final qPCR melting curves ensured an exclusively target specific amplification (Fig. S3). The results of the qPCR experiments, visualized as bar graphs (Fig. 8) indicate that all oxidases are constitutively expressed since there is base expression of every oxidase under all oxygen conditions.

The absolute copy numbers were normalized by the copy number of the 16S rRNA gene whose expression level was constant under all oxygen concentrations (Fig. S5). The expression level of *rpoA* was not stable under the different oxygen concentrations.

The *bd* oxidase of *E. luteus*, which is the sole oxidase present, is slightly higher expressed with rising oxygen conditions with the highest expression level at 1% oxygen. No data was gathered for 10%, since *E. luteus* is not able to grow at oxygen levels over 4% (Tegtmeier *et al*. 2018). Attempts to expose anaerobically precultured cell suspensions to 10% oxygen for eight hours led to very unstable levels of the *bd* oxidase and also the control gene (16S rRNA gene). The results were therefore not included. The *bd* oxidase of *G. colitermitum* and *O. terrae* are also constitutively expressed and only undergo minimal changes under changing oxygen levels.

The expression levels of the cbb_3 type high affinity oxidase of *G. colitermitum* and *O. terrae* show an opposing pattern (Fig. 8). Between 0% and 1% oxygen, *G. colitermitum* has a relatively low cbb_3 oxidase expression level (about 2% of the *bd* oxidase expression level), while the expression is immensely upregulated (about 500 times) at 10% oxygen, exceeding the *bd* oxidase expression level about tenfold. On the contrary to this, the expression level of *ccoN* of *O. terrae* is decreasing with increasing oxygen concentrations with the highest expression level at 0% oxygen. While the cbb_3 is the oxidase with the highest expression level at 0% O_2, it has the lowest expression level at O_2 levels higher than 0.01%.

Finally, the third terminal oxidase of *O. terrae*, the low-affinity bo_3 oxidase (*cyoB*) is expressed constitutively at constant level. The *cyoB* gene of *G. colitermitum* was not further investigated since the oxidase is most likely not complete (see 4.2.2).

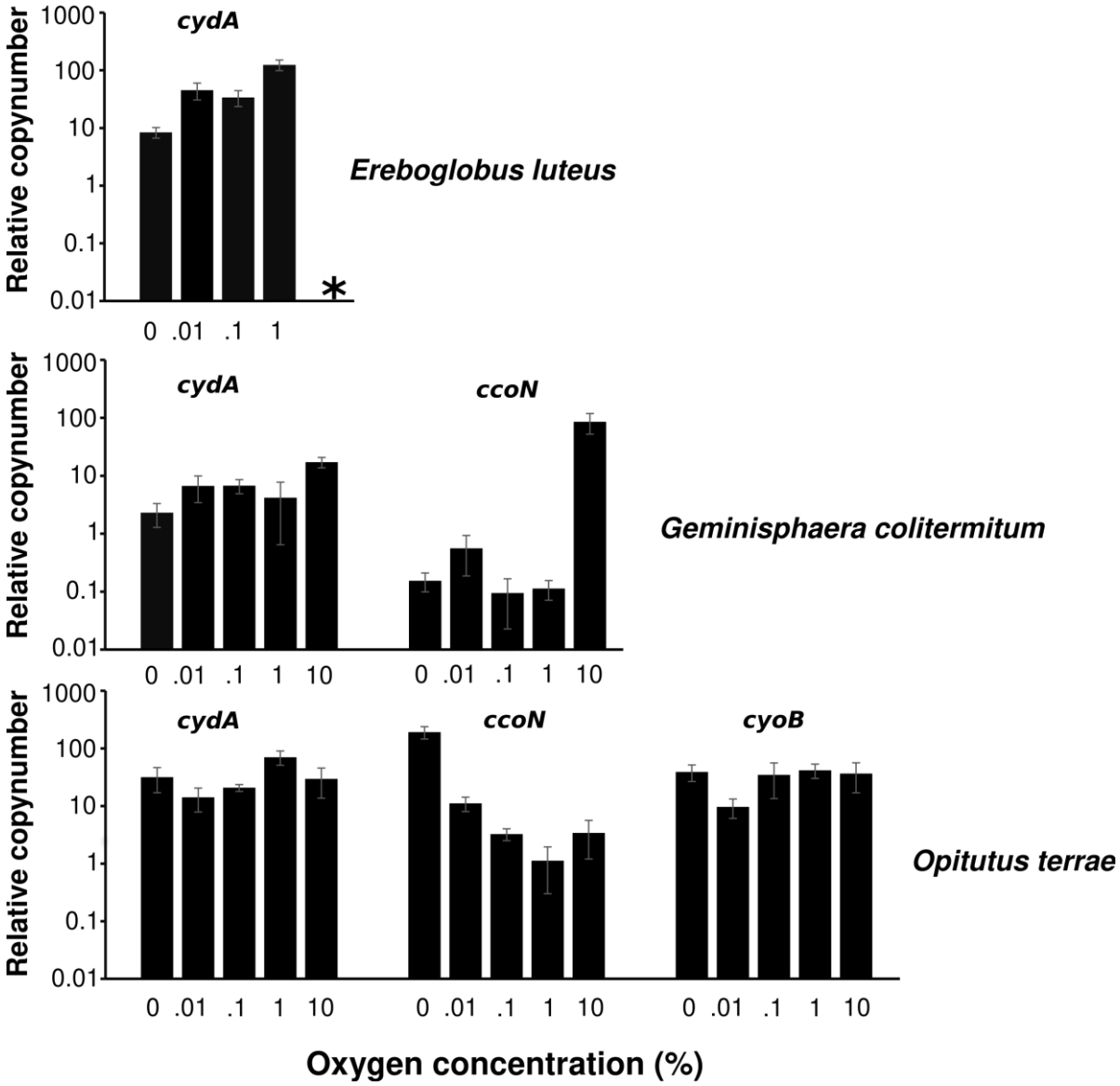

Figure 8: Terminal oxidase expression levels of *Opitutaceae*. The bar graphs show the copy number (copy number per ng RNA used in the cDNA synthesis) of the respective gene relative to the copy number of the 16S rRNA gene (multiplied by 10^6). The three organisms *Ereboglobus luteus*, *Geminisphaera colitermitum* and *Opitutus terrae* are displayed in separate rows of bar graphs. The different oxidases genes *cydA*, *ccoN* and *cyoB* are shown in separate columns. The asterix indicates missing data of *E. luteus* at 10% oxygen. This data point is missing because *E. luteus* is not growing at oxygen concentration over 4% (Tegtmeier *et al.* 2018).

3.1.5 Microrespiration experiments

Graphs of oxygen consumption curves were obtained by visualizing the microsensor data (Fig. 9). In the beginning of the experiments, the buffer-filled reaction chamber was monitored for a few minutes to ensure stability of the signal. Addition of washed cells led to a certain oxygen reduction by the cells, probably caused by oxidation of the internal sugar

reservoirs of the cells. The addition of 10 mM glucose to the chambers led to a stronger oxygen reduction, which indicates bacterial respiration induced by glucose addition.

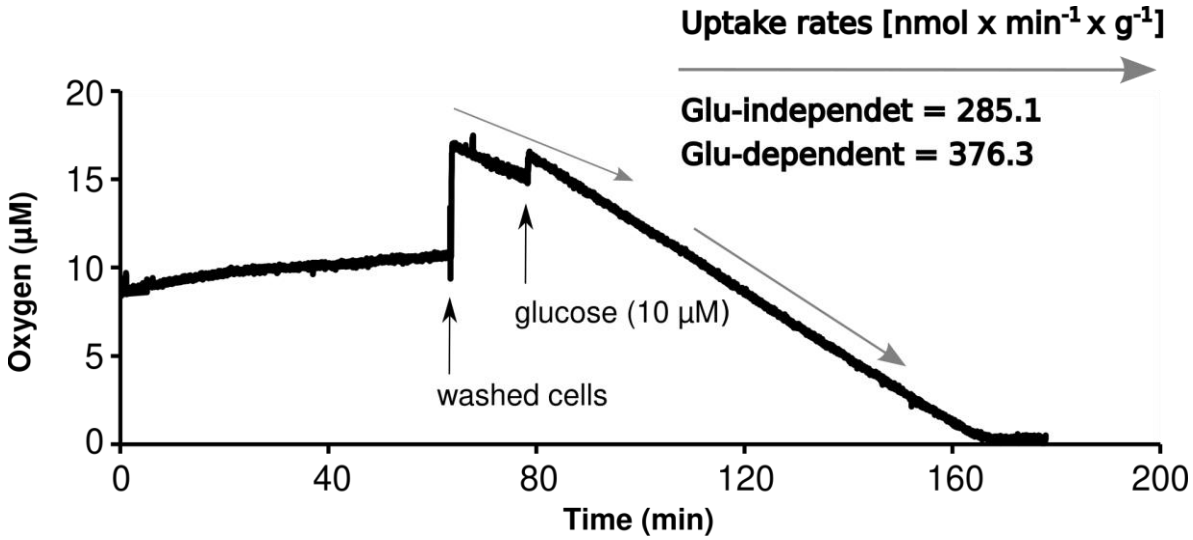

Figure 9: Microrespiration experiment. The microrespiration chamber was filled with anoxic buffer using standard plastic syringes and needles. The oxygen contamination during the transfer is enough to reach an oxygen level of around 10 µM. After the signal of the microsensor stabilized under stirring, washed cells were added to the chamber to an estimated OD of 1. After some time glucose was added to start the respiratory oxygen reduction. The slope of oxygen removal was used to calculate the oxygen reduction rate [nmol × min^{-1} × g^{-1}] of the cells.

The slopes of the curves were used to determine oxygen uptake rates of the cells. The uptake rates were normalized by the OD of the cell suspension in the chambers (Tab. 4). The oxygen uptake rates of *E. luteus* and *O. terrae* change only slightly when cultured under 1% oxygen compared to anoxic cultivation. While the rate of *E. luteus* decreases, the rate of *O. terrae* increases. Contrary to this, the oxygen uptake rate of *G. colitermitum* strongly increases about two-fold when cultured under 1% oxygen.

Table 4: Oxygen uptake rates: (nmol × min^{-1} × g^{-1}) and affinity (nM) of *Opitutaceae*.

	v_{max} (microsensor)		v_{max} (globin deoxyg.)		K_S (nM)	
O_2 concentration	0%	1%	0%	1%	0%	1%
E. luteus	401.4	354.1	312.3	427.8	22.1	20.4
G. colitermitum	1901.2	4239.0	565.8	2705.4	27.9	26.4
O. terrae	4937.6	5813.4	2235.4	6006.8	132.8	47.4

In the lower micromolar ranges of the curves (Fig. 9), the oxygen reduction rate decreases. The initial goal was to use the decrease in in oxygen reduction rate to calculate the oxygen affinities of the cells based on Michaelis-Menten kinetics (Tab. 4). The resolution of the microsensors did not allow a determination of K_S values below 0.5 µM. As a consequence, it is not possible to measure affinities that match those of published high-affinity oxidases (*cbb*$_3$ oxidase: K_S = 7 nM; Preising *et al*. 1996; *bd* oxidase: K_S = 3 nM; D´mello 1996).

3.1.6 Deoxygenation of myoglobin

The deoxygenation of oxy-myoglobin was used as an alternative method to follow the oxygen uptake kinetics of *Opitutaceae*. The oxygen uptake rates of the different *Opitutaceae* strains all increased when pre-cultivated under 1% oxygen when compared to anoxic precultivation. (Tab. 4, Fig. 11). While the rate of *E. luteus* increases only slightly, the rates of *O. terrae* and *G. colitermitum* are strongly increasing.

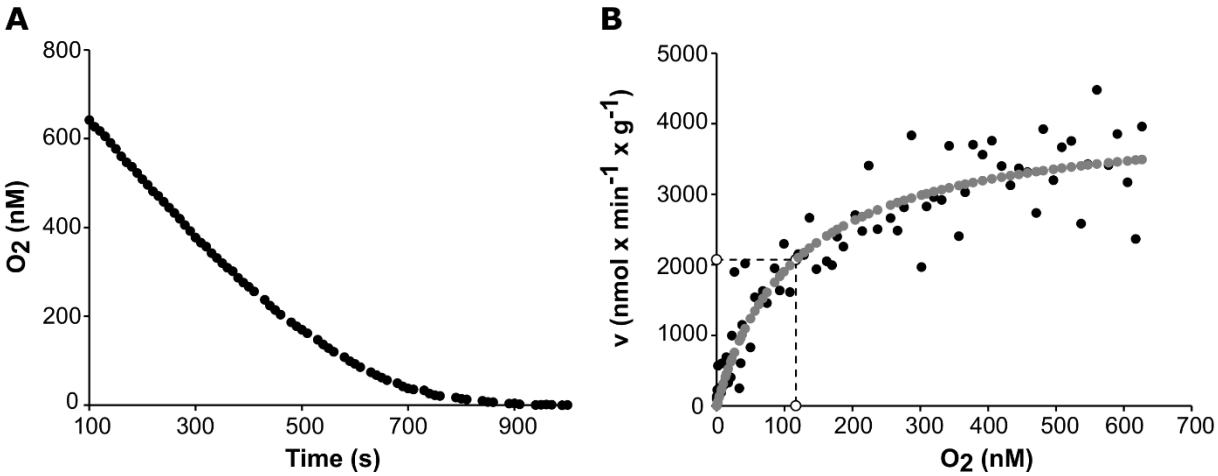

Figure 10: Kinetics of myoglobin deoxygenation by *Opitutus terrae*. A) The oxygen concentration was calculated from the spectrophotometrically measured ratios of the myoglobin peaks at 581 nm and 560 nm. One point was measured every ten seconds until the ratios did not change anymore. B) The oxygen uptake rates at every point were plotted against the respective oxygen concentration (black dots). Mean squared error regression was used to create a model that fits the data points optimally while following Michaelis-Menten kinetics (grey squares).

The oxygen uptake affinities of the three *Opitutaceae* strains were determined by analyzing the deoxygenation curves using the mean squared error regression assuming Michaelis-Menten kinetics. The affinities of *E. luteus* and *G. colitermitum* are both below 50 nM and don´t seem to change with differential oxygen conditions during pre-cultivation. Compared to this, the affinity of *O. terrae* is significantly higher when pre-cultivated under 1% oxygen (Tab. 4, Fig. 11).

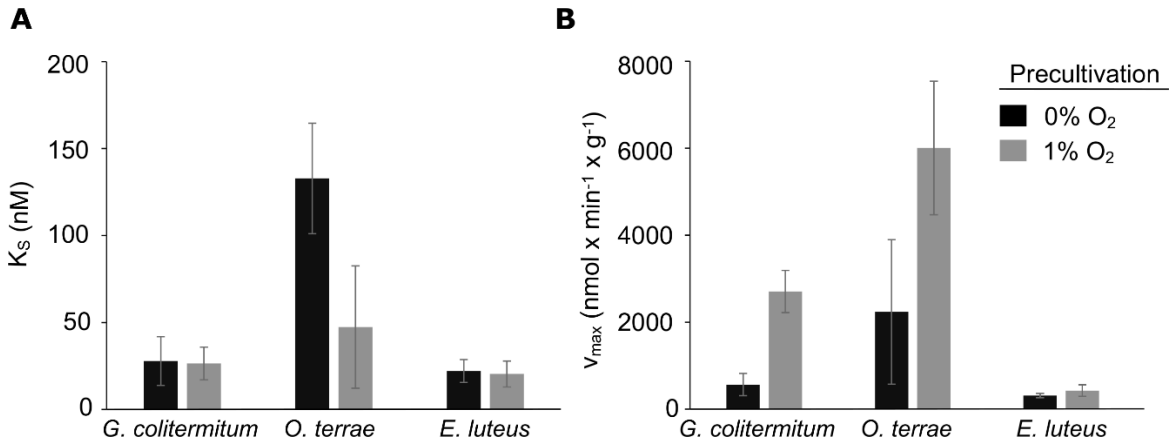

Figure 11: Oxygen uptake physiology of *Opitutaceae*. Both graphs show the results of the experiments that were based on the deoxygenation of myoglobin after precultivation under anoxic conditions (black bars) and under 1% oxygen (grey bars). A) Oxygen uptake affinity of *Opitutaceae*. B) Maximal oxygen uptake rates (v_{max}) of *Opitutaceae*.

3.2 Flagellate-associated *Opitutales* in termite guts

3.2.1 Overview of *Verrucomicrobiota* MAGs

The 2312 bacterial and archaeal metagenome-assembled genomes (MAGs) include 90 MAGs that were classified as members of the phylum *Verrucomicrobiota*, including 83 MAGs classified as *Opitutales*. The MAGs were recovered from metagenomes of 23 different termite species from six different termite families (Tab. 5). The majority of the MAGs belong to the family Kalotermitidae and only one MAG was from a higher termite (fam. Termitidae). 87 MAGs were of medium quality (>50% completeness, <10% contamination) and three MAGs were of high quality (>90% completeness, <5% contamination). Each termite ID represents an individually sampled termite nest. A summary of all MAG characteristics can be found in the supplementary materials (Tab. S7).

Table 5: Metagenomes that yielded *Verrucomicrobiota* MAGs

Host			Number of
ID	**Species**	**Familiy**	**MAGs**
Lower termites			
Hs463	*Hodotermopsis sjoestedtii*	Archotermopsidae	1
Po218	*Porotermes adamsoni*	Archotermopsidae	3
Pq454	*Porotermes quadricollis*	Archotermopsidae	1
Zx50	*Zootermopsis sp.*	Archotermopsidae	2
Hm464	*Hodotermes mossambicus*	Hodotermitidae	2
Cc175	*Cryptotermes cavifrons*	Kalotermitidae	8
Cd354	*Cryptotermes dudleyi*	Kalotermitidae	4
Ct408	*Calcaritermes temnocephalus*	Kalotermitidae	7
Gsp477	*Glyptotermes sp.*	Kalotermitidae	10
Gx481	*Glyptotermes sp.*	Kalotermitidae	7
Gx485	*Glyptotermes sp.*	Kalotermitidae	3
Im510	*Incsisitermes marginipennis*	Kalotermitidae	1
Iy174	*Incisitermes snyderi*	Kalotermitidae	1
Kf353	*Kalotermes flavicollis*	Kalotermitidae	2
Nc350	*Neotermes castaneus*	Kalotermitidae	5
Ncb351	*Neotermes cubanus*	Kalotermitidae	8
Nm470	*Neotermes meruensis*	Kalotermitidae	7
Pcl387	*Procryptotermes leewardensis*	Kalotermitidae	7
Roe453	*Roisinitermes ebogensis*	Kalotermitidae	3
Md513	*Mastotermes darwiniensis*	Mastotermitidae	2
Cf509	*Coptotermes formosanus*	Rhinotermitidae	2
Pc512	*Prorhinotermes canalifrons*	Rhinotermitidae	3
Higher termites			
TD116	*Odontotermes sp.*	Termitidae	1

3.2.2 Phylogenomic analysis

A phylogenomic tree of all *Verrucomicrobiota* MAGs and selected reference genomes was built with the Genome Taxonomy Database Toolkit (GTDB-Tk, Chaumeil *et al.* 2020). The reference genomes included at least one genome per genus, ensuring a broad coverage of the phylum. The phylogenomic analysis revealed several lineages that solely consist of termite gut MAGs (MAG groups I–V, Fig. 12) with the exception of MAG group IV, which includes one MAG that was recovered from a cow rumen metagenome (UBA1183, Parks *et al*. 2017). Furthermore, six MAGs belong to the *Opitutales* family *Opitutaceae,* four MAGs belong to the verrucomicrobial order *Methylacidiphilales* and one MAG to the verrucomicrobial class *Lentisphaeria* (genus *Victivalles*). All the colored MAG groups represent an independent phylogenomic lineage. All MAG groups likely represent at least family-level lineages as revealed by Average nucleic acid identity (ANI) analysis and relative evolutionary distance (RED) analysis, both of which are included in the GTDB taxonomy. The original classification of the MAGs and the used *Opitutales* genomes predicted by GTDB can be found in the supplementary materials (Tab. S8).

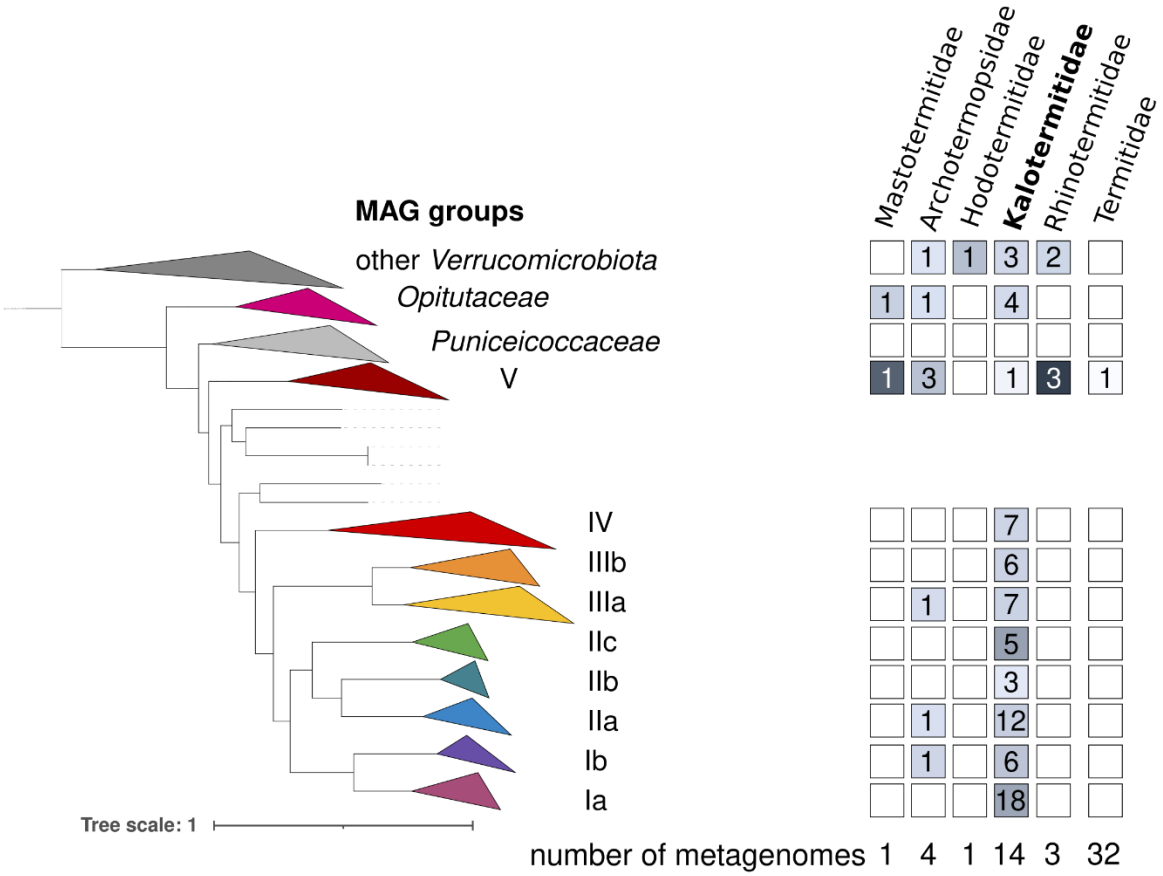

Figure 12: Phylogenomic classification of the *Verrucomicrobiota* MAGs recovered from gut metagenomes of different termite families. The phylogenomic analysis revealed nine different MAG groups (Group I–V) that fall into the order of *Opitutales*. MAG groups I–III and V solely consist of MAGs recovered from termite gut metagenomes, while MAG group IV includes one MAG recovered from cow rumen. Other *Opitutales* MAGs belong to MAG group V (dark red) and to the family *Opitutaceae* (purple) but none to the family *Puniceicoccaceae* (light grey). A few more MAGs belong other verrucomicrobial orders (dark grey). A selection of *Planctomycetota* genomes was used as outgroup (not shown). B) The most apical, termite-specific lineages (MAG group I–IV) were mostly recovered from Kalotermitidae metagenomes with the exception of a few MAGs from Archotermopsidae. The other groups are represented by more different termite families including one MAG from higher termites. The relative abundance of sequencing reads that were assigned to the different MAG groups per termite family is shown as a color gradient in the heatmap.

3.2.3 Distribution of the MAGs to the termite host metagenomes

The apical MAG groups I–IV consist of genomes from Archotermopsidae and mainly Kalotermitidae. The more basal groups MAG group V, *Opitutaceae* and also the non-*Opitutales Verrucomicrobiota* consist more evenly distributed of Mastotermitidae, Archotermopsidae, Kalotermitidae, Rhinotermitidae and Termitidae (subfam.: Macrotermitinae). The only MAG from higher termites (TD116_bin.50) belongs to MAG group V. No MAGs belong to the second *Opitutales* family *Puniceicoccaceae*. Other than

the restriction to Archotermopsidae and *Kalotermitidae*, no obvious pattern is visible in the distribution of the MAG hosts in the tree (Fig. S10).

3.2.4 Characteristics of MAGs

The genome size of the analyzed genomes varied between 1 Mbp and 5 Mbp (Fig. 13A). Within MAG groups I–IV, the genomes are much smaller (1–1.5 Mbp) than in MAG group V and the selected reference genomes (2.5–5 Mbp).

The analysis of the GC contents revealed that the apical groups with reduced genome sizes have a slightly lower GC content (40–55%) compared to more basal *Opitutales* and other *Verrucomicrobiota* (50–61%). A detailed overview of the characteristics of the MAGs can be found in the supplementary materials (Tab. S7).

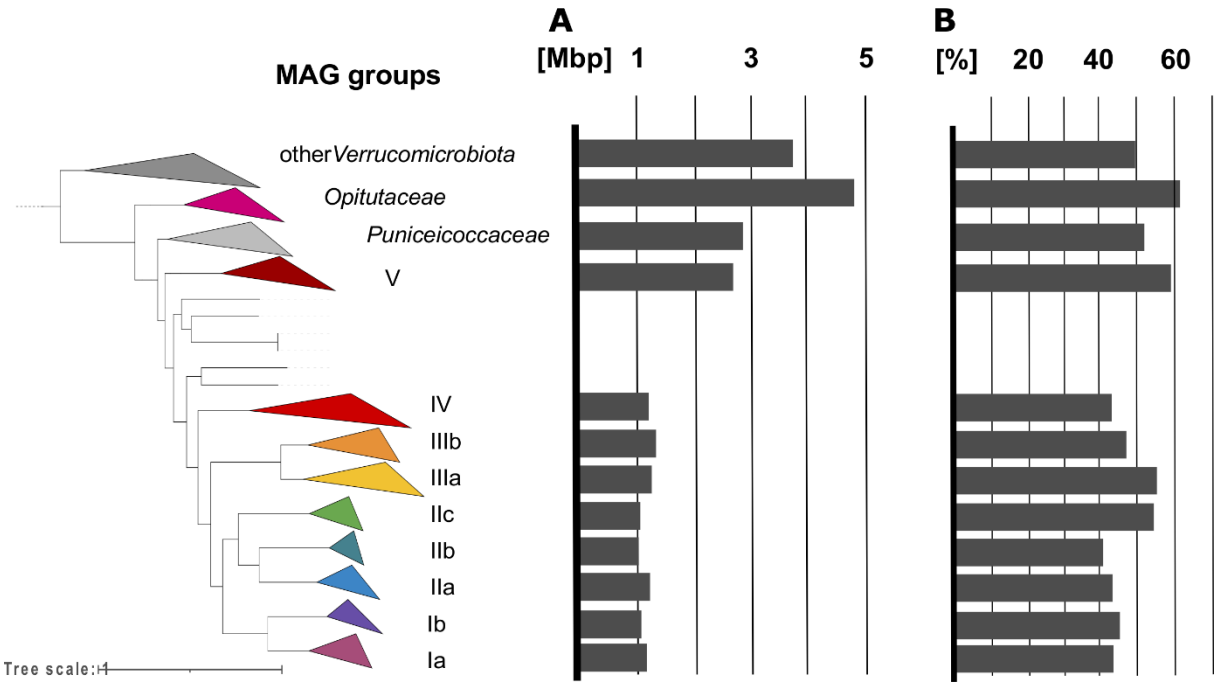

Figure 13: Genome characteristics of the *Verrucomicrobiota* MAGs. A) The average genome size of the apical MAG groups I–IV is between 1 and 1.5 Mbp. The genome sizes of MAG group V, the selected *Opitutaceae* and *Puniceicoccaceae* genomes and the other selected *Verrucomicrobiota* genomes varies between 2.5 and 5 Mbp. The genome sizes were corrected by the completeness of the MAGs. B) The GC contents of the apical groups are between 40 and 55% while the GC contents of the basal groups is between 50 and 61%.

3.2.5 Phylogenetic analysis of the MAGs.

Extracted 16S rRNA genes of the MAGs were analyzed by adding them to the Dictyoptera database (DictDb4, Mikaelyan *et al*. 2015b). Only 38 of 77 MAGs that belong to MAG groups I–V included a 16S rRNA gene and were included in the phylogenetic analysis. Additionally, three 16S rRNA genes of low-quality MAGs were included. Except MAG group IV and MAG group IIa, none of the groups solely consist of sequences from MAGs

(Fig. 14). Sequences from clone libraries of termite gut homogenates and flagellate suspensions are often closely related to the MAGs. Sequences of the intra-nuclear symbionts of *Trichonympha agilis*, *Candidatus* Nucleococcus kirbyi and *Candidatus* Nucleococcus trichonymphae, fall into the range of MAG group II. The 16S rRNA genes of the recently described Ciliate endosymbionts with highly-reduced genomes, *Candidatus* Pinguicoccus supinus and *Candidatus* Organicella extenuata, are not closely related to the MAG groups and are more closely related to other uncultured *Opitutales* clones.

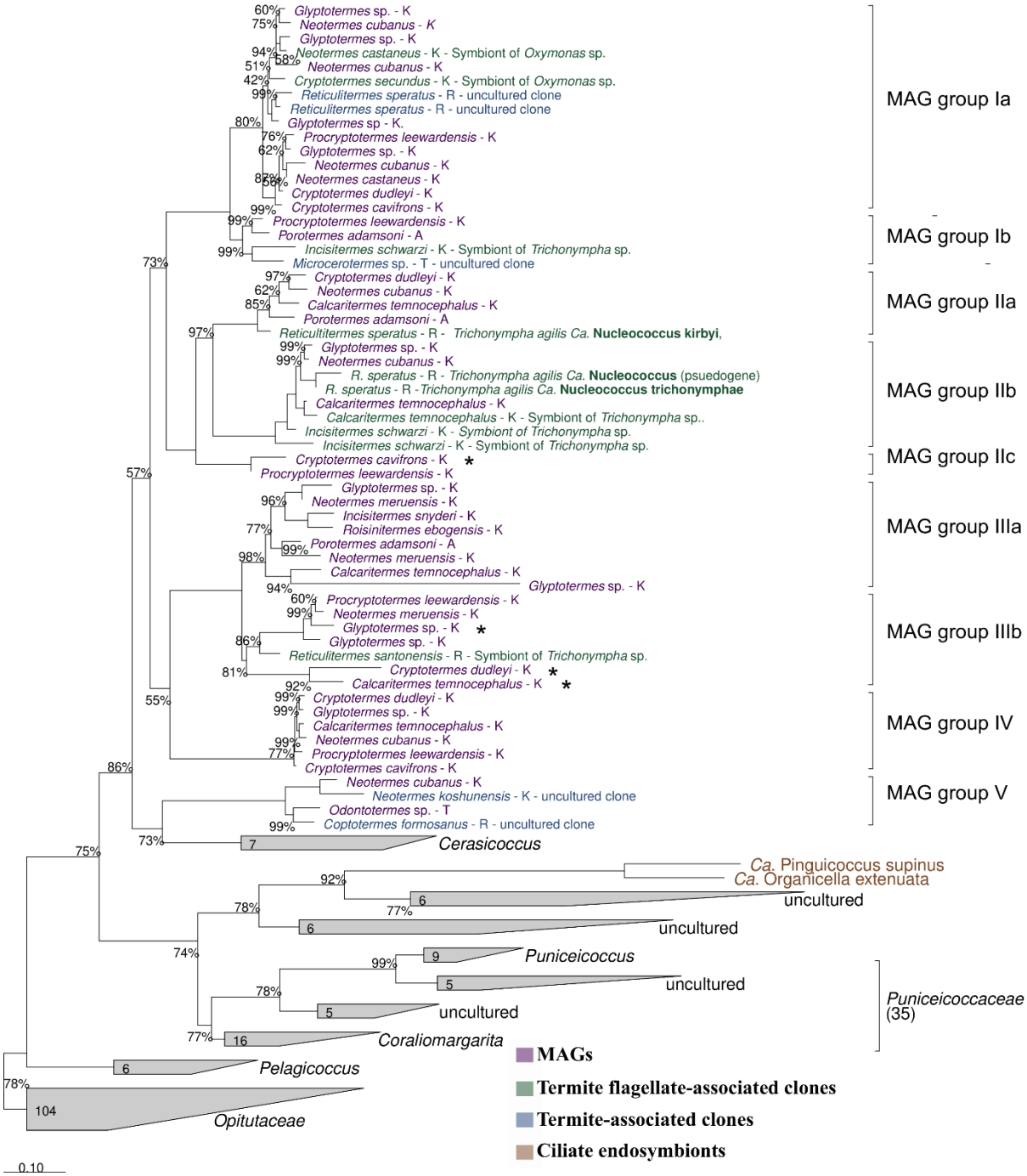

Figure 14: Phylogenetic analysis of *Opitutales* 16S rRNA genes. The MAG groups that were assigned in the phylogenomic analysis can be found again in the phylogenetic analysis of the 16S rRNA gene. The position of the MAGs (purple) among several sequences from termites (blue) and their symbiotic flagellates (green) are shown. The labels indicate the termite host of the MAGs and the other clones. The respective termite families Kalotermitidae (K), Rhinotermitidae (R), Archotermopsidae (A) and Termitidae (T) are encoded in the labels. Sequences of recently published endosymbionts of aquatic ciliates with ultra-reduced genomes were also added to the analysis (brown). Nodes that show sequences from low-quality MAGs (<50% completeness, >10% contamination) and unbinned sequences are labeled with an asterix.

3.2.6 Localization of *Opitutales* MAGs in the termite gut

Whole gut homogenates and flagellate suspensions of available termite workers were used as samples for visualization of and localization of *Opitutales* symbionts. Signals of *Opitutales* were found in several different flagellates of different termites that were available, and that yielded MAGs. *Opitutales* signal was found in FISH samples prepared with flagellate suspensions of *Cryptotermes havilandi* (Ch595, Fig. 15AB), *Coptotermes formosanus* (Cf555, Fig. 15D) and *Reticulitermes lucifugus* (Rl597, Fig. 15C) as well as other termites that were not included in the figure. The flagellates were identified based on morphology and compared to literature about termites and their flagellates (e.g.: Yamin 1979). *Stephanonympha*-like flagellates and *Devescovina*-like flagellates were identified in preparations of *Cryptotermes havilandi* (Fig. 15B). The *Opitutales* signal was detected in both cell types, but not all cells have the signal, at least not to the same extend. The strong EUB1 signal between the cells is likely caused by autofluorescence of wood particles left in the sample. The signal of the general bacteria probe and the *Opitutales*-specific probe are not entirely overlapping. A closer look to the *Stephanonympha*-like cells, identified by the round shape and the numerous nuclei, discloses a distribution of the *Opitutales* signal over the whole cell (Fig. 15A). A co-localization with the nuclei was not observed. (*Spiro*)-*Trichonympha*-like and *Microjoenia*-like cells were found in preparations of *Reticulitermes lucifugus* (Fig. 15C). In this case, the round-shaped *Opitutales* signals were restricted to the bigger *Trichonympha*-like cell while the EUB1 signal was more prominent in the smaller cells. In *Coptotermes formosanus*, a termite with no MAGs in MAG groups I–IV, not *Opitutales* signal was found in the *Pseudotrichonympha*-like flagellates and other flagellates (Fig. 15D).

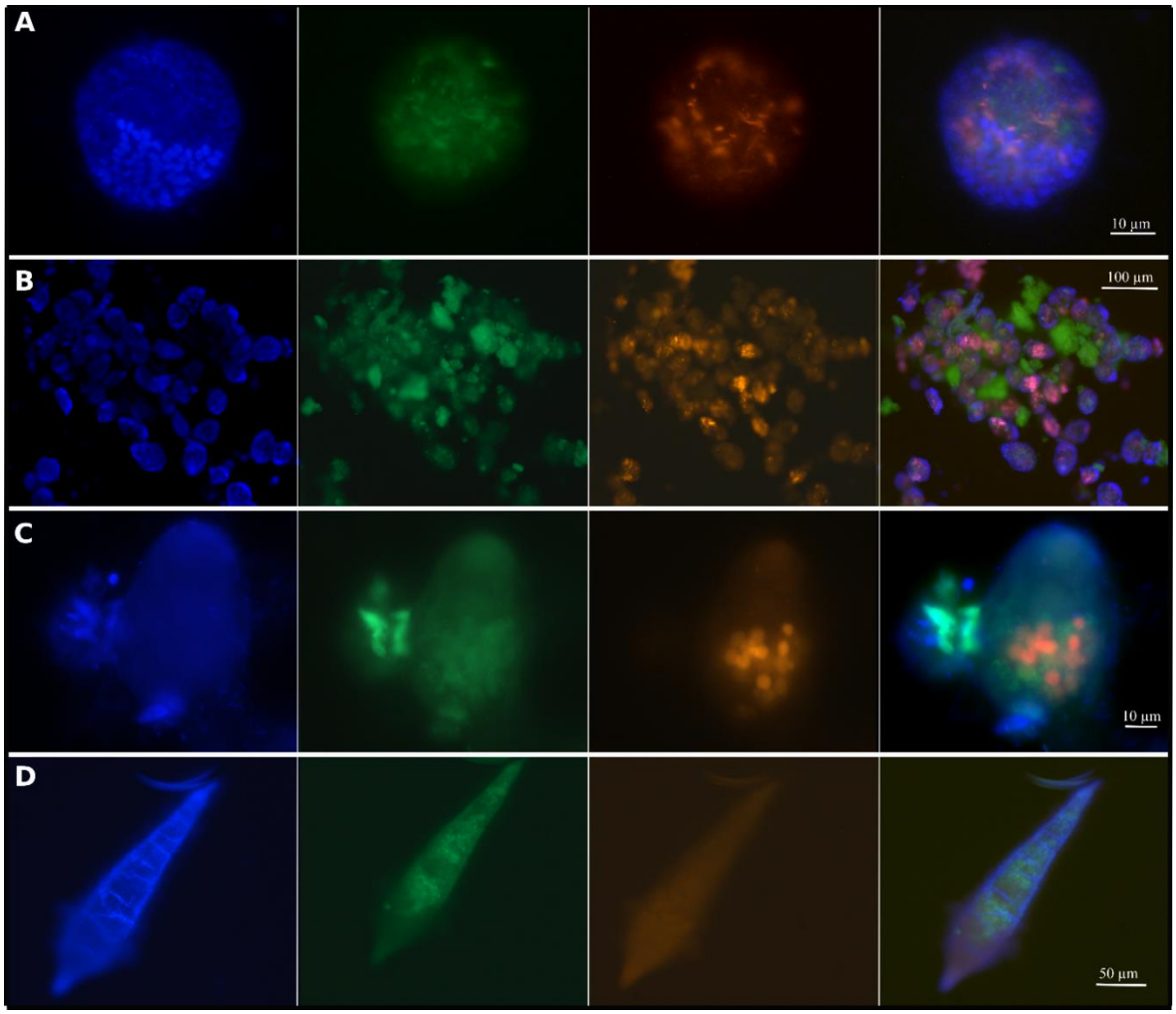

Figure 15: Localization of *Opitutales* symbionts with fluorescence *in-situ* hybridization (FISH). All samples were hybridized for 4–6 h at 20% formamide. The first column includes DAPI images. The second column includes the signal of fluorescein-labeled probe EUB1, a general Bacteria probe that is discriminating some *Verrucomicrobiota* and *Planctomycetota*. The signal of an *Opitutales*-specific probes, labeled with Cy3 is included in the third column. Finally, the last column includes merged images of the first three columns. The samples were prepared from flagellate suspension from A,B) *Cryptotermes havilandi* (Ch595), C) *Reticulitermes lucifugus* (Rl597) and D) *Coptotermes formosanus* (Cf555).

3.3 Functional analysis of the *Opitutales* MAGs

3.3.1 Central carbon metabolism

A first overview about the functional capacity was gained by checking the composition of the central metabolism (Fig. 16). The typical enzymes that are part of glycolysis are only partly present. No PTS system was found in all MAG groups. A number of multi-facilitator transporters (MFS) was found in the MAGs, however, no direct identification as glucose transporters was possible. The first step of glycolysis, the activation of glucose, is catalyzed by hexokinase. A hexokinase was detected in members of *Opitutaceae* and other *Opitutales* like *Coraliomargarita akajimensis* but not in all MAG groups. A similar pattern was found for fructose-1,6-bisphosphate aldolase, an enzyme catalyzing the reversible splitting of fructose-1,6-bisphosphate to dihydroxyacetone phosphate (DHAP) and glyceraldehyde 3-phosphate (G3P). The final step of glycolysis, the transfer of a phosphate group from phosphoenolpyruvate to ADP is catalyzed by pyruvate kinase, which was not found in the MAGs but is present in *Opitutaceae* and some other *Opitutales* genomes. An enzyme catalyzing the same reaction, pyruvate phosphate dikinase, was found in all investigated genomes. The pyruvate:ferredoxin oxidoreductase is connecting glycolysis to the TCA cycle via acetyl-CoA and is present in most investigated genomes. The TCA cycle is almost completely absent in MAG groups I–IV (reduced genome sizes) but present in MAG group V, *Opitutaceae* and other *Opitutales*.

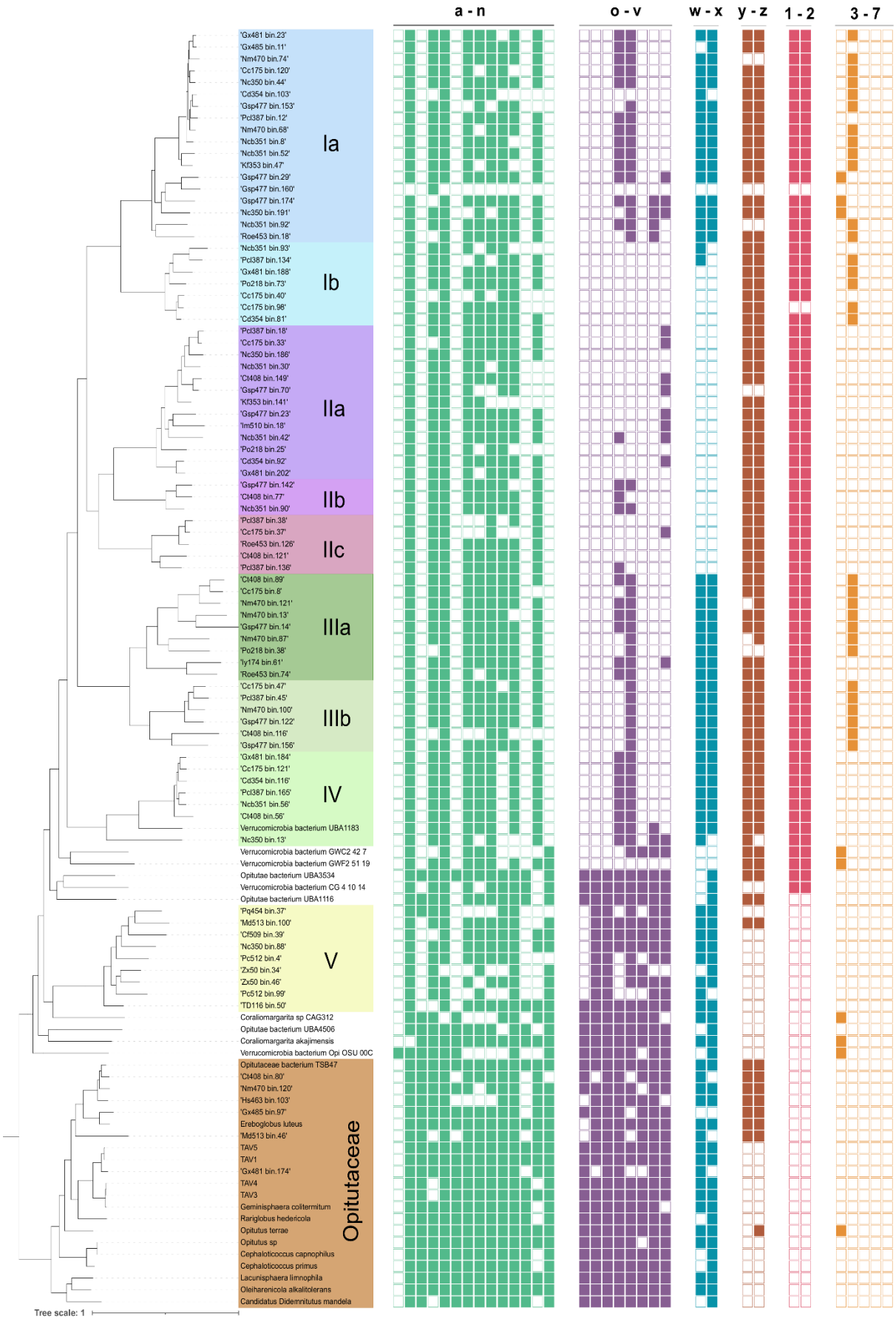

a: Glucose PTS system, **b**: MFS transporter, **c**: Hexokinase, **d**: Glucose-6-phosphate isomerase, **e**: Phosphofructokinase, **f**: Fructose-1,6-bisphosphate, **g**: Triose isomerase, **h**: Glycerol-3-phosphate dehydrogenase, **i**: Phosphoglyerol kinase, **j**: Phosphoglucomutase, **k**: Enolase, **l**: Pyruvate kinase, **m**: Pyruvate:ferredoxin oxidoreductase, **n**: PEP carbo **o**: Pyruvate dehydrogenase, **p**: citrate synthase, **q**: Acconitase, **r**: 2-Oxoglutarate dehydrogenase, **s**: Succinyl-CoA synthetase, **t**: Succinate dehydrogenase, **u**: Fumarase **v**: Malate dehydrogenase, **w**: Acetate:succinate CoA transferase, **x**: Succinyl-CoA synthetase, **y**: OPA transporter model 1, **z**: OPA transporter model 2, **1**: Nucleotide transporter **2**: Nucleotide transporter model 2, **3**: [FeFe] hydrogenase - A, **4**: [FeFe] hydrogenase - B, **5**: [FeFe] hydrogenase - C, **6**: [Fe] hydrogenase, **7**: [NiFe] hydrogenase

Figure 16: Central metabolism of *Opitutales*. Glycolysis (green) is only partly complete in MAG groups I–V and complete in *Opituaceae*. The genes/complexes absent in MAG groups I–V are a glucose PTS system, hexokinase, fructose-1,6-bisphosphate aldolase and pyruvate kinase. Most enzymes that consist the TCA cycle (purple) are absent in MAG groups I–IV but are present in more basal genomes. Exceptions are 2-oxo-glutarate dehydrogenase and succinyl-CoA synthetase which were found in MAG groups I, III and IV. ATP production via acetate succinate CoA transferase (ASCT) and succinyl CoA synthetase (blue) is possible in MAG groups Ia and III–V. A transporter for phosphosugars (brown) was found only in MAG groups I–IV and one branch of *Opitutaceae*. Nucleotide transporters (red) were found in MAG groups I–IV. Group B [FeFe] hydrogenases (orange) were found in MAG groups I and III.

3.3.2 Sugar phosphate transporters

An uptake system for sugar phosphates was found in MAG groups I–IV, aquatic metagenomes and a few insect gut-related *Opitutaceae* using two different models (Fig. 16). The transporters were not found in MAG group V and the remaining *Opitutaceae*. BLAST searches revealed that the transporters of the MAGs are not directly derived from the ones in *Opitutaceae* but more closely related to transporters of *Rickettsia prowazekii*. A phylogenetic analysis of characterized transporters and transporters from termite gut metagenomes showed that they are closest related to transporters of uncultured *Paracedibacterales* (candidate family UBA11393) from the termite gut (Fig. 17). No characterized transporters are closely related. The phylogeny of the sugar phosphate transporters of the MAGs reflects the phylogeny of the MAGs themselves.

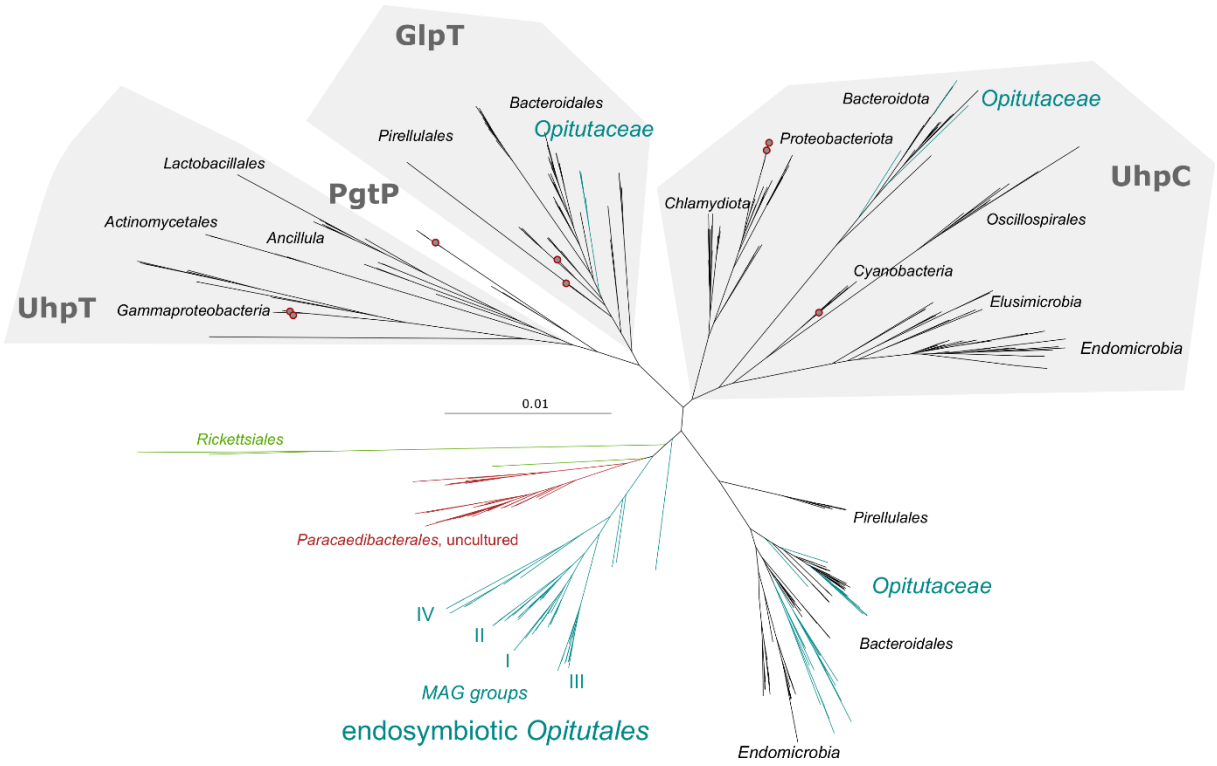

Figure 17: Maximum-likelihood tree of the sugar phosphate transporters of *Opitutales*. Sugar phosphate transporters of the *Opitutales* MAGs (dark green) were closest related to transporters of uncultured *Paracedibacterales* (red) from the termite gut and *Rickettsiales* (light green). Characterized transporters (red dots) are only distantly related to homologs of endosymbiotic *Opitutales*. The colored areas mark the different transporters (UhpT: hexose-6-phosphate transporter, UhpC: Glucose-6-phosphate transporter, GlpT: Glycerol-3-phosphate transporter, PgtP: 3-phosphate transporter). Tree and analysis by Tom Kropp; adapted.

3.3.3 Further carbon metabolism

Genes for glycogen degradation and biosynthesis were found in all investigated *Opitutales* MAGs. The only exception is an amylase, or an alternative glycogen hydrolyzing enzyme which was not found in any of the genomes.

The only phosphoenolpyruvate (PEP) utilizing enzyme found in MAG groups I–V was pyruvate phosphate dikinase. Pyruvate kinase was only found in *Opitutaceae* and other basal *Opitutales*. Other PEP-utilizing enzymes like PEP carboxylase and PEP carboxykinase were not found in any of the investigated genomes.

Acetyl-CoA is a central metabolite that is involved in many pathways. Genes for the acetyl-CoA utilizing enzymes acetate kinase, acetyl-CoA ligase and acetyl-CoA hydrolase were not found in any of the investigated genomes. Only acetate kinase was found in some *Opitutaceae*. An acetate succinate CoA transferase was found in all genomes except MAG

groups Ib and II. Furthermore, acetyl-CoA is the precursor of fatty acid biosynthesis. The first step, catalyzed by Acetyl-CoA carboxylase, as well as all further steps of fatty acid biosynthesis were found in all investigated genomes. Also, the genes required for peptidoglycan biosynthesis starting from fructose-6-phosphate were found in all investigated genomes.

Alternatives to the Embden-Meyerhof-Parnas pathway are absent or incomplete. The pentose phosphate pathway is lacking among other genes the phosphogluconate dehydrogenase while the Entner-Doudoroff pathway is lacking several enzymes including the key enzyme 2-keto-deoxy-6-phosphogluconate (KDPG) aldolase. Also, the phosphoketolase pathway as an alternative bypass of fructose-1,6-bisphosphate aldolase is absent in all MAGs.

Several further potential features were investigated using HMM searches. A wide-spread feature of members of the PVC superphylum, compartmentalization was investigated by searching for bacterial microcompartment (BMC) shell proteins BMC-P and BMC-H. Both were not present in all MAG groups but were found in certain *Opitutaceae* and MAGs, related to *Methylacidiphilales*.

3.3.4 Nucleotide transporters

Nucleotide transport proteins (NTTs) were found in MAG groups I–IV and four other MAGs recovered from mainly ground water metagenomic data that are basal to MAG group IV. All other investigated genomes are lacking NTTs (Fig. 16). Two different models were used to find the NTTs are yielded the same result. Two separate MAGs were found to not include NTTs. A phylogenetic analysis of the *Opitutales* NTTs, further NTTs from termite gut metagenomes and several characterized NTTs shows that NTTs from *Opitutales* are deep-branching in not in close relation to NTTs from other groups (Fig. 18). No characterized transporter falls within the radiation of *Opitutales*.

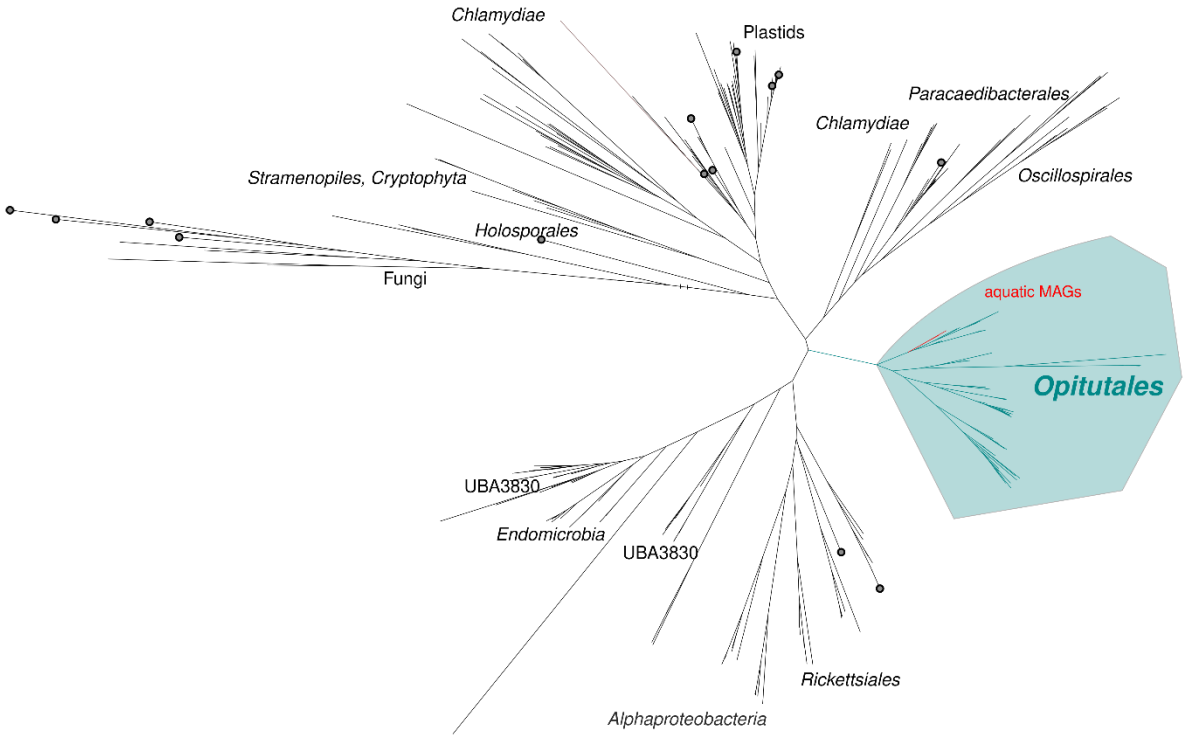

Figure 18: Phylogenetic analysis of nucleotide transporters (NTTs) of *Opitutales*. The tree includes transporters from *Opitutales* (green), other termite gut MAGs and several characterized transporters (grey dots). NTTs of MAGs from aquatic environments basal to the termite gut MAG groups I–IV are shown in red. The tree was generated by Undine Mies and adapted.

3.3.5 Hydrogenases

Hydrogenases were found in MAG groups I and III but were absent in all other MAG groups. With exception of MAG group IV, hydrogenases are present in the same MAG groups that retained ASCT and SCS (Fig. 16). Classification using the web tool of the hydrogenase database (HydDB, Søndergaard *et al.* 2016) revealed that most hydrogenases of *Opitutales* were [FeFe] hydrogenases of group B and only a few hydrogenases of *Opitutaceae* classified as [FeFe] hydrogenases of group A. A phylogenetic analysis with all MAG-derived hydrogenases of *Opitutales* and all classified hydrogenases of HydDB supports the web tool classification (Fig. 19). Other hydrogenases like [NiFe] hydrogenases or [Fe] hydrogenases were not found.

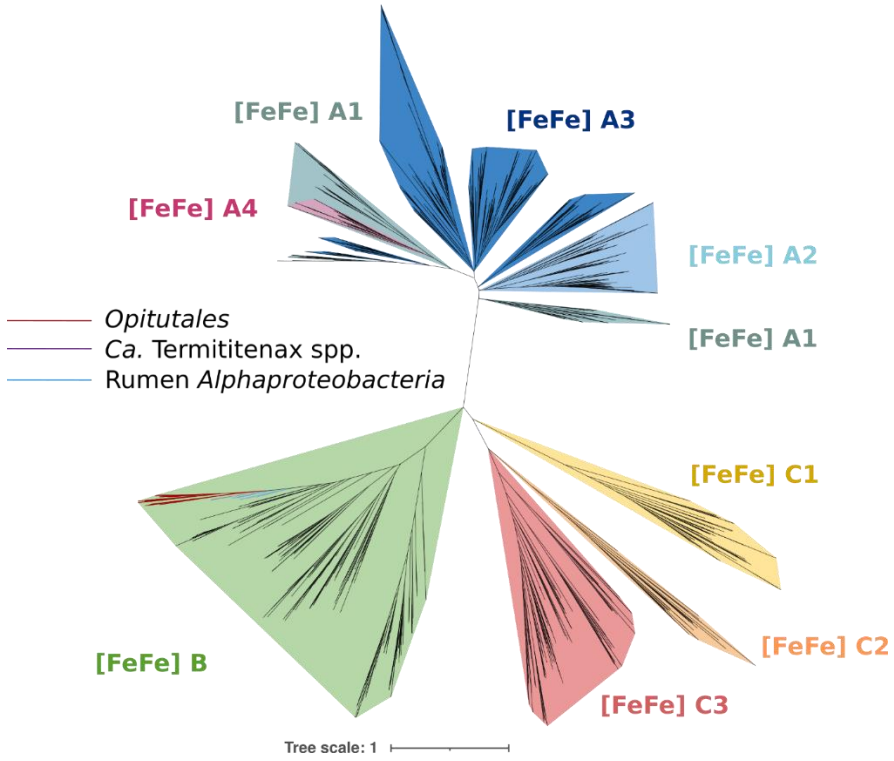

Figure 19: Maximum-likelihood tree of [FeFe] hydrogenases. The tree includes hydrogenases of the *Opitutales* MAGs and over 1228 classified [FeFe] hydrogenases retrieved from the hydrogenase database (HydDB, Søndergaard *et al.* 2016). The different hydrogenase groups are marked with different colors. *Opitutales* hydrogenases (red branches) belong to group B of [FeFe] hydrogenases and are most closely related to *Candidatus* Termititenax spp. (purple branches) and rumen-associated *Alphaproteobacteria* (blue branches).

Blast searches revealed that the closest relatives of *Opitutales* [FeFe] hydrogenases of group B are hydrogenases from rumen-associated *Alphaproteobacteria* (Xie *et al.* 2021) and from *Margulisbacteriota* (*Candidatus* Termititenax spp.)that are attached to *Spirochaetota* ectosymbionts of termite gut flagellates (Utami *et al.* 2019).

3.3.6 Oxygen relationship of *Opitutales* MAGs

Further HMMR searches revealed that MAG groups I–IV are completely lacking a respiratory chain including NADH oxidoreductase, succinate dehydrogenase, cytochrome *c* reductase, and all types of terminal oxidases (Fig. 20). Complete respiratory chains were found in genomes of MAG group V, *Opitutaceae* and other *Opitutales*. These included several sets of terminal oxidases of the bd-type, *cbb*$_3$-type and *bo*$_3$-type. Defense mechanisms against reactive oxygen species (ROS) like hydrogen peroxide or superoxide groups were not found in the apical MAG groups I–IV. Catalases were absent in almost all genomes that were investigated. The presence of superoxide dismutases was limited to the FeMn type. The respective genes were found most basal genomes and only a few MAGs from groups I–IV. The NADH:rubredoxin system that is used as oxygen defense mechanism was only found in *Opitutales* and MAG group V but absent in the more apical groups.

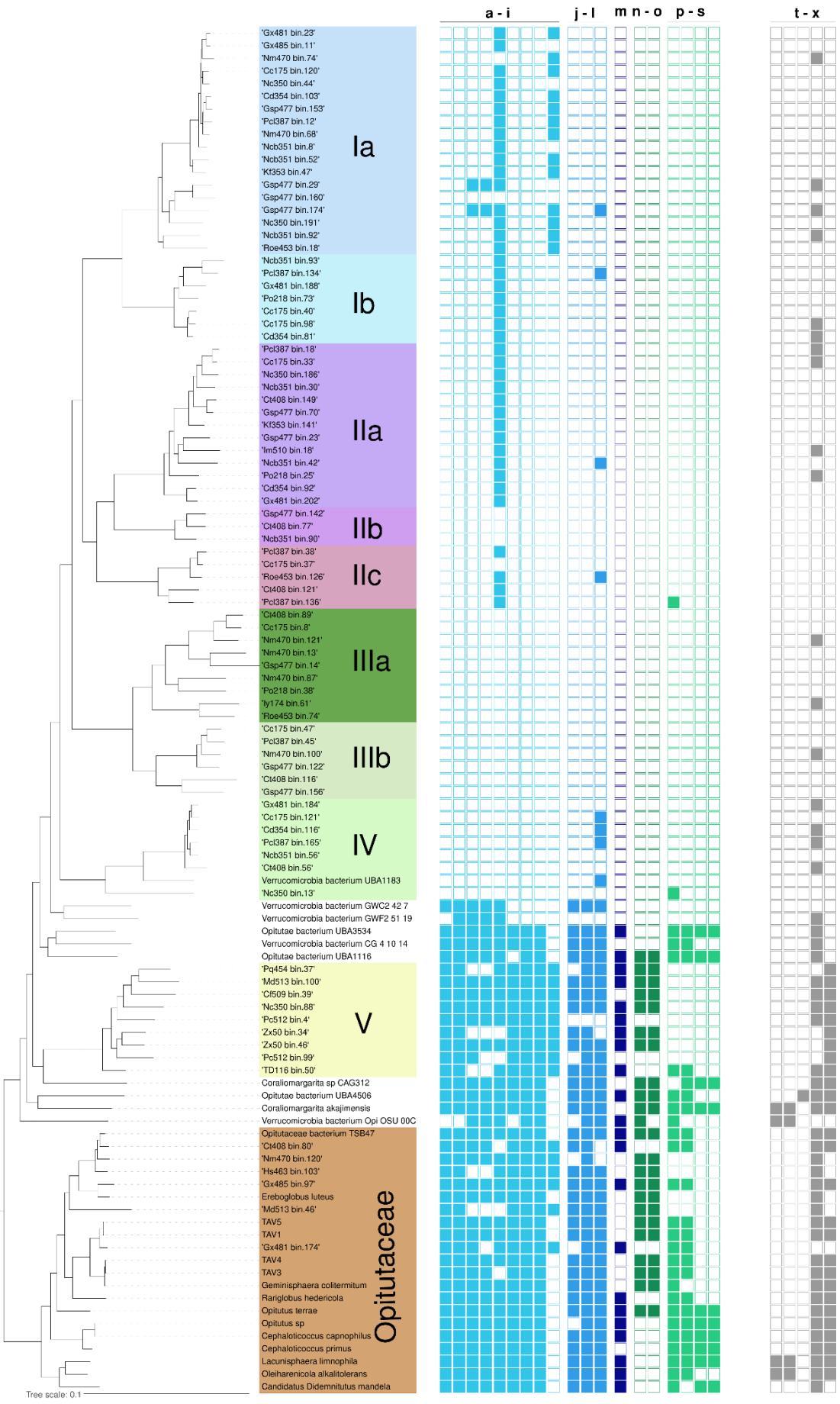

a: nuoC, **b**: nuoB, **c**: nuoE, **d**: nuoF, **e**: nuoG, **f**: nuoK, **g**: nuoL, **h**: nuoM, **i**: nuoN, **j**: sdhC, **k**: sdhA, **l**: sdhB, **m**: Cytochrome bc_1 complex, **n**: cydA, **o**: cydB, **p**: ccoN, **q**: ccoO, **r**: cyoB, **s**: cyoA, **t**: Catalase model 1, **u**: Catalase model 2, **v**: Superoxide dismutase (CuZn), **w**: Superoxide dismutase (FeMn), **x**: NADH:rubredoxin oxidoreductase

Figure 20: Oxygen relationship of *Opitutales*. The apical MAG groups I–IV are lacking a NADH oxidoreductase (complex I, turquoise), succinate dehydrogenase (complex II, light blue), cytochrome *c* reductase (complex III, dark blue) and any terminal oxidases (complex IV, dark green and light green). All more basal genomes have complete respiratory chain with a combination of *bd* oxidase and heme copper oxidases. No investigated genomes have a catalase as defense mechanism for reactive oxygen species. A superoxide dismutase (FeMn type) was found in most *Opitutaceae* and MAG group V and in a few members of the apical MAG groups (I–IV). An NADH:rubredoxin oxidoreductase complex was found in most of the basal genomes from *Opitutaceae* and MAG group V.

3.3.7 Cell maintenance

All MAGs contained genes for the proteins involved in essential processes like transcription (*rpoABCD*), protein folding and stability (*groLS*, *dnaK*), tRNA modification (*mnmAEG*), replication (*dnaEQ*), ribosomal proteins and enzymes involved in translation.

3.3.8 Amino acid biosynthesis and uptake

Complete pathways for the biosynthesis of amino acids were searched using HMMER. The results were visualized in a presence/absence map (Fig. 21). Amino acids derived from phosphoenolpyruvate, and 2-oxo-glutarate are absent in all MAGs with reduced genomes (MAG groups I–IV). Furthermore, only the genes for biosynthesis of glycine from serine, for the transamination of alanine from pyruvate and for the biosynthesis of aspartate and asparagine from oxaloacetate were present in most MAGs. All amino acid biosynthesis pathways were complete in the basal genome of MAG group V, *Opitutaceae* and other *Opitutales* genomes.

Amino acid transporters were found in most investigated genomes, including all MAGs of MAG groups I–IV. Many Hidden Markov Models (HMMs) found multiple transporters, whose identification and substrate prediction were not possible. The identified transporters included LeuT, a transporter for hydrophobic amino acids, ArcD, a transporter for basic amino acids and more unspecific transporters.

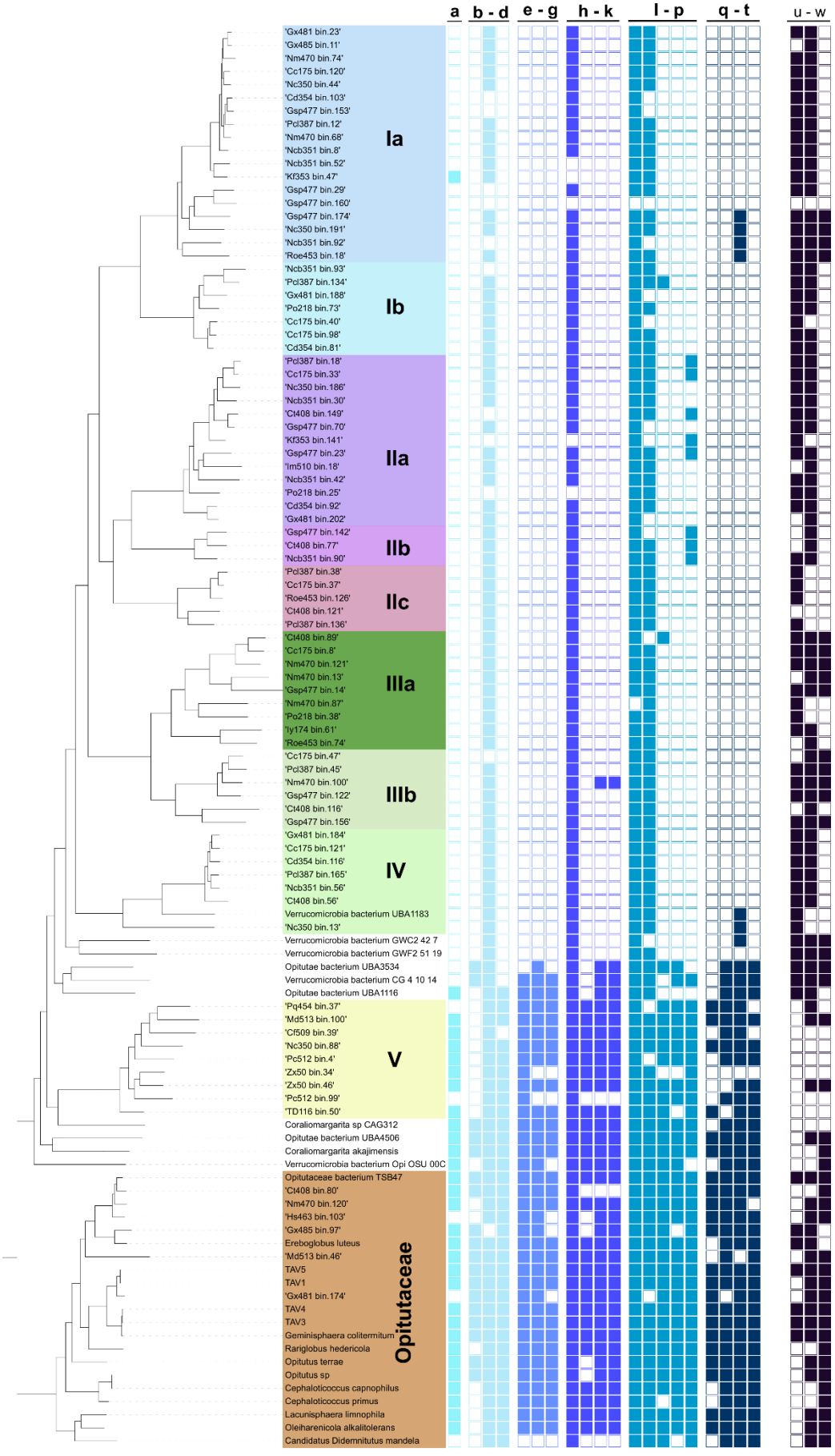

a: Histidine, **b**: Serine, **c**: Glycine, **d**: Cystein, **e**: Tryptophane, **f**: Phenylalanine, **g**: Tyrosine, **h**: Alanine, **i**: Valine, **j**: Leucine, **k**: Isolleucine, **l**: Aspartate, **m**: Asparagine, **n**: Methionine, **o**: Threonine, **p**: Lysine, **q**: Glutamate, **r**: Glutamine, **s**: Arginine, **t**: Proline, **u**: LeuT, **v**: MFS, **w**: ArcD

Figure 21: Amino acid metabolism of *Opitutales*. The presence-absence map of the amino acid biosynthesis pathways (blue shades) is sorted by the typical starting point of the biosynthesis in the central carbon metabolism. With exception of glycine, alanine, aspartate and asparagine, all amino acid biosynthesis pathways are absent or highly incomplete in the MAG groups I–IV. MAG group V, *Opitutaceae* and other *Opitutales* encode for all pathways. Different types of amino acid transporters were found in some MAGs and the other genomes (black). These include muli-fascilitator transporters (MFS), a transporter for hydrophobic amino acids (LeuT) and a transporter for basic amino acids (ArcD).

3.3.9 Protein segregation systems

All MAGs and investigated genomes were searched for protein segregation systems. All subunits of the Sec system, including the binding subunits SecA and SecB and the tunnel subunits SecYEG were found in all investigated genomes including the MAGs with reduced genomes. Additionally, the signal recognition particle (SRP) receptor FtsY was found in all genomes. Another protein translocations system, the twin arginine translocation (TAT) including all subunits TatABC was found in all non-reduced genomes but was absent in MAG groups I–IV.

4 DISCUSSION

4.1 Phylogenomic analysis of *Opitutaceae*

The phylogenomic analysis of *Opitutaceae* (Fig. 5) shows a distinct separation to other *Verrucomicrobiota* and other members of the PVC superphylum. *Opitutaceae* comprise eight different genera of described species and even more genera that consist of uncultivated members. Some genera and species require re-classification. The most basal *Opitutaceae*, *Oleiharenicola alkalitolerans* and *Lacunisphaera* spp. were isolated from aquatic environments. The genome-based taxonomy of GTDB re-classified O*leiharenicola alkalitolerans* as a species within the genus *Lacunisphaera* (Parks *et al.* 2018). The genome assembly of *Opitutus* sp. 57933 (IMG ID: 57933, assembly from *Cephalotes* sp. ant gut) forms a group with the other ant gut symbionts *Cephaloticoccus capnophilus* and *Cephaloticoccus primus*. Analysis of the average nucleotide identity (ANI) and relative evolutionary divergence (RED-value) revealed that all three genomes belong to the same genus, suggesting to rename *Opitutus sp.* 57933 to be a member of the genus *Cephaloticoccus*. Similarly, the *Opitutaceae* strain TSB47, whose closest relative is *Ereboglobus luteus*, should be classified a member of the genus *Ereboglobus*. Both of these results were also in agreement with the re-classification in GTDB. The TAV strains (TAV1–5), including *Geminisphaera colitermitum* (TAV2) are the youngest group of *Opitutaceae*. Again, in agreement with GTDB classification, ANI-analysis suggest that all TAV strains are members of the same genus (*Geminisphaera*) but only two different species (species boundary = 95% ANI, Jain *et al*. 2018). Generally, the phylogenomic tree follows an evolution from free-living to host-associated lifestyle within *Opitutaceae*, suggesting that the ancestor of *Opitutaceae* was free-living.

4.2 The oxygen relationship of *Opitutaceae*

4.2.1 Cultivation of *Opitutaceae*

Routine cultivation of the three investigated strains *Ereboglobus luteus*, *Opitutus terrae* and *Geminisphaera colitermitum* was performed in non-reduced medium under a N_2/CO_2 headspace. Complete reduction of the medium was observed by color change of resazurin in the medium and was achieved by all three strains. Growth continued after the medium was reduced, suggesting a fermentative metabolism. All three strains grew in the presence of oxygen up to 1%, while *G. colitermitum* and *O. terrae* also grew under atmospheric oxygen. These results are in agreement with Tegtmeier *et al*. 2018, confirming their hypothesis that the original description of *O. terrae* as an anaerobe (Chin *et al.* 2001) and *G. colitermitum*

as an obligate aerobe (Wertz *et al.* 2018) are incorrect. (Micro)-aerobic respiration was ensured by growth on acetate which was observed in all three strains, similar to the results of Tegtmeier *et al.* 2018, who also confirmed respiratory metabolism by HPLC analysis of the metabolic intermediates.

4.2.2 Respiratory chains *Opitutaceae*

Bacterial electron transport chains (ETCs) can come in multiple different flavors, allowing them to switch between different aerobic (Arai 2011) – but also between aerobic and anerobic respiratory pathways (Chen and Strous 2013). Aerobic ETCs often contain different terminal oxidases that allow adaptation to changing oxygen conditions (e.g.: Cotter and Gunsalus 1992, Arai 2011). All *Opitutaceae* strains encode a complete aerobic respiratory chain, including differential terminal oxidases. Interestingly, a common feature of all *Opitutaceae* and even most *Verrucomicrobiota* and *Chlamydiota* reference genomes was the lack of a bc_1 complex (complex III). However, with the exception of *Ereboglobus luteus*, this complex is functionally replaced by the alternative complex III (ACIII, Refojo *et al.* 2012). These findings are in agreement with other studies of *Verrucomicrobiota* (Kruse *et al.* 2019; Awala *et al.* 2021) and *Opitutaceae* members (Tegtmeier *et al.* 2018). The absence of ACIII in *E. luteus* can be explained by the fact that its only oxidase (*bd* oxidase) is a quinole oxidase, hence, rendering a cytochrome *c* reductase unnecessary. In the case, of *Geminisphaera colitermitum*, Wertz *et al.* reported the absence of the bc_1 complex and the missing link from the quinole pool to the cbb_3-type cytochrome *c* oxidase (Wertz *et al.* 2018). My results show that this missing link is most likely fulfilled by the alternative complex III. The basal aerobic respiratory chain of *Opitutaceae* consists of a NADH oxidoreductase (complex I), a succinate dehydrogenase (complex II), an alternative complex III (complex III), an ATP synthase (complex V) and a differential set of terminal oxidases (complex IV). Three main types of oxidases were found in our analysis (Fig. 5) including two heme-copper oxidases (bo_3 oxidase and cbb_3 oxidase) and the *bd*-type quinole oxidase. Other subtypes of A-type HCOs, B-type HCOs and also the related nitric oxide reductases (NOR) were not found within *Opitutaceae* and are likely absent in all *Verrucomicrobiota* (Fig. 7).

The *bd* oxidase is absent in the basal *Opitutaceae* groups including *Cephaloticoccus*- and *Lacunisphaera* species, whereas the apical groups all contain a *bd* oxidase. Phylogenetic analysis of the *bd* oxidases revealed two phylogenetic origins of the *bd* oxidase in *Opitutaceae* (Fig. 6). The *bd* oxidase of the soil-inhabiting *Opitutus terrae* and closely related uncultivated *Opitutaceae* are closely related to oxidases of members of the PVC

superphylum, suggesting vertical transmission. On the other hand, oxidases of the apical group, consisting of most host-associated *Opitutaceae* and the fresh-water inhabiting *Nibricoccus aquaticus*, are most closely related to oxidases of *Bacteriodota*, suggesting a horizontal transmission of the oxidase genes from the environment. These findings suggest an initial loss of the bd oxidase in *Opitutaceae* and a potential re-acquisition of the oxidase within their host-associated environments. A *bd* oxidase was also found in *Geminisphaera colitermitum* and the related TAV strains, however it was not detected in the report by Wertz *et al.* 2018.

The bo_3-type heme copper oxidase is a low-affinity oxidase that was well characterized in the model organism *Escherichia coli* (Lemieux *et al.* 1992; Schulz and Chan 1998). The catalytic subunit *cyoB* is related to other heme copper oxidases, especially to A-type HCOs like the aa_3 oxidase (*coxA*). Hence, the identification of the exact variant of A-type HCOs can be difficult. Within *Opitutaceae*, the bo_3 oxidase was found in all members except *Ereboglobus luteus*, *Geminisphaera colitermitum* as well as the strains TAV3 and TAV4 that likely are the same species than *G. colitermitum* (Fig. 5). Besides their phylogenetic position (Fig. 7), further characteristics support the identification as bo_3 oxidases. While the aa_3 oxidase consists of four subunits (CoxABCD), the bo_3 oxidase consists of five subunits (CyoABCDE). The *cyoE* gene is encoding for the protoheme IX farnesyltransferase, an enzyme responsible for the biosynthesis of heme *o* and therefore necessary for a functional bo_3 oxidase (Saiki *et al.* 1992). The *cyoE* genes was found in all respective *Opitutaceae* within close neighborhood to the other genes of the operon, supporting their identification as bo_3 oxidases. The genomes of *G. colitermitum*, TAV3 and TAV4 also contain a copy of the catalytic subunit CyoB (Fig. 7). However, there are no further subunits found in these genomes, suggesting a non-functional oxidase as indicated in Figure 5. These results confirm the reports of Wertz *et al.* 2018.

The third oxidase present in *Opitutaceae*, the cbb_3 oxidase belongs to the more distantly related C-type HCOs (Fig. 7). With exception of the cockroach gut symbiont *Ereboglobus luteus*, the cbb_3 oxidase was found in all so far described members of *Opitutaceae* (Fig. 5) confirming previous reports (Tegtmeier *et al.* 2018; Wertz *et al.* 2018). Phylogenetically, cbb_3 oxidases of *Opitutaceae* comprise two distinct groups. Both groups are related to other members of the PVC superphylum and were likely vertically transmitted. Interestingly, a few species including *Geminisphaera colitermitum* contain two copies of the cbb_3 oxidase, a phenomenon that was previously described in *Pseudomonas* species (Comolli and

Donohue 2004), where one copy is used at low oxygen conditions while the other is constitutively expressed (Arai 2011). The *cbb*$_3$ oxidase consist of up to four subunits (CcoNOPQ), however, only the subunits CcoNOP are required or oxygen reduction activity (Zufferey *et al.* 1996), while CcoQ was reported to be involved in complex stabilization in *Pseudomonas spp*. (Kohlstaedt *et al.* 2017). Subunit CcoQ is generally absent in *Opitutaceae*. One copy of the *cbb*$_3$ oxidase of *G. colitermitum* shows a gene fusion of the subunits CcoNO, however, like in all other *Opitutaceae*, there is no subunit CcoP in the direct neighborhood of this CcoNO, suggesting that this copy of the *cbb*$_3$ oxidase might be unfunctional. He *et al.* found the alternative complex III in various MAGs and genomes from the phylum *Verrucomicrobiota*, often in close gene neighborhood to the *cbb*$_3$ oxidase genes, supporting their co-functionality in respiration (He *et al.* 2017). However, ACIII and *cbb*$_3$ oxidase are not in direct gene neighborhood in *Opitutaceae*.

Generally, this study shows that *Opitutaceae* have various sets of terminal oxidases from the *bd* oxidase family and A- and C-type HCOs that they can use for (micro-) aerobic respiration in their respective environments. Most oxidases are likely derived from more ancestral members of the PVC superphylum, however, some host-associated *Opitutaceae* acquired their *bd* oxidase gene via HGT from *Bacteroidota* after their *Opitutaceae* ancestors likely lost it.

4.2.3 Transcription level of terminal oxidases

Ereboglobus luteus, *Geminisphaera colitermitum* and *Opitutus terrae* were chosen as model organisms because they represent three different variations of respiratory chains that can be found in *Opitutaceae*. Transcription levels of the oxidases were analyzed using qPCR in order to investigate whether a differential set of terminal oxidases has an effect on the transcriptional response to changing oxygen conditions. The *bd* oxidase of *Opitutacea*e strains seems to be constitutively expressed under all oxygen conditions. While the expression level of *O. terrae* and *G. colitermitum* do not differ significantly, the *bd* oxidase of *E. luteus* is at an about ten-fold higher expression level between anoxic and microoxic (1% O_2) conditions. Apparently, the *bd* oxidase is constitutively expressed under anoxic conditions and upregulated when *E. luteus* is exposed to oxygen. This could be an adaptation to its habitat, the cockroach gut. When exposed to oxygen for longer periods, *E. luteus* can upregulate the expression of its oxidase in order to have have an advantage in competition for oxygen at low concentrations.

The *cbb*$_3$ oxidase is generally considered a high-affinity oxidase and was shown to be upregulated at low oxygen partial pressures in *Azorhizobium caulinodans* (Mandon *et al.* 1994), *Bradyrhizobium japonicum* (Preisig *et al.* 1996), *Ralstonia solanacearum* (Colburn-Clifford and Allen 2010) and *Pseudomonas aeruginosa* (Comolli and Donehue 2004, Arai 2011). The regulation of the *cbb*$_3$ oxidase has been well studied in *P. aeruginosa* where Arai showed that *P. aeruginosa* uses three low-affinity oxidases comprising of an *aa*$_3$ oxidase (used at nutrient starvation), a *bo*$_3$ oxidase (used at iron starvation) and a cyanide-insensitive-type *bd* oxidase (used when other oxidases are downregulated). Out of the two *cbb*$_3$ oxidases of *P. aeruginosa*, one is constitutively expressed, while the other is upregulated at low oxygen levels (Arai 2011). Opposing to these results, *G. colitermitum* seems to prefer its *bd*-type high-affinity oxidase at low oxygen concentrations and upregulates its *cbb*$_3$ oxidase at high oxygen concentrations. However, the lack of a typical low-affinity oxidase, might also open the need of a strategy to cope with higher oxygen concentrations. The solution in this scenario might be the upregulation of the second oxidase, the *cbb*$_3$ oxidase, which can often be necessary in the natural habitat of *G. colitermitum*, the termite gut. Interestingly, the *cbb*$_3$ type oxidases of *G. colitermitum* and *O. terrae* show a differential expression pattern when pre-cultivated under different oxygen conditions. In *O. terrae*, the *cbb*$_3$ oxidase is the oxidase with the highest expression level at 0% oxygen, while it has the lowest expression level at oxygen levels higher oxygen levels than 0.01% when compared to its other oxidases. Other than its *cbb*$_3$ oxidase, the high-affinity *bd* oxidase and the low-affinity *bo*$_3$ oxidase of *Opitutus terrae* were constitutively expressed and not changing in expression level when pre-cultivated under different oxygen levels (Fig. 8). The reason for this regulations could be explained by the ecology of *O. terrae*. As a rice paddy soil bacterium (Chin *et al.* 2001), *O. terrae* mainly experiences anoxic conditions but may be exposed to oxygen when the soil dries out. However, it is possible that *O. terrae* is more prevalent in other soil environments where it is exposed to more fluctuant oxygen conditions. Frequently changing oxygen conditions may have led to the expression pattern of the terminal oxidases, where a high-affinity and a low-affinity oxidase are constitutively expressed to cope with those changes rapidly. The upregulation of the *cbb*$_3$ oxidase at very low oxygen levels could enable *O. terrae* to utilize traces of oxygen in the mostly anoxic rice paddy soil.

The low-affinity *bo*$_3$-type quinole oxidase was intensely studied in *Escherichia coli*, where it is, among other oxidases and respiration-associated genes, regulated by the global regulator FNR (Unden and Trageser 1991; Salmon *et al.* 2003; Unden *et al.* 2014). Under anoxic conditions, both the *bo*$_3$ and *bd* oxidase of *E. coli* are negatively regulated by FNR

while the AraA regulon upregulates the *bd* oxidase and downregulates the bo_3 oxidase allowing high-affinity oxygen scavenging (Cotter and Gunsalus 1992). The expression level of *cydAB* of *E. coli* was shown to be highest at 7% oxygen saturation (~20 µM) and decreasing at lower and higher oxygen concentrations. At higher oxygen levels (10–15% and higher), the expression level of *cyoBA* was maximal in *E. coli* (Tseng *et al.* 1996). A homolog of FNR was found in some *Opitutaceae* including *Opitutus terrae*, however its regulation in *Opitutaceae* has not been studied yet. In *P. aeruginosa*, the global transcriptional regulator ANR is responsible for the regulation of the high-affinity oxidases (Comolli and Donohue 2004; Kawakami *et al.* 2010). Homologous sequences of these regulators were also found in the genomes of *Opitutaceae* by BLAST searches, but their involvement in the regulation of the terminal oxidases can only be speculated. However, also a constitutive expression of high-affinity oxidases (Brzuszkiewicz *et al*. 2011; Dank *et al.* 2021) and low-affinity oxidases (Trojan *et al.* 2021) has been reported in previous studies suggesting that the results found in *Opitutaceae* are not uncommon in nature.

4.2.4 Rates and affinities of oxygen uptake

The oxygen uptake physiology of *Opitutaceae* was studied with spectrophotometric measurement of the deoxygenation of myoglobin and microelectrode measurements. The latter method was only used to measure oxygen uptake rates since the available microsensors were not sensitive enough to measure oxygen uptake kinetics. The glucose-induced acceleration of oxygen reduction observed during the microsensor measurements (example: Fig. 9) supports the hypothesis that *Opitutaceae* can energetically benefit from aerobic glucose oxidation, although they are capable of fermentation (Tegtmeier *et al.* 2018). Glucose-independent oxygen reduction of washed cell suspensions might be fueled by internal reserve compounds of the cells. The alternative method, the deoxygenation of globins, was previously used to measure kinetics of purified enzymes and membrane fractions in the low nanomolar ranges (Preisig *et al.* 1996; D´mello and Poole 1995; D´mello *et al.* 1996) and should be sufficient to measure the oxygen reduction physiology of *Opitutaceae*.

Comparing the oxygen uptake rates of *Opitutaceae* when measured spectrophotometrically to the rates measured with microelectrodes shows clear differences in absolute values but a similar trend (Tab. 4). The uptake rate of *Ereboglobus luteus* was generally lower than that of the other two strains with the maximal rates measured for *Opitutus terrae*. The rates follow the same trend than the growth rates that were described earlier (Tegtmeier *et al.* 2018). With

exception of *E. luteus* measured with microelectrodes, all experiments involving cells that were pre-cultivated at 1% oxygen had higher uptake rates than at 0%, suggesting an upregulation of the oxidases. Interestingly, these upregulations at 1% oxygen could not be detected in the qPCR experiments (Fig. 8). The uptake rates of *E. luteus* were not changing strongly when cultured under different oxygen conditions which is in agreement with the constitutive expression of the *bd* oxidase that was measured by qPCR experiments (Fig. 8). The uptake rates of *Geminisphaera colitermitum* and *Opitutus terrae* were increasing 1.5-fold to 2-fold (microsensor measurements) and 3-fold to 5-fold (spectrophotometric measurements). Generally, *Opitutaceae* seem to have relatively low oxygen uptake rates. The maximal rate measured for *Opitutaceae* (6006.8 nmol × g^{-1} × min^{-1}, measured for *O. terrae*) is about 50-fold lower that oxygen uptake rates reported for aerobic *E. coli* cultures (333 µmol × g^{-1} × min^{-1}, Andersen and Mayenburg 1980).

In this study, 20 nM was set as the lower detection limit of the myoglobin-based experiment measuring the oxygen uptake kinetics of *Opitutaceae*. The fractional oxygenation of myoglobin at 20 nM is still about 2.5% (calculations based on K_M = 786 nM, reported in Appleby and Bergersen 1980), which is reasonable to measure using the spectrophotometric approach. Previous studies that used the same approach have used the deoxygenation of myoglobin above 100 nM, however leghemoglobin was available in these studies (Bergersen and Turner 1980; D´mello *et al.* 1996).

The oxygen uptake affinities of cell suspensions of *Opitutaceae* (Fig. 11, Tab. 4) were generally lower (K_S = 20 – 120 nM) than reported for the purified enzyme complexes of the *bd* oxidase (K_M = 3 – 8 nM, D´mello *et al.* 1996) and the membrane preparations of the *cbb*$_3$ oxidase (K_M = 7 nM, Preisig *et al.* 1996) but higher than the reported affinities for preparations of the low-affinity *bo*$_3$ oxidase of *E. coli* (K_M = 0.15 – 0.35 µM, D´mello and Poole 1995). However, other than purified than the K_M value of enzymes, the K_S value of cell suspensions is the result of multiple cellular processes and not only dictated by the oxidase affinities. The oxygen uptake affinity (K_S) of *G. colitermitum* and *E. luteus* were constant between 20 and 30 nM and not changing significantly when the cells were pre-cultivated under differential oxygen concentrations (Fig. 11, Tab. 4). Contrary to this, the oxygen uptake affinity of *O. terrae* was lower when pre-cultivated under anoxic conditions (132.8 nM) compared to pre-cultivation at 1% oxygen (47.4 nM). This trend is opposite than expected based on the transcription levels, where the high-affinity *cbb*$_3$ oxidase is downregulated at 1% oxygen compared to 0% oxygen. Potentially, the *cbb*$_3$ oxidase does

not contribute significantly to the total oxygen affinity of the cells. Another explanation would be that the *cbb*$_3$ oxidase of *O. terrae* is not a high-affinity oxidase, a phenomenon that was previously reported in *Rhodobacter capsulatus* (Swem and Bauer 2002). Similarly, *Pseudomonas aeruginosa* uses the *cbb*$_3$ oxidase as its main terminal oxidase at all oxygen concentrations by applying multiple isosubunits of the oxidase depending on the environmental conditions (Hirai *et al*. 2016). Comparing the terminal oxidase expression levels of *O. terrae* to the oxygen uptake affinity also allows to draw another conclusion. The downregulation of the *cbb*$_3$ oxidase also results in the *bd* oxidase being the major HATOx available. Assuming that the oxygen uptake affinity of the cells is a result of the combination of the different available oxidases, this could mean that the higher affinity of *O. terrae* at 1% is a result of the downregulation of a potential lower-affinity *cbb*$_3$ oxidase and a resulting dominance of the high-affinity *bd* oxidase. However, other factors like a differential oxidase mRNA half-life time and differential specific enzyme activities are also important factors in the oxygen uptake physiology, hence, a strict correlation between oxidase transcription level and oxygen uptake affinities and rates is not always expected and would require further investigations in *Opitutaceae*.

The measurement of oxygen concentrations in the range of the K_M of the high-affinity oxidases (~5 nM) require the utilization of the high-affinity leghemoglobin. Protein preparations of faba bean root nodules did not contain any leghemoglobin. Future experiments could use leghemoglobin to potentially show even lower oxygen affinities for *Opitutaceae* cell suspensions.

4.2.5 Ecological relevance of microaerobic respiration

Members of *Opitutaceae* can utilize diverse sets of high- and low-affinity terminal oxidases in their genomes to respire oxygen in their respective habitats. Although differing from previous reports, all so far cultivated members of *Opitutaceae* are facultative anaerobes that have the potential to thrive at microaerobic conditions (Tegtmeier *et al.* 2018). Following the evolution of *Opitutaceae* from free-living to host-associated environments, some *Opitutaceae* have lost their low-affinity oxidases which are likely no longer needed in oxygen-scarce insect gut environments. *Opitutaceae* seem to be a small-scale model for this global pattern, that has been described based on the analysis of 673 prokaryotic genomes from all environments by Morris and Schmidt (Morris and Schmidt 2013) and was continued with a stronger focus on the termite gut (Dietrich and Brune, unpublished data, Fig. 3). Gut-inhabitting microorganisms like *Geminisphaera colitermitum* or *Ereboglobus luteus* have to

cope with an oxygen gradient from the gut wall to the gut center, as shown by microelctrode measurements in termites and cockroaches (Brune *et al.* 1995, Sprenger *et al.* 2007). Microaerobes reduce the penetrating oxygen and thereby allow the strictly anaerobic processes in the gut center to occur. Therfore, host-associated, microaerobic *Opitutaceae* are potentially important players in the in guts of termites and cockroaches.

Although microaerobic potential is certainly of high relevance to understand the true physiology and ecology of microorganisms, it is often overlooked (Morris and Schmitt 2013, Berg *et al*. 2022). While bacteria are mostly cultivated at either atmospheric oxygen concentrations or at anoxic conditions, these conditions often do not reflect the real conditions the bacteria face in natural habitats. Future studies should focus on the role of the different high-affinity oxidases in the differential response to changing oxygen conditions to get a broader understanding of the biology involved. As suggested by the mostly constitutively expressed oxidases in *Opitutaceae*, the long-known regulations and characteristics of well-studied organisms like *Escherichia coli* or *Pseudomonas aeruginosa* are not representative for all groups and all environments. Estimations on an organism's ecology based on modern transcriptomic and metabolomic methods are certainly a great improvement for the field but do not replace sophisticated physiological experiments.

4.3 *Opitutales* associated with flagellates in the termite gut

4.3.1 Classification of the *Opitutales* MAGs from termite guts

With the exception of one MAG (TD116_bin.50) that was recovered from the gut of an *Odontotermes* species, all 83 *Opitutales* MAGs represent lower termite metagenomes, dominated by members of Kalotermitidae. Only one additional uncultured higher termite clone from a *Microcerotermes* species is known (Hongoh *et al.* 2005). Additionally, Arora *et al.* found *Opitutales* in low abundances associated with lower termites, but almost never with higher termites (Arora *et al*. 2022). Although they are restricted to lower termites, *Opitutales* represented by our MAGs inhabit the gut of several lower termite species. The unique feature of higher termites, the loss of flagellates (Lo and Eggleton 2011; Brune 2014), could suggest that a potential association of *Opitutales* with termite gut flagellates might be the reason for the absence of *Opitutales* in higher termites (family: Termitidae). *Opitutales* MAGs account for about 6% of the 1392 total MAGs recovered from lower termites and could be assembled from every investigated lower termite metagenome except for *Reticulitermes santonensis* (Rs511). Members of *Opitutales* have been detected as parts of the termite gut microbiome in previous studies (Stevenson *et al.* 2004; Hongoh *et al.* 2003; Hongoh *et al*. 2005; Nakajima *et al*. 2005; Wertz *et al.* 2018), including several strains associated with termite gut flagellates (Yang *et al.* 2005) and even intranuclear symbionts of termite gut flagellates (Sato *et al.* 2014). However, their low abundance and restricted number of isolated species led to only minor interest in *Opitutales* and *Verrucomicrobiota* termite gut symbionts. *Geminisphaera colitermitum* and related TAV strains are the only isolated and characterized *Verrucomicrobiota* from the termite gut (Stevenson *et al.* 2004; Wertz *et al.* 2018). The abundance and diversity of *Opitutales* MAGs found in our termite gut metagenomes compared to earlier studies might help shed light on this uncultivated bacterial lineage.

Phylogenomic analysis and classifications of the MAGs revealed that they form nine MAG-specific groups that are likely family-level lineages within the order *Opitutales*. This opens a whole new view on the importance of *Opitutales* in the gut of lower termites. Further analysis of the characteristics of the MAGs revealed that the MAGs belonging to MAG groups I–IV have strongly reduced genomes sizes (1–1.3 Mbp) and GC contents (40–50%) compared to more basal *Opitutales* (2.5–4.5 Mbp, 50–65% GC, Fig. 13). Both, reduced genomes and a lowered GC content are common features that were found in endosymbiotic bacteria (Hershberg and Petrov 2010; McCutcheon and Moran 2012), also within

endosymbionts of termite gut flagellates (Ikeda-Ohtsubo and Brune 2009; Ikeda-Ohtsubo *et al*. 2016; Kuwahara *et al.* 2016; Strassert *et al.* 2016). This provides first indications that *Opitutales* MAGs of group I–IV represent potential endosymbionts of termite gut flagellates. MAGs of group V and the more basal *Opitutaceae* are not reduced in genome size and do not have a lowered GC content and most likely represent free-living lineages.

4.3.2 Localization of *Opitutales* within termite gut flagellates

Previous fluorescence *in situ* hybridization (FISH) studies *Trichonympha* spp. revealed a co-inhabitation of *Endomicrobia* and *Desulfovibrio* endosymbionts, that were spatially separated within their flagellate hosts (Sato *et al.* 2008). *Desulfovibrio* endosymbionts are arranged in parallel rows at the anterior part of the *Trichonympha* cell, while *Endomicrobia* were located in the posterior part (Sato *et al.* 2008; Strassert *et al.* 2012). Also, cells of the putative homoacetogenic *Candidatus* Adiutrix intracellularis showed highest densities in the ectoplasm of the anterior part of *Trichonympha* cells, although they were detected throughout the cell (Ikeda-Ohtsubo *et al.* 2016). The FISH experiments of my study showed a signal of *Opitutales* in several different flagellate species from different termite species, where they were dispensed all over the cells with no clear localization pattern. Images from a gut suspension of *Cryptotermes havilandi* (Fig. 15AB) show that two different flagellate species (most likely *Stephanonympha sp*. and *Devescovina sp*.) were present and both were inhabited by *Opitutales*. However, not all cells of both species seem to be inhabited by *Opitutales*. The experiments also indicated that some flagellate species like *Pseudotrichonympha* sp. (Fig. 15D) are never inhabited by *Opitutales*. This indicates that although *Opitutales* seem to be associated with a lot of different flagellate species, they are likely still specific for them and not inhabiting every flagellate species.

4.3.3 Are *Opitutales* endosymbionts co-evolving with their hosts?

Flagellates typically co-evolve with their lower termite hosts (Ohkuma and Brune 2010; Brune and Dietrich 2015), and also the flagellates themselves may co-evolve with their prokaryotic endosymbionts (Noda *et al*. 2007; Ikeda-Ohtsubo and Brune 2009; Desai *et al.* 2010). Phylogenomic analysis of the *Opitutales* MAGs did not reveal clear evolutionary patterns with these putative symbionts and their termite hosts (Fig. S10). MAGs from the same metagenomes do not form phylogenomic clusters, suggesting no co-evolution of the endosymbiont and their termite hosts. A recent update on the Kalotermitidae phylogeny (Buček *et al.* 2022) highlights the species richness of Kalotermitidae and also shows misclassifications of some genera, however, this also does not explain the absence of

evolutionary patterns between *Opitutales* and their termite host phylogeny. My results indicate that *Opitutales* might not be permanent inhabitants of the flagellates, although obligate host dependency is suggested by significant genome reduction and their environmental restriction to flagellate-inhabited lower termites. However, since the MAGs were recovered from whole-gut metagenomes, the potential flagellate hosts of the respective MAGs cannot be identified. A potential future study including clone libraries of the concerned termite gut flagellates could shed more light on the cospeciation of *Opitutales* and termite gut flagellates. Additionally, co-localization with flagellate-specific probes and *Opitutales*-specific probes could show whether or not every cell of one flagellate species is colonized by *Opitutales* and if certain *Opitutales* lineages are specific for individual flagellate species.

4.4 Functional analysis of *Opitutales* MAGs

4.4.1 Central carbon metabolism

The large genome reduction of *Opitutales* from MAG groups I–IV (Fig. 13) suggests massive gene losses and loss of functions. The conservation of genes for all core cellular processes like replication, transcription or translation indicates that there are no major gaps within the MAGs suggesting reliable genome assembly. *Opitutales* with reduced genomes lost several genes belonging to glycolysis, which is an important central pathway of anabolism and catabolism in many prokaryotes and eukaryotes. Basal *Opitutale*s have conserved all genes necessary for a complete glycolysis while endosymbiotic *Opitutales* with reduced genomes lost certain genes. All MAGs are lacking genes for a glucose PTS system, but contain several genes of unspecific MFS transporters that could encode potential sugar importers. All MAGs (group I–V) are also lacking genes for hexokinase, an enzyme responsible for glucose phosphorylation. The absence of hexokinase was also reported for *Burkholderiales* endosymbionts of fungi (Uehling *et al*. 2017), *Burkholderiales* endosymbionts of insect-pathogenic flagellates (Zakharova *et al.* 2021) but also for different endosymbionts of termite gut flagellates (Strassert *et al.* 2016; Hongoh *et al.* 2008b). Similarly to these cases, the acquisiton of sugar phosphate transporters from the organophosphate:P_i antiporter (OPA) family potentially rendered these genes unnessecary, causing their subsequent loss in the genomes. The OPA transporters from *Opitutales* are present in MAG groups I–IV and a subgroup of *Opitutaceae*. The transporters of MAG groups I–IV are most closely related to transporters of uncultured *Paracedibacterales* (candidate family: UBA11393) from the termite gut and transporters from *Rickettsiales* (Fig.

17). Therefore, *Opitutales* most likely gained these transporters via horizontal gene transfer in the termite gut. Well-characterized glycerol-3-phosphate transporters (*glpT*) from *Rickettsia spp*. (Audia and Winkler 2006) and hexose-6-phosphate transporters (*uhpC*) of *Chlamydiota* and other bacteria were more distantly related (Reid *et al.* 2000; Schwöppe *et al.* 2002). Accordingly, a prediction of the type of transported sugar phosphate is highly speculatative and would require further analysis. Nevertheless, *Opitutales* can most likely supplement their metabolism with sugar phosphates from their hosts cytoplasm. The uptake of key genes via HGT, along with massive genome reduction is a mechanism that is thought to allow rapid adaptation to a new functional niche and the establishment of endosymbiosis. For example, aphid endosymbionts have gained vitamin biosynthesis genes via which allows them to compensate for another endosymbiont's gene deficiencies (Manzano-Marín *et al*. 2020). Further, a member of the microbiome associated to beetle eggs underwent massive genome reduction after acquisition of genes that encode for an anti-fungal compound (Waterworth *et al.* 2020). However, the mechanisms responsible HGT and genome integration are not always clear (Arnold *et al*. 2022).

Another key enzyme of glycolysis, fructose-1,6-bisphosphate aldolase, was absent in all MAGs (groups I–V). A phosphoketolase pathway, as described in *Bifidobacteriales* (Meile *et al*. 2001), can be excluded because the respective genes were not found in MAG groups I–V. Hence, it remains puzzling how this gap can be overcome in *Opitutales*. Moreover, all MAGs are lacking pyruvate kinase, an enzyme that is usually used to yield ATP and produce the important metabolic intermediate pyruvate. However, this gap is likely overcome by using pyruvate phosphate dikinase (PPDK). Other than pyruvate kinase, PPDK is reversible (Wood *et al.* 1997). While it is usually driven PEP-directed in C4-plants (Edwards and Nakamoto 1985), pathogenic protozoa (Rodriguez-Contreras and Hamilton 2014) and some bacteria (Olson *et al*. 2017), it can be used pyruvate-directed and ATP-forming in flagellates and bacteria (Slamovits and Keeling 2006), including *Opitutales* MAGs. This is in agreement with the findings that the MAGs can produce acetyl-CoA from pyruvate using pyruvate:ferredoxin oxidoreductase connecting glycolysis to further metabolic pathways.

The TCA cycle, while present in all *Opitutaceae* and genomes from MAG group V, was lost in most MAGs (groups I–IV). However, most MAGs from groups I, III, IV retained genes for 2-oxo-glutarate dehydrogenase and succinyl-CoA synthetase. Interestingly, the exact same genes are the only remnants of the TCA cycle of parasitic *Rickettsiales* where they were assumed to be fueled by deamination products of glutamate and glutamine (Driscoll *et*

al. 2017; Castelli *et al.* 2021). Acetyl-CoA is a central intermediate and starting point of many metabolic processes including some ATP-forming processes that can be used for energy conservation. Both typical energy conserving enzymes, acetyl-CoA synthetase and acetate kinase were not found in all MAGs suggesting that *Opitutales* MAGs cannot conserve energy by substrate-level phosphorylation (SLP) from acetyl-CoA. Also, the non-energy-conserving acetyl-CoA hydratase which splits acetate and CoA was not found in all MAGs. However, an acetate succinate CoA transferase (ASCT), an enzyme that transfers the CoA group from acetate to succinate forming succinyl-CoA, was found in all MAGs except MAG group II (Fig. 16). The conservation of both ASCT and succiyl-CoA synthetase (SCS) could suggest energy conservation via SLP in *Opitutales* MAGs (Fig. 22). The combination of these two complexes was shown to be used for energy conservation and acetate production in parasitic trypanosomatid flagellates (Van Hellomond *et al* 1998; Mochizuki *et al*. 2020). Interestingly, these reactions are mainly present in mitochondrion-like and hydrogenosome-like organelles of the parasitic trypanosomatid flagellates (Leger *et al.* 2017). In several bacteria, including symbionts of humans, insects and other animals, ASCT has been evolved to replace the function of SCS in an incomplete TCA cycle (Kwong *et al.* 2018). In MAG group II, ASCT and SCS were lost, closing this potential pathway for energy conservation.

4.4.2 Energy metabolism

Energy conservation via fermentative processes always comes along with the need to get rid of surplus electrons that accumulate as reducing equivalents. In the case of *Opitutales,* the need to recycle NADH produced by glyceraldehyde phosphate dehydrogenase and reduced ferredoxin produced by PFOR is apparent. Reduced ferredoxin could be recycled by hydrogenases that were found in the same MAG groups that also retained ASCT/SCS as a potential pathway for substrate-level phosphorylation (Fig. 16), with the exception of MAG group IV who retained ASCT/SCS but do not have hydrogenases. The hydrogenases are not present in the genomes basal to the MAGs with reduced genomes, suggesting horizontal acquisition of the genes. The closest relatives of these hydrogenases, identified by BLAST searches, were hydrogenases from rumen-associated *Alphaproteobacteria* and from *Margulisbacteriota* attached to spirochaetal ectosymbionts of termite gut flagellates. Accordingly, the genes were likely acquired despite genome reduction in the termite gut. The hydrogenases of *Opitutales* were classified as group B [FeFe] hydrogenases, a potentially ancestral group with no characterized reference (Greening *et al.* 2016). These hydrogenases are organized by either two [4Fe4S] clusters or three [4Fe4S] clusters and one

[2Fe2S] cluster and were predicted to be very oxygen-sensitive and used in a hydrogen-evolving direction (Greening *et al.* 2016; Wolf *et al.* 2016). The production of hydrogen as an electron sink is commonly found in fermentative bacteria, and could allow *Opitutales* to recycle ferredoxin. The gene neighborhood and phylogenetic classification do not suggest that the hydrogenases are bifurcating NADH, which means that it remains unclear how NADH is recycled in endosymbiotic *Opitutales* (MAG groups I–IV). However, the exact functionality of the hydrogenases remains speculative due to the lack of characterized members. However, the lack of pathways for anerobic respirations, lactate dehydrogenase or alcohol dehydrogenase results in a need of reducing equivalent recycling that could potentially be overcome by hydrogen production. Fermentative bacteria need to be able to maintain the electrochemical potential of their membranes (Buckel and Thauer 2013). Similar to many other fermentative bacteria, endosymbiotic *Opitutales* retained an ATP synthase which allows them to create membrane potential on the cost of ATP.

4.4.3 Peptidoglycan biosynthesis

The cell wall of endosymbionts is often retained in relatively young endosymbionts like endosymbionts of termite gut flagellates (Kuwahara *et al.* 2016; Zheng *et al.* 2017) but also in verrucomicrobial endosymbionts of ciliates (Serra *et al.* 2020; Williams *et al.* 2021). Similarly, all *Opitutales*, including the potential endosymbionts, retained the genes for peptidoglycan biosynthesis. The whole order of *Opitutales* seems to be an exception within the mainly peptidoglycan-less PVC superphylum (Wagner and Horn 2006). Endosymbionts that underwent even further genome erosion often rely on certain cell wall building blocks of their hosts (Shigenobu *et al.* 2000) or are completely dependent on host-derived membranes (Husnik and McCutcheon 2016) and therefore are on the frontier between endosymbiont and organelle (Tamames *et al.* 2007).

4.4.4 ATP/ADP antiporters

Opitutales from MAG groups I–IV encode for ATP/ADP antiporters (NTTs) that putatively enables them to scavenge for ATP of the host cell. NTTs have been described in intracellular parasites like Microsporida fungi (Heinz *et al*. 2014), *Rickettsia* (Audia and Winkler 2006) and *Chlamydiota* (Bou Khalil *et al.* 2016) but were also found in free-living bacteria (Major *et al.* 2017). NTTs were only found in MAG groups I–IV as well as four ground-water MAGs basal to MAG group IV (Fig. 16), suggesting an acquisition via horizontal gene transfer (HGT). Phylogenetic analysis of the NTTs of the MAGs (Fig. 18) revealed that *Opitutales* NTTs form a deep-branching group. BLAST searches found NTTs from *Chlamydiota* and

Rickettsiales as closest relatives. The absence of *Chlamydiota* from the termite gut and the presence of the NTTs in MAGs from fresh-water metagenomes suggest that the NTTs were likely not acquired in the termite gut. The ability of ATP scavenging can be advantageous for the energy metabolism and potentially DNA and RNA metabolism in *Opitutales* and opens up a whole new ecological niche in the termite gut.

4.4.5 Oxygen relationship of *Opitutales* MAGs

Although *Opitutaceae*, including host-associated and termite gut-inhabiting species, are microaerobes that possess diverse sets of terminal oxidases to cope with differential oxygen conditions in their environments (Chapter 4.2), all *Opitutales* with reduced genomes (MAG groups I–IV) lack all elements of a respiratory chain including all terminal oxidases and NADH dehydrogenase (Fig. 20). Their intracellular location within anaerobic flagellates likely made it unnecessary to retain the respective genes. *Opitutales* from MAG group V still have complete respiratory chains with a *bd*-type terminal oxidase that enables them respire oxygen at a high affinity. Assuming a free-living lifestyle within the gut of lower termites, MAG group V can use its respiratory chain to respire oxygen that is present in a steep gradient from the gut wall to the gut center (Brune *et al.* 1995). Other than *Opitutaceae* and MAG group V, the MAGs with reduced genomes also lack all types of defense mechanisms against reactive oxygen species (ROS) like hydrogen peroxide or superoxide. The loss of ROS defense mechanisms was also reported in other termite gut flagellate endosymbionts (Strassert *et al*. 2016, Kuwahara *et al.* 2017) and can also be explained by its redundancy for an intracellular endosymbiont of an anerobic flagellate.

4.4.6 Amino acid metabolism

Endosymbionts of termite gut flagellates like *Candidatus* Endomicrobium trichonymphae, *Candidatus* Azobacteroides pseudotrichonymphae or *C*andidatus Adiutrix intracellularis retained the majority of amino acid biosynthesis pathways despite significant genome reduction and were therefore thought to supply their host with certain amino acids (Hongoh *et al*. 2008a; Hongoh *et al*. 2008b; Ikeda-Ohtsubo *et al.* 2016). The exchange of amino acids is a common feature in nutritional symbiosis and has been reported for intracellular aphid symbionts (Degnan *et al.* 2009; Price *et al.* 2013), cockroach fat body endosymbionts (Neef *et al.* 2011) and endosymbionts of trypanosomatid flagellates (Silva *et al.* 2018). The loss of most amino acid biosynthesis pathways in *Opitutales* MAGs (groups I–IV, Fig. 21) therefore distinguishes them from other symbionts of termite gut flagellates and implies that they are depended on amino acid supply by their flagellate hosts. This is also supported by the

presence of a number of amino acid transporters in *Opitutales* MAGs that can potentially be used for amino acid scavenging.

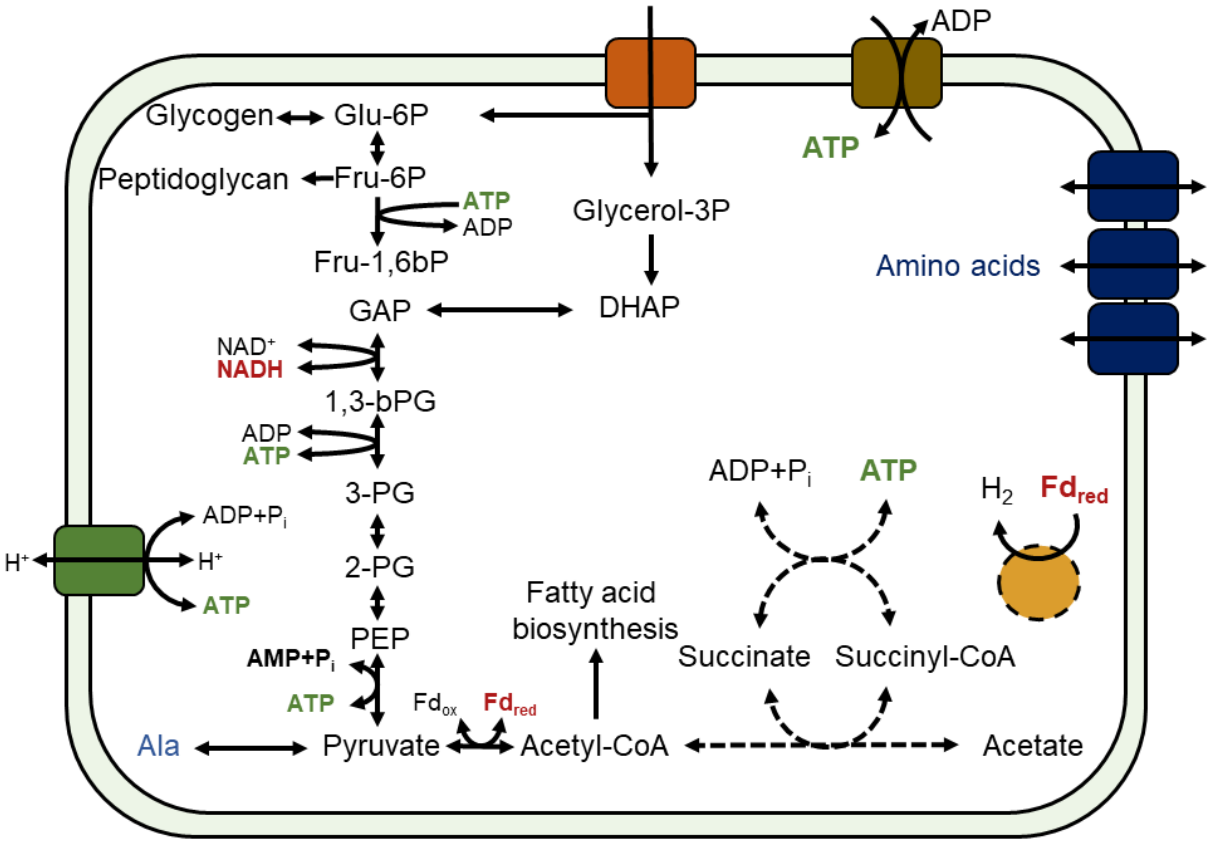

Figure 22: Metabolic map of *Opitutales* endosymbionts. Sugar phosphate transporters (orange) are used to import glycerol-3-phosphate (Glycerol-3P) or potentially glucose-6-phosphate (Glu-6P). Glycerol-3-phosphate is further imported into the energy-yielding part of glycolysis and further metabolized via dihydroxyacetonephosphate (DHAP), glyceraldehyde-3-phosphate (GAP), 1,3-bisphosphoglycerate (1,3-bPG), 3-phophoglycerate (3-PG), 2-phosphoglycerate (2-PG) to phosphoenol-pyruvate (PEP). ATP is yielded by the AMP-forming pyruvate phosphate dikinase producing pyruvate. Pyruvate:ferredoxin oxidoreductase (PFOR) is producing acetyl-CoA from pyruvate, forming reduced ferredoxin as a side product. Acetyl-CoA can be used to synthesize fatty acids but can also be further metabolized by acetate succinate CoA transferase and succinyl-CoA synthetase yielding ATP and acetate. Some reactions were lost in MAG group II (dashed lines). Transporters for nucleotides (brown) and amino acids (blue) are present in all *Opitutales* endosymbionts. Additionally, am ATP synthase (green) was found in all MAGs. Reducing equivalents NADH and ferredoxin are labeled in red. An [FeFe] hydrogenase could be used to produce hydrogen from reduced ferredoxin.

4.5 Nature of the *Opitutales*–flagellate symbiosis

4.5.1 Ecological consideration

The massive genome reduction of *Opitutales* (MAG groups I–IV) and their localization, are strong evidence for the endosymbiotic relationship of *Opitutales* (MAG groups I–IV) with their flagellate hosts, however, the nature of this symbiosis is rather unclear. Neither the fluorescence in situ hybridization experiments, nor the genome analysis indicate that the investigated *Opitutales* are intranuclear symbionts of the flagellates like it was shown for *Candidatus* Nucleococcus trichonymphae and *Candidatus* Nucleococcus kirbyi (Sato *et al.* 2014). Phylogenetic analysis of the *Opitutales* 16S rRNA genes revealed that these intranuclear symbionts are most closely related to MAG group IIb (Fig. 14). Consistent with this, MAG groups IIb and IIc have the smallest genome sizes (Fig. 13) and lost several functions that were retained in the other MAGs (example: ASCT/SCS, [FeFe] hydrogenases) suggesting that MAG groups IIb and IIc are putatively precursors of the intranuclear *Opitutales*. *Candidatus* Nucleococcus sp. were reported to be symbionts of *Trichonympha spp*. flagellates within the gut of *Reticulitermes speratus* (family: Rhinotermitidae). However, no MAGs with reduced genome sizes were recovered from Rhinotermitidae metagenomes, and even FISH experiments of flagellate suspensions from *Reticulitermes santonensis* and *Reticulitermes lucifugus* showed no co-localization of the *Opitutales* signal and the flagellate nuclei. Intranuclear symbionts of termite gut flagellates with a similar morphology than *Candidatus* Nucleococcus spp. have been reported in numerous earlier studies (Kirby1944; Rösel *et al.* 1996; Radek 1997; Brugerolle and Radek 2006). Possibly, intranuclear *Opitutales* are more widespread than reported so far, however, the *Opitutales* MAGs investigated in this study likely do not represent intranuclear lineages. Future FISH-based studies could use *Opitutales*- and flagellate-specific probes to achieve a more comprehensive overview of which flagellates are associated with *Opitutales*.

The nature of the symbiosis between termite gut flagellates and *Opitutales* symbionts is not obvious yet. Endosymbiotic *Opitutales* are obligately dependent on amino acid and sugar phosphate supply by their flagellate hosts and potentially also rely on ATP uptake. The functional analysis of the *Opitutales* MAGs did not reveal potential metabolic products like essential amino acids, vitamins or secondary metabolites that could be beneficial for their host, suggesting a rather parasitic than mutualistic lifestyle. Localization of *Opitutales* with fluorescence *in situ* hybridization showed that not all flagellate cells are inhabited by *Opitutales* to the same extend suggesting that *Opitutales* might not me permanently

inhabiting the flagellate cells. Additionally, *Opitutales* differentiate from other termite gut flagellate symbionts by the absence of a cospeciation pattern of the MAGs and their termite hosts. Localization experiments also showed that *Opitutales* are found as endosymbionts of several different flagellate species and do not seem to be specific for certain lineages like it was reported for other flagellate symbionts. All these results suggest that *Opitutales* could be parasitic endosymbionts of termite gut flagellates. The lack of the ATP producing ASCT/SCS pathway in MAG group II and their even smaller genome sizes compared to the other reduced MAG groups, indicate that MAG group II represents the most-proceeded endosymbionts with an even stronger dependency on ATP uptake by their hosts.

4.5.2 Conclusions

Opitutales are the first example of termite gut bacteria where some members have potentially evolved to putative parasites of cellulolytic flagellates. Similar to other flagellate endosymbionts, the transition from a free-living to endosymbiotic lifestyle came along with significant genome reduction and the acquisition of several key genes (nucleotide transporters and sugar phosphate transporters). Some transporter genes were likely acquired via horizontal gene transfer from other termite gut bacteria, and enabled *Opitutales* to thrive on ATP and sugar phosphates that are present in the host cytoplasm. The broad range of potentially parasitic *Opitutales* and their termite hosts suggest that they are common members of the microbiome of kalotermitid termites. In order to gain a deeper understanding of the transition and evolution of this symbiosis, future investigations should improve the specific localization of certain MAG groups with microscopy but should also focus on covering the total range of *Opitutales* associated with flagellate with clone libraries. Although metagenome-based studies have a great potential to investigate the potential of uncultured microorganisms, they can not replace cultivation-based studies to confirm the assumptions and hypothesis about an organism's cell biology, metabolism and ecological niche (Lewis *et al.* 2021).

4.6 General conclusions

This dissertation shows that members of the verrucomicrobial order *Opitutales* are diverse and important members of free-living and host-associated environments. A prominent feature of free-living and host-associated *Opitutales* is their diverse respiratory equipment which enables them to scavenge for oxygen in their temporarily or permanently oxygen scarce environments. The family *Opitutaceae* is especially prominent in host-associated environments like cockroach or termite guts where they are classical sugar fermenters but can also contribute to the aerobic respiratory oxygen reduction which is crucial for the anaerobic processes in the gut center. The example of *Opitutaceae* elucidates that investigations on bacterial groups that seem to have a basic metabolism are still important to achieve a broader understanding of their biology. Termite gut *Opitutales* have evolved to become endosymbionts of termite gut flagellates where they potentially parasitically scavenge for sugar phosphates, amino acids and ATP. The conservation of certain key genes along with the take up of certain genes from the environment seem to be important factors that drive the process of endosymbiosis in *Opitutales* but likely also in other endosymbionts of termite gut flagellates. These studies revealed a small fraction of the possibly great diversity of *Verrucomicrobiota* and *Opitutales* and underlines that these groups were clearly under-sampled. The great number of metagenome-derived genomic data of uncultured *Verrucomicrobiota* corroborates the great potential of these methods to study the diversity, function and importance of *Opitutales* in other environments. However, also cultivation-based methods help to evaluate the assumptions made based on genomic and metagenomic experiments.

5 REFERENCES

Alteio LV, Schulz F, Seshadri R, Varghese N, Rodriguez-Reillo W, Ryan E, Goudeau D, Eichorst SA, Malmstrom RR, Bowers RM, Katz LA, Blanchard JL, Woyke T (2020) Complementary Metagenomic Approaches Improve Reconstruction of Microbial Diversity in a Forest Soil. *mSystems* **10**:e00768–19

Altschul SF, Madden TL, Schäffer AA, Zhang J, Zhang Z, Miller W, Lipman DJ (1997) Gapped BLAST and PSI-BLAST: a new generation of protein database search programs. *Nucleic Acids Res* **25**:3389–402

Amann RI, Binder BJ, Olsen R, Chisholm SW, Devereux R, Stahl DA (1990) Combination of 16S rRNA-targeted oligonucleotide probes with flow cytometry for analyzing mixed microbial populations. *Appl Environ Microbiol* **56**:1919–25

Anders H, Power JF, MacKenzie AD, Lagutin K, Vyssotski M, Hanssen E, Moreau JW, Stott MB (2015) *Limisphaera ngatamarikiensis* gen. nov., sp. nov., a thermophilic, pink-pigmented coccus isolated from subaqueous mud of a geothermal hotspring. *Int J Syst Evol Microbiol* **65**:1114–21

Andersen KB, Mayenburg K (1980) Are growth rates of *Escherichia coli* in batch cultures limited by respiration? *J Bacteriol* **144:**114–23

Appleby CA, Bergersen FJ (1980) Preparation and experimental use of leghaemoglobin. In: Bergersen FJ (ed.). Methods of evaluating biological nitrogen fixation. John Wiley and Sons Ltd., Chichester, United Kingdom, 315-35.

Arai H (2011) Regulation and function of versatile aerobic and anaerobic respiratory metabolism in *Pseudomonas aeruginosa*. *Front Microbiol* **2**:103

Arnold BJ, Huang I-T, Hanage W-P (2022) Horizontal gene transfer and adaptive evolution in bacteria. *Nat Rev Microbiol* **20**:206-18

Arora J, Kinjo Y, Šobotník J, Buček A, Clitheroe C, Stiblik P, Roisin Y, Žifčáková L, Park YC, Kim KY, Sillam-Dussès D, Hervé V, Lo N, Tokuda G, Brune A, Bourguignon T (2022) The functional evolution of termite gut microbiota. *Microbiome* **10**:78

Audia JP, Winkler HH (2006) Study of the five Rickettsia prowazekii proteins annotated as ATP/ADP translocases (Tlc): Only Tlc1 transports ATP/ADP, while Tlc4 and Tlc5 transport other ribonucleotides. *J Bacteriol* **188**:6261–8

Awala SI, Gwak J-H, Kim Y-M, Kim S-J, Strazzulli A, Dunfield PF, Yoon H, Kim G-J, Rhee S-K (2021) Verrucomicrobial methanotrophs grow on diverse C3 compounds and use a homolog of particulate methane monooxygenase to oxidize acetone. *ISME J* **15**:3636–46

Baek K, Song J, Cho J-C, Chung EJ, Choi A (2019) *Nibricoccus aquaticus* gen. nov., sp. nov., a new genus of the family *Opitutaceae* isolated from hyporheic freshwater. *Int J Syst Evol Microbiol* **69**:552–7

Berg JS, Ahmerkamp S, Pjevac P, Hausmann B, Milucka J, Kuypers MMM (2022) How low can they go? Aerobic respiration by microorganisms under apparent anoxia. *FEMS Microbiol Rev* **46**:1-14

Bergersen FJ, Turner GL (1979) Systems utilizing oxygenated leghemoglobin and myoglobin as sources of free dissolved O_2 at low concentrations for experiments with bacteria. *Anal Biochem* **90**:165–74

Bergersen FJ, Turner GL (1980) Properties of terminal oxidase systems of bacteroids from root nodules of soybean and cowpea and of N-fixing bacteria grown in continuous culture. *J Gen Microbiol* **188**:235–52

Bignell DE, Eggleton P (2000) Termites in ecosystems. In: Abe T, Higashi M, Bignell DE (eds.). Termites: Evolution, Sociality, Symbiosis, Ecology, Kluwer Academic Publications, Dordrecht, Netherlands, 363–387

Bignell DE (2010) Termites. In: Reay D, Smith P, van Amstel A (eds.). Methane and climate change. Earthscan, London, United Kingdom, 62–73

Boga H, Ji R, Ludwig R, Brune A (2007) *Sporotalea propionica* gen. nov. sp. nov., a hydrogen-oxidizing, oxygen-reducing, propionigenic firmicute from the intestinal tract of a soil-feeding termite. *Arch Microbiol* **187**:15–27

Bogachev A, Murtazina RA, Skulachev VP (1997) The Na+/e- stoichiometry of the Na+-motive NADH: quinone oxidoreductase in *Vibrio alginolyticus*. *FEBS lett* **409**:475–7

Borisov VB, Forte E, Davletshin A, Mastronicola D, Sarti P, Giuffre A (2013) Cytochrome *bd* oxidase from *Escherichia coli* displays high catalase activity: An additional defense against oxidative stress. *FEBS Lett* **587**:2214–8

Bou Khalil JY, Benamar S, Baudoin J-P, Croce O, Blanc-Tailleur C, Pagnier I, Raoult D, La Scola B (2016) Developmental cycle and genome analysis of "*Rubidus massiliensis*," a new *Vermamoeba vermiformis* pathogen. *Front Cell Infect Microbiol* **6**:31

Bourguignon T, Lo N, Dietrich C, Šobotník J, Sidek S, Roisin Y, Brune A, Evans TA (2018) Rampant host switching shaped the termite gut microbiome. *Curr Biol* **28**:649-54

Breznak JA, Brune A (1994) Role of microorganisms in the digestion of lignocellulose by termites. *Annu Rev Entomol* **39**:453–87

Breznak JA (2000) Termites. In: Abe T, Higashi M, Bignell DE (eds.). Termites: Evolution, Sociality, Symbiosis, Ecology, Kluwer Academic Publications, Dordrecht, Netherlands, 209–231

Breznak JA, Leadbetter JR (2002) Termite gut spirochetes. In: Dworkin M, Falkow S, Rosenberg E, Schleifer, K-H, Stackebrandt E (eds.). The prokaryotes: an online electronic resource for the microbiological community, 3rd edn, Springer, New York City, USA, 318-29

Brugerolle G, Radek R (2006). Symbiotic protozoa of termites. In: König H, Varma A (eds.). Soil Biology. Springer-Verlag, Heidelberg, Germany, 243–269.

Brune A, Emerson D, Breznak JA (1995) The termite gut microflora as an oxygen sink: microelectrode determination of oxygen and pH gradients in guts of lower and higher termites. *Appl Environ Microbiol* **61**: 2681–7

Brune A, Kühl M (1996) pH profiles of the extremely alkaline hindguts of soil-feeding termites (Isoptera: Termitidae) determined with microelectrodes. *J Insect Physiol* **42**:1121–7

Brune A (2014) Symbiotic digestion of lignocellulose in termite guts. *Nat Rev Microbiol* **12**:168–80

Brune A, Dietrich C (2015) The gut microbiota of termites: digesting the diversity in the light of ecology and evolution. *Annu Rev Microbiol* **69**:145–166

Brune A (2018) Methanogens in the digestive tract of termites. In: Hackstein J (ed.). (Endo)symbiotic Methanogenic Archaea. Springer-Verlag, Heidelberg, Germany, 81–101.

Brzuszkiewicz E, Weiner J, Wollherr A, Thürmer A, Hüpeden J, Lomholt HB, Kilian M, Gottschalk G, Daniel R, Mollenkopf H-J, Meyer TF, Brüggemann H (2011) Comparative genomics and transcriptomics of *Propionibacterium acnes*. *PLoS One* **6**:e21581

Buček A, Šobotník J, He S, Shi M, McMahon DP, Holmes EC, Rosin Y, Lo N, Bourguignon T (2019) Evolution of termite symbiosis informed by transcriptome-based phylogenies. *Curr Biol* **29**:3728–34

Buček A, Wang M, Šobotník J, Hellemanns S, Sillam-Dussès D, Mizumoto N, Stiblík P, Clitheroe C, Lu T, Gonzáles Plaza JJ, Mohogan A, Rafanomezantsoa JJ, Fisher B, Engel MS, Roisin Y, Evans TA, Scheffrahn R, Bourguignon T (2022) Molecular phylogeny reveals the past transoceanic voyages of drywood termites (Isoptera, Kalotermitidae). *Mol Biol Evol* msac093

Buckel W, Thauer RK (2013) Energy conservation via electron bifurcating ferredoxin reduction and proton/Na+ translocating ferredoxin oxidation. *Biochim Biophys Acta* **1827**:94–113

Castelli M, Lanzoni O, Nardi T, Lometto S, Modeo L, Potekhin A, Sassera D, Petroni G (2021) '*Candidatus* Sarmatiella mevalonica' endosymbiont of the ciliate *Paramecium* provides insights on evolutionary plasticity among Rickettsiales. *Environ Microbiol* **23**:1684–701

Chang HY, Hemp J, Chen Y, Fee Ja, Gennis RB (2009) The cytochrome ba3 oxygen reductase from Thermus thermophilus uses a single input channel for proton delivery to the active site and for proton pumping. *PNAS* **106**:16169–73

Chaumeil P-A, Mussig AJ, Hugenholtz P, Parks DH (2019) GTDB-Tk: a toolkit to classify genomes with the Genome Taxonomy Database. *Bioinformatics* **36**:1925–7

Chen IA, Chu K, Palaniappan K, Pillay M, Ratner A, Huang J, Huntemann M, Varghese N, White JR, Seshadri R, and Smirnova T (2019) IMG/M v.5.0: an integrated data management and comparative analysis system for microbial genomes and microbiomes. Nucleic Acids Res **47**:D666–D677

Chen J, Strous M (2013) Denitrification and aerobic respiration, hybrid electron transport chains and co-evolution. *Biochim Biophys Acta* **1827**:136–44

Cherrier M, Brune A (2003) The gut microenvironment of helicid snails (Gastropoda: Pulmonata): in-situ profiles of pH, oxygen, and hydrogen determined by microsensors. *Can J Zool* **81**:928–35

Chin KJ, Liesack W, Janssen PH (2001) *Opitutus terrae* gen. nov., sp. nov., to accommodate novel strains of the division 'Verrucomicrobia' isolated from rice paddy soil.Int. J Syst Evol Microbiol **51**:1965–8

Cho J-C, Hanssen PH, Shieh WY, Hedlund BP (2015) *Opitutaceae*. In: Trujillo ME, Dedysh S, DeVos P, Hedlund B, Kämpfer P, Rainey FA, Whitman WB (eds.). Bergey's Manual of Systematics of Archaea and Bacteria. John Wiley and Sons, Inc, Hoboken, USA, 536

Choo YJ, Lee K, Song J, Cho JC (2007) *Puniceicoccus vermicola* gen. nov., sp. nov., a novel marine bacterium, and description of *Puniceicoccaceae* fam. nov., Puniceicoccales ord. nov., *Opitutaceae* fam. nov., *Opitutales* ord. nov. and *Opitutae* classis nov. in the phylum 'Verrucomicrobia'. *Int J Syst Evol Microbiol* **57**:532–7

Chouvenc T, Šobotník J, Engel MS, Bourguignon T (2021) Termite evolution: mutualistic associations, key innovations, and the rise of Termitidae. *Cell Mol Life Sci* **78**:2749–69

Cleveland LR (1924) The physiological and symbiotic relationships between the intestinal protozoa of termites and their host, with special reference to *Reticulitermes flavipes* Kollar. *Biol Bull Mar Biol Lab* **46**:117–227

Colburn-Clifford J, Allen C (2010) A *cbb*$_3$-type cytochrome c oxidase contributes to *Ralstonia solanacearum* R3bv2 growth in microaerobic environments and to bacterial wilt disease development in tomato. *Mol Plant Microbe Interact* **23**:1042–52

Comolli JC, Donohue TJ (2004) Differences in two *Pseudomonas aeruginosa cbb*$_3$ cytochrome oxidases. *Mol Microbiol* **51**:1193–203

Cotter PA, Gunsalus RP (1992) Contribution of the *fnr* and *arcA* gene products in coordinate regulation of cytochrome *o* and *d* oxidase (*cyoABCD* and *cydAB*) genes in *Escherichia coli*. *FEMS Microbiol Lett* **91**:31–6

Crofts AR (2004) The cytochrome bc_1 complex: function in the context of structure. *Annu Rev Physiol* **66**:689–733

Cunningham LM, Pitt M, Williams HD (1997) The *cioAB* genes from *Pseudomonas aeruginosa* code for a novel cyanide-insensitive terminal oxidase related to the cytochrome bd quinol oxidases. *Mol Microbiol* **24**:579–91

Daims H, Brühl A, Amann RI, Schleifer K-H, Wagner M (1999) The domain-specific probe EUB338 is insufficient for the detection of all bacteria: Development and evaluation of a more comprehensive probe set. *Syst Appl Microbiol* **22**:434–44

Daims H, Stoecker K, Wagner M (2005) Fluorescence in situ hybridization for the detection of prokaryotes. In: Molecular Microbial Ecology. 213–29

Dank A, van Mastrigt O, Boeren S, Lillevang SK, Abee T, Smid EJ (2021) *Propionibacterium freudenreichii* thrives in microaerobic conditions by complete oxidation of lactate to CO_2. *Environ Microbiol* **23**:3116–29

Davies RG, Eggleton P, Jones DT, Gathorne-Hardy FJ, Hernández LM (2003) Evolution of termite functional diversity: analysis and synthesis of local ecological and regional influences on local species richness. J Biogeogr 30:847–77

Degnan PH, Yu S, Sisneros N, Wing RA, Moran NA (2009) *Hamiltonella defensa*, genome evolution of protective bacterial endosymbiont from pathogenic ancestors. *PNAS* **106**:9063–8

Derrien M, Vaughan EE, Plugge CM, de Vos WM (2004) *Akkermansia muciniphila* gen. nov., sp. nov., a human intestinal mucin-degrading bacterium. *Int J Syst Evol Microbiol* **54**:1469–76

Desai MS, Strassert JFH, Meuser K, Hertel H, Ikeda-Ohtsubo W, Radek R, Brune A (2010) Strict cospeciation of devescovinid flagellates and Bacteroidales ectosymbionts in the gut of dry-wood termites (*Kalotermitidae*). *Environ Microbiol* **12**:2120–32

Desai MS, Brune A (2012) *Bacteroidales* ectosymbionts of gut flagellates shape the nitrogen-fixing community in dry-wood termites. *ISME J* **6**:1302–13

Dietrich C, Köhler T, Brune A (2014) The cockroach origin of the termite gut microbiota: Patterns in bacterial community structure reflect major evolutionary events. *Appl Environ Microbiol* **80**:2261–9

D´mello R, Poole RK (1995) The oxygen affinity of cytochrome bo_3 in *Escherichia coli* determined by the deoxygenation of oxyleghemoglobin and oxymyoglobin: Km values for oxygen are in the sub-micromolar range. *J Bacteriol* **177**:867–70

D´mello R, Hill S, Poole RK (1996) The cytochrome *bd* quinol oxidase in *Escherichia coli* has an extremely high oxygen affinity and two oxygen-binding haems: implications for regulation of activity in vivo by oxygen inhibition. *Microbiol* **142**: 755–63

Dolan M (2001) Speciation of termite gut protists: the role of bacterial symbionts. *Int Microbiol* **4**:203–8

Driscoll TP, Verhoeve VI, Guilotte ML, Lehman SS, Rennoll SA, Beier-Sexton M, Sayeedur Rahman M, Azad AF, Gillespie JJ (2017) Wholly Rickettsia! reconstructed metabolic profile of the quintessential bacterial parasite of eukaryotic cells. *mBio* **8**:e00859–17

Ebert A, Brune A (1997) Hydrogen concentration profiles at the oxic-anoxic interface: a microsensor study of the hindgut of the wood-feeding lower termite Reticulitermes flavipes (Kollar). *Appl Environ Microbiol* **63**:4039–46

Eddy SR (2011) Accelerated profile HMM searches. *PLoS Comput Biol* **7**:e1002195

Edwards GE, Nakamoto H (1985) Pyruvate,Pi dikinase and NADP-Malate dehydrogenase in C4 photosynthesis: properties and mechanism of light/dark regulation. *Ann Rev Plant Physiol* **36**:255–86

El-Gebali S, Mistry J, Bateman A, Eddy SR, Luciani A, Potter SC, Qureshi M, Richardson LJ, Salazar GA, Smart A, Sonnhammer ELL, Hirsch L, Paladin L, Piovesan D, Tosatto SCE, Finn RD (2019) The Pfam protein families database in 2019. *Nucleic Acids Res* **47**:D427–D432

Engel P, Moran NA (2013) The gut microbiota of insects–diversity in structure and function. *FEMS Microbiol Rev* **37**:699–735

Falkowski PG, Fenchel T, Delong EF (2008) The microbial engines that drive Earth's biogeochemical cycles. *Science* **320**:1034–9

Fang H, Chen W, Wang B, Li X, Liu S-J, Yang H (2015) Cultivation and characterization of symbiotic bacteria from the gut of *Reticulitermes chinensis*. *Appl Environ Biotechnol* **1**:3–12

Fenchel T, Finlay B (2008) Oxygen and the spatial structure of microbial communities. *Biol Rev* **83**:553–69

Feng X, Zou Q-H, Zhang X-Y, Ye M-Q, Du Z-J (2020) *Oceanipulchritudo coccoides* gen. nov., sp. nov., isolated from marine sediment within the family *Puniceicoccaceae*. *Int J Syst Evol Microbiol* **70**:5654–64

Figueirêdo RECR, Vasconcellos A, Policarpo IS, Alves RRN (2015) Edible and medicinal termites: a global overview. *J Ethnobiol Ethnomed* **11**:29

Fuchs G (2014) Zentrale Stoffwechselwege. In: Fuchs G (ed.). Allgemeine Mikrobiologie. Thieme, New York, USA, **8**:246–279

Fuhrman JA, McCallum K, Davis AA (1993) Phylogenetic diversity of subsurface marine microbial communities from the Atlantic and Pacific Oceans. *Appl Environ Microbiol* **59**:1294–302

Fuerst JA (2013) The PVC superphylum: exceptions to the bacterial definition? *Antonie van Leeuwenhoek* **104**:451–66

Gaju-Ricard M, Notario MJ, Mora R, Alcaide E, Moreno T, Molero-Baltanás R, Bach C (2002) Termite damage to buildings in the province of Cordoba, Spain. *Sociobiology* 40:75–85

Gilroy R, Ravi A, Getino M, Pursley I, Horton DL, Alikhan N-F, Baker D, Gharbi K, Hall N, Watson M, Adriaenssens EM, Foster-Nyarko E, Jarju S, Secka A, Antonio M, Oren A, Chaudhuri RR, La Ragione R, Hildebrand F, Pallen MJ (2021) Extensive microbial diversity within the chicken gut microbiome revealed by metagenomics and culture. *Peer J* **9**:e10941

Greening C, Ambarish B, Carere CR, Jackson CJ, Taylor MC, Stott MB, Cook GM, Morales SE (2016) Genomic and metagenomic surveys of hydrogenase distribution indicate H_2 is a widely utilised energy source for microbial growth and survival. *ISME J* **10**:761-77

Haft DH, Selengut, White O (2003) The TIGRFAMs database of protein families. *Nucleic Acids Res* **31**:371–3

He S, Stevens SLR, Chan L-K, Bertilsson S, del Rio TG, Tringe SG, Malmstrom RR, McMahon KD (2017) Ecophysiology of freshwater *Verrucomicrobia* inferred from metagenome-assembled genomes. *mSphere* **2**: e00277–17

Hedlund BP, Gosink JJ, Staley JT (1997) *Verrucomicrobia* div. nov., a new division of the bacteria containing three new species of *Prosthecobacter*. *Antonie Van Leeuwenhoek* **72**:29–38

Heinz E, Hacker C, Dean P, Mifsud J, Goldberg AV, Williams TA, Nakjang S, Gregory A, Hirt RP, Lucocq JM, Kunji ERS, Embley TM (2014) Plasma membrane-located purine nucleotide transport proteins are key components for host exploitation by microsporidian intracellular parasites. *PLoS Path* **10**:e1004547

Hemp J, Robinson DE, Ganesan KB, Martinez TJ, Kelleher NL, Gennis RB (2006) Evolutionary migration of a post-translationally modified active-site residue in the protonpumping heme-copper oxygen reductases. *Biochemistry* **45**:15405–10

Hemp J, Han H, Roh JH, Kaplan S, Martinez TJ, Gennis RB (2007) Comparative genomics and site-directed mutagenesis support the existence of only one input channel for protons in the C-family (*cbb_3* oxidase) of heme−copper oxygen reductases. *Biochemistr*y **46**:9963–72

Henrici AT, Johnson DE (1935) Studies of freshwater bacteria. II. Stalked bacteria, a new order of Schizomycetes. *J Bacteriol* **30**:61–93

Hershberg D, Petrov PA (2010) Evidence that mutation is universally biased towards AT in bacteria. *PLoS Genet* **6**:e1001115

Hervé V, Liu P, Dietrich C, Sillam-Dussès D, Stiblik P, Šobotník J, Brune A (2020) Phylogenomic analysis of 589 metagenome-assembled genomes encompassing all major prokaryotic lineages from the gut of higher termites. *Peer J* **8**:e8614

Hirai T, Osamura T, Ishii M, Arai H (2016) Expression of multiple *cbb*$_3$ cytochrome *c* oxidase isoforms by combinations of multiple isosubunits in *Pseudomonas aeruginosa*. PNAS **113**:12815–9

Holland HD (2006) The oxygenation of the atmosphere and oceans. *Phil Trans R Soc B* **361**:903–15

Hongoh Y, Ohkuma M, Kudo T (2003) Molecular analysis of bacterial microbiota in the gut of the termite *Reticulitermes speratus* (Isoptera; *Rhinotermitidae*). *FEMS Microbiol Ecol* **44**:231–42

Hongoh Y, Deevong P, Inoue T, Moriya S, Trakulnaleamsai S, Ohkuma M, Vongkaluang C, Noparatnaraporn N, Kudo T (2005) Intra- and interspecific comparisons of bacterial diversity and community structure support coevolution of gut microbiota and termite host. *Appl Environ Microbiol* **71**:6590–9

Hongoh Y, Sharma VK, Prakash T, Noda S, Toh H, Taylor TD, Kudo T, Sakaki Y, Toyoda A, Hattori M, Ohkuma M (2008a) Genome of an endosymbiont coupling N_2 fixation to cellulolysis within protist cells in termite gut. *Science* **322**:1108–9

Hongoh Y, Sharma VK, Prakash T, Noda S, Taylor TD, Kudo T, Sakaki Y, Toyoda A, Hattori M, Ohkuma M (2008b) Complete genome of the uncultured Termite Group 1 bacteria in a single host protist cell. *PNAS* **105**:5555–60

Hongoh Y (2011) Toward the functional analysis of uncultivable, symbiotic microorganisms in the termite gut. *Cell Mol Life Sci* **68**:1311–25

Hou S, Makarova KS, Saw JHW, Senin P, Ly BV, Zhou Z, Ren Y, Wang J, Galperin MY, Omelchenko MV, Wolf YI, Yutin N, Koonin EV, Stott MB, Mountain BW, Crowe MA, Smirnova AV, Dunfield PF, Feng L, Wang L, Alam M (2008) Complete genome sequence of the extremely acidophilic methanotroph isolate V4, *Methylacidiphilum infernorum*, a representative of the bacterial phylum *Verrucomicrobia*. *Biol Direct* **3**:26

Husnik F, McCutcheon JP (2016) Repeated replacement of an intrabacterial symbiont in the tripartite nested mealybug symbiosis. *PNAS* **13**:E5416–24

Hyatt D, Chen G, Locascio PF, Land ML, Larimer FW, Hauser LJ (2010) Prodigal, prokaryotic gene recognition and translation initiation site identification. *BMC Bioinfo* **11**:119–119

Iida T, Ohkuma M, Ohtoko K, Kudo T (2000) Symbiotic spirochetes in the termite hindgut: phylogenetic identification of ectosymbiotic spirochetes of oxmonad protists. *FEMS Microbiol Ecol* **34**:17–26

Inward D, Beccaloni G, Eggleton P (2007) Death of an order: a comprehensive molecular phylogenetic study confirms that termites are eusocial cockroaches. *Biol Lett* **3**:331–5

Ikeda-Ohtsubo W, Brune A (2009) Cospeciation of termite gut flagellates and their bacterial endosymbionts: *Trichonympha* species and '*Candidatus* Endomicrobium trichonymphae'. *Mol Ecol* **18**:332–42

Ikeda-Ohtsubo W, Strassert JFH, Köhler T, Mikaelyan A, Gregor I, McHardy AC, Green Tringe S, Hugenholtz P, Radek R, Brune A (2016) '*Candidatus* Adiutrix

intracellularis', an endosymbiont of termite gut flagellates, is the first representative of a deep-branching clade of Deltaproteobacteria and a putative homoacetogen. *Environ Microbiol* **18**:2548–64

Jain C, Rodriguez-R LM, Phillippy AM, Konstantinidis KT, Aluru S (2018) High throughput ANI analysis of 90k prokaryotic genomes reveals clear species boundaries. *Nat Comm* **9**:5114

Jones DT, Eggleton P (2010) Global biogeography of termites: a compilation of sources. In: Bignell D, Roisin Y, Lo N (eds.). Biology of Termites: A Modern Synthesis. Springer, Dordrecht, Netherlands, 477–98.

Kaila VRI, Wikström M (2021) Architecture of bacterial respiratory chains. *Nat Rev Microbiol* **19**:319–30

Kant R, van Passel MWJ, Sangwan P, Palva A, Lucas S, Copeland A, Lapidus A, Glavina del Rio T, Dalin E, Tice H, Bruce D, Goodwin L, Pitluck S, Chertkov O, Larimer FW, Land ML, Hauser L, Brettin TS, Detter JC, Han S, de Vos WM, Janssen PH, Smidt H (2011) Genome sequence of "*Pedosphaera parvula*" Ellin514, an aerobic verrucomicrobial isolate from pasture soil. *J Bacteriol* **193**:11

Kao W-C, Hunte C (2014) The molecular evolution of the Q_o motif. *Genome Biol Evol* **7**:1894–910

Kappler A, Brune A (2002) Dynamics of redox potential and changes in redox state of iron and humic acids during gut passage in soil-feeding termites (*Cubitermes* spp.). *Soil Biol Biochem* **34**:221–7

Katoh K, Stanley DM (2013) MAFFT multiple sequence alignment software version 7: improvements in performance and usability. *Mol Biol Evol* **30**:772–80

Kawakami T, Kuroki M, Ishii M, Igarashy Y, Arai H (2010) Differential expression of multiple terminal oxidases for aerobic respiration in *Pseudomonas aeruginosa*. *Environ Microbiol* **12**:1399–412.

Kirby H (1941) Organisms living on and in protozoa. In: Calkins GN, Summers FM (eds.) Protozoa in biological research. Columbia Univ Press, New York, USA, 1009–113

Kirby H (1944). The structural characteristics and nuclear parasites of some species of *Trichonympha* in termites. *Univ Calif (Berkeley) Publ Zool* **49**:185–282.

Köhler T, Dietrich C, Scheffrahn RH, Brune A (2012) High-resolution analysis of gut environment and bacterial microbiota reveals functional compartmentation of the gut in wood-feeding higher termites (*Nasutitermes* spp.). *Appl Envrion Microbiol* **78**:4691–701

Kohlstaedt M, Buschmann S, Langer JD, Xi H, Michel H (2017) Subunit CcoQ is involved in the assembly of the cbb_3-type cytochrome c oxidases from *Pseudomonas stutzeri* ZoBell but not required for their activity. *Biochim Biophys Acta* **1858**:231–8

Krumova K, Cosa G (2016) Overview of reactive oxygen species. In: Nonell S, Flors C (eds.). Singlet Oxygen: Applications in Biosciences and Nanosciences, The Royal society of chemistry, London, United Kingdom, 1–21

Kruse T, Ratnadevi CM, Erikstad H-A, Birkeland N-K (2019) Complete genome sequence analysis of the thermoacidophilic verrucomicrobial methanotroph "*Candidatus* Methylacidiphilum kamchatkense" strain Kam1 and comparison with its closest relatives. *BMC Genomics* **20**:642

Kühl M, Rickelt LF, Thar R (2008) Combined imaging of bacteria and oxygen in biofilms. *Appl Environ Microbiol* **73**:6289–95

Kuhnigk T, Branke J, Krekerler D, Cypionka H, König H (1996) A feasible role of sulfate-reducing bacteria in the termite gut. *System Appl Microbiol* **19**:139–49

Kuwahara H, Yuki M, Izawa K, Ohkuma M, Hongoh Y (2016) Genome of '*Ca*. Desulfovibrio trichonymphae', an H_2-oxidizing bacterium in a tripartite symbiotic system within a protist cell in the termite gut. *ISME J* **11**:766–76

Kuzma MM, Hunt S, Layzell DB (1993) Role of oxygen in the limitation and inhibition of nitrogenase activity and respiration rate in individual soybean nodules. *Plant Physiol* **101**:161–9

Kwong WK, Zheng H, Moran NA (2018) Convergent evolution of a modified, acetate-driven TCA cycle in bacteria. *Nat Microbiol* **2**:17067

Leger MM, Kolisko M, Kamikawa R, Stairs CW, Kume K, Čepička I, Silberman JD, Andersson JO, Xu F, Yabuki A, Eme L, Zhang Q, Takishita K, Inagaki Y, Simpson AGB, Hashimoto T, Roger AJ (2017) Organelles that illuminate the origins of *Trichomonas* hydrogenosomes and *Giardia* mitosomes. *Nat Ecol Evol* **1**:0092

Lemieux L, Calhoun MW, Thomas JW, Ingledew J, Gennis RB (1992) Determination of the ligands of the low spin heme of the cytochrome o ubiquinol oxidase complex using site-directed mutagenesis. *J Bacteriol Chem* **267**:2105–13

Lemos RS, Gomes CM, Santana M, LeGall J, Xavier AV, Teixeira M (2001) The 'strict' anaerobe *Desulfovibrio gigas* contains a membrane-bound oxygen-reducing respiratory chain. *FEBS Lett* **496**:40–3.

Letunic I, Bork P (2019) Interactive tree of life (iTOL) v4: recent updates and new developments. *Nucleic Acids Res* **47**:W256–W259

Lewis WH, Tahon G, Geesink P, Sousa DZ, Ettema TJG (2021) Innovations to culturing the uncultured microbial majority. *Nat Rev Microbiol* **19**:225-40

Liesack W, Stackebrandt E (1992) Occurrence of novel groups of the domain Bacteria as revealed by analysis of genetic material isolated from an Australian terrestrial environment. *J Bacteriol* **174**:5072–8

Lin JY, Russel JA, Sanders JG, Wertz JT (2016) *Cephaloticoccus* gen. nov., a new genus of 'Verrucomicrobia' containing two novel species isolated from *Cephalotes* ant guts. *Int J Syst Evol Microbiol* **66**:3034–40

Lin S-Y, Hameed A, Liu Y-C, Hsu Y-H, Hung M-H, Lai W-A, Young C-C (2017) *Ruficoccus amylovorans* gen. nov., sp. nov., an amylolytic and nitrate-reducing diazotroph of the family *Puniceicoccaceae*. *Int J Syst Evol Microbiol* **67**:956–62

Lo N, Engel MS, Cameron S, Nalepa CA, Tokuda G, Grimaldi D, Kitade O, Krishna K, Klass K-D, Maekawa K, Miura T, Thompson GJ (2007) Save Isoptera: A comment on Inward *et al. Biol Lett* **3**:562–3

Lo N, Eggleton P (2011) Termite phylogenetics and co-cladogenesis with symbionts. In: Bignell DE, Roisin Y, Lo N (eds.). Biology of Termites: A Modern Synthesis, Springer, Heidelberg, Germany, 27–50

Lopera J, Miller IJ, McPhail KL, Kwan JC (2017) Increased biosynthetic gene dosage in a genome-reduced defensive bacterial symbiont. *mSystems* **2**: e00096–17

Lu Z, Imlay JA (2021) When anaerobes encounter oxygen: mechanisms of oxygen toxicity, tolerance and defense. *Nat Rev Microbiol* **19**:774–85

Ludwig W, Strunk O, Westram R, Richter L, Meier H, Yadhukumar, Buchner A, Lai T, Steppi S, Jobb G, and Förster W (2004) ARB: a software environment for sequence data. *Nucleic Acids Res* **32**:1363–71

Major P, Embley M, Williams TA (2017) Phylogenetic diversity of NTT nucleotide transport proteins in free-living and parasitic bacteria and eukaryotes. *Genome Biol Evol* **9**:480–7

Mandon K, Kaminiski PA, Elmerich C (1994) Functional analysis of the *fixNOQP* region of *Azorhizobium caulinodans*. *J Bacteriol* **176**:2560–8

Manzano-Marín A, Coeur-d´acier A, Clamens A-L, Orvain C, Cruaud C, Barbe V, Jousselin E (2020) Serial horizontal transfer of vitamin-biosynthetic genes enables the establishment of new nutritional symbionts in aphids' di-symbiotic systems. *ISME J* **14**:259-73

Marteyn B, West NP, Browning DF, Cole JA, Shaw JG, Palm F, Mounier J, Prévost M-C, Sansonetti P, Tang CM (2010) Modulation of *Shigella* virulence in response to available oxygen *in vivo*. *Nature* **465**:355–8

McCutcheon JP, Moran NA (2012) Extreme genome reduction in symbiotic bacteria. *Nat Rev Microbiol* **10**:13–26

Meile L, Rohr LM, Geissmann TA, Herensperger M, Teuber M (2001) Characterization of the D-xylulose 5-phosphate/D-fructose 6-phosphate phosphoketolase gene (*xfp*) from *Bifidobacterium lactis*. *J Bacteriol* **183**:2929–36

Melo AMP, Bandeiras TM, Teixeira M (2004) New insights into type II NAD(P)H:quinone oxidoreductases. *Microbiol Mol Biol Rev* **68**:603–16

Mendler K, Chen H, Parks DH, Hug LA, Doxey AC (2019) AnnoTree: visualization and exploration of a functionally annotated microbial tree of life. *Nucleic Acids Res* **47**:4442–8

Mi H, Lazareva-Ulitsk, Loo R, Kejariwal A, Vandergriff J, Rabkin S, Guo N, Muruganujan A, Doremieux O, Campbell MJ, Kitano H, Thomas PD (2005) The PANTHER database of protein families, subfamilies, functions and pathways. *Nucleic Acids Res* **33**:D284–D288

Mikaelyan A, Dietrich C, Köhler T, Poulsen M, Sillam-Dussès D, Brune A (2015a) Diet is the primary determinant of bacterial community structure in the guts of higher termites. *Mol Ecol* **24**:5284-95

Mikaelyan A, Köhler T, Lampert N, Rohland J, Boga H, Meuser K, Brune A (2015b) Classifying the bacterial gut microbiota of termites and cockroaches: A curated phylogenetic reference database (DictDb). *Syst Appl Microbiol* **38**:472–82

Mikaelyan A, Meuser K, Brune A (2017a) Microenvironmental heterogeneity of gut compartments drives bacterial community structure in wood- and humus-feeding higher termites. *FEMS Microbiol Ecol* **93**:fiw210

Mikaelyan A, Thompson CL, Meuser K, Zheng H, Rani P, Plarre R, Brune A (2017b) High-resolution phylogenetic analysis of *Endomicrobia* reveals multiple acquisitions of endosymbiotic lineages by termite gut flagellates. *Environ Microbiol Rep* **9**:477–83

Minh BQ, Nguyen MAT, Von Haeseler A (2013) Ultrafast approximation for phylogenetic bootstrap. *Mol Biol Evol* **30**, 1188–95

Mitchell P (1975) Proton motive redoxmechanism of the cytochrome *b*-c_1 complex in the respiratory chain: proton motive ubiquinone cycle. *FEBS lett* **56**:1–6

Mitchell JD (2002) Termites as pests of crops, forestry, rangeland and structures in South Africa and their control. *Sociobiology* **40**:47–69

Mochizuki K, Inaoka DK, Mazet M, Shiba T, Fukuda K, Kurasawa H, Millerioux Y, Boshart M, Balogun EO, Harada S, Hirayama K, Bringaud F, Kita K (2020) The ASCT/SCS cycle fuels mitochondrial ATP and acetate production in *Trypanosoma brucei*. *Biochim Biophys Acta Bioenerg* **1861**:148283

Morris RL, Schmidt TM (2013) Shallow breathing: bacterial life at low O_2. *Nat Rev Microbiol* **11**:205–12

Myers KN, Conn D, Brown AMV (2021) essential amino acid enrichment and positive selection highlight endosymbiont's role in a global virus-vectoring pest. *mSystems* **6**:e01048–20

Nakajima H, Hongoh Y, Usami R, Kudo T, Ohkuma M (2005) Spatial distribution of bacterial phylotypes in the gut of the termite *Reticulitermes speratus* and the bacterial community colonizing the gut epithelium. *FEMS Microbiol Ecol* **54**:247–55

Neef A, Latorre A, Peretó J, Silva FJ, Pignatelli M, Moya A (2011) Genome economization in the endosymbiont of the wood roach *Cryptocercus punctulatus* due to drastic loss of amino acid synthesis capabilities. *Genome Biol Evol* **3**:1437–48

Nguyen LT, Schmidt HA, Von Haeseler A, Minh BQ (2015) IQ-TREE: A fast and effective stochastic algorithm for estimating maximum-likelihood phylogenies. *Mol Biol Evol* **32**, 268–74

Noda S, Iida T, Kitade O, Nakajima H, Kudo T, Ohkuma M (2005) Endosymbiotic Bacteroidales Bacteria of the Flagellated Protist *Pseudotrichonympha grassii* in the Gut of the Termite *Coptotermes formosanus*. *Appl Environ Microbiol* **71**:8811–17

Noda S, Kitade O, Inoue T, Kawai M, Kanuka M, Hiroshima K, Hongoh Y, Constantino R, Uys V, Zhong J, Kudo T, Ohkuma M (2007) Cospeciation in the triplex symbiosis of termite gut protists (*Pseudotrichonympha spp*.), their hosts, and their bacterial endosymbionts. **16**:1257–66

Noda S, Hongoh Y, Sato T, Ohkuma M (2008) Complex coevolutionary history of symbiotic Bacteroidales bacteria of various protists in the gut of termites. *BMC Ecol Biol* **9**:158

O´Brien RW, Breznak JA (1984) Enzymes of acetate and glucose metabolism in termites. *Insect Biochem* **14**:639–43

Ohkuma M, Sato T, Noda S, Ui S, Kudo T, Hongoh Y (2007) The candidate phylum 'Termite Group 1' of bacteria: phylogenetic diversity, distribution, and endosymbiont members of various gut flagellated protists. *FEMS Microbiol Ecol* **60**:467–76

Ohkuma M (2008) Symbiosis of flag345ellates and prokaryotes in the gut of lower termites. *Trends Microbiol* **16**:345–52

Ohkuma M, Brune A (2010) Diversity, structure, and evolution of the termite gut microbial community. In: Bignell DE, Roisin Y, Lo N (eds.). Biology of Termites: A Modern Synthesis, Springer, Heidelberg, Germany, 413–38

Olson DG, Hörl M, Fuhrer T, Cui J, Zhou J, Maloney MI, Amador-Noguez D, Tian L, Sauer U, Lynd LR (2017) Glycolysis without pyruvate kinase in *Clostridium thermocellum*. *Metab Eng* **39**:169–80

Oren A, Garrity GM (2021) Valid publication of the names of forty-two phyla of prokaryotes. *Int J Syst Evol Microbiol* **71**:005056

Otsuka S, Ueda H, Suenaga T, Uchino Y, Hamada M, Yokota A, Senoo K (2013) *Roseimicrobium gellanilyticum* gen. nov., sp. nov., a new member of the class Verrucomicrobiae. *Int J Syst Evol Microbiol* **63**:1982–6

Ouwerkerk JP, Aalvink S, Belzer C, de Vos WM (2016) *Akkermansia glycaniphila* sp. nov., an anaerobic mucin-degrading bacterium isolated from reticulated python faeces. *Int J Syst Evol Microbiol* **66**:4614–20

Parks DH, Imelfort M, Skennerton CT, Hugenholtz P, Tyson GW (2015) CheckM: Assessing the quality of microbial genomes recovered from isolates, single cells, and metagenomes. *Genome Res* **25**:1043–55

Parks DH, Rinke C, Chuvochina M, Chaumeil P-A, Woodcroft BJ, Evans PN, Hugenholtz P, Tyson GW (2017) Recovery of nearly 8,000 metagenome-assembled genomes substantially expands the tree of life. *Nat Microbiol* **2**:1533–42

Parks DH, Chuvochina M, Waite DW, Rinke C, Skarsheweski A, Chaumeil P-A, Hugenholtz P (2018) A standardized bacterial taxonomy based on genome phylogeny substantially revises the tree of life. *Nat Biotechnol* **36**:996–1007

Pereira MM, Santana M, Teixeira M (2001) A novel scenario for the evolution of heme-copper oxygen reductases. *Biochim Biophys Acta* **1505**:185–208.

Picone N, Blom P, Hogendoorn C, Frank J, van Alen T, Pol A, Gagliano AL, Jetten MSM, D´Allesandro W, Quatrini P, Op den Camp HJM (2021) Metagenome assembled genome of a novel verrucomicrobial methanotroph from Pantelleria Island. *Front Microbiol* **12**:666929

Pinos S, Pontarotti P, Raoult D, Baudoin JP, Pagnier I (2016) Compartmentalization in PVC super-phylum: evolution and impact. *Biol Direct* **11**:38

Pitt A, Schmidt J, Koll U, Hahn MW (2020) *Rariglobus hedericola* gen. nov., sp. nov., belonging to the Verrucomicrobia, isolated from a temperate freshwater habitat. *Int J Syst Evol Biol* **70**:1830–6

Ploug H (2001) Small-scale oxygen fluxes and remineralization in sinking aggregates. *Limnol Oceanogr* **46**:1624–31

Pol A, Heijmans K, Harhangi HR, Tedesco D, Jetten MSM, Op den Camp HJM (2007) Methanotrophy below pH 1 by a new Verrucomicrobia species. *Nature* **450**:874–8

Poole RK, Hill S (1997) Respiratory protection of nitrogenase activity in *Azotobacter vinelandii*–Roles of the terminal oxidases. *Biosci Rep* **17:**307–17

Preisig O, Zufferey R, Thöny-Meyer L, Appleby CA, Hennecke H (1996) A high affinity cbb3-type cytochrome oxidase terminates the symbiosis-specific respiratory chain of *Bradyrhizobium japonicum*. *J Bacteriol* **78**:1532–36

Price DRG, Feng H, Baker JD, Bavan S, Luetje CW, Wilson ACC (2013) Aphid amino acid transporter regulates glutamine supply to intracellular bacterial symbionts. *PNAS* **111**:320–5

Qui Y-L, Kuang X-Z, Shi X-S, Yuan X-Z, Guo R-B (2014) *Terrimicrobium sacchariphilum* gen. nov., sp. nov., an anaerobic bacterium of the class 'Spartobacteria' in the phylum Verrucomicrobia, isolated from a rice paddy field. *Int J Syt Evol Microbiol* **64**:1718–23

Radek R (1997) *Spirotrichonympha minor* n. sp., a new hypermastigote termite flagellate. *Eur J Protistol* **33**:360–74.

Rast P, Glöckner I, Boedeker C, Jeske O, Wiegand S, Reinhardt R, Schumann P, Rhode M, Spring S, Glöckner FO, Jogler C, Jogler M (2017) Three Novel Species with Peptidoglycan Cell Walls form the New Genus *Lacunisphaera* gen. nov. in the Family *Opitutaceae* of the Verrucomicrobial Subdivision 4. *Front Microbiol* **8**:202

Reid TD, Brunham RC, Shen C, Gill SR, Heidelberg JF, White O, Hickey EK, Peterson J, Utterback T, Berry K, Bass S, Linher K, Weidman J, Khouri H, Craven B, Bowman C, Dodson R, Gwinn M, Nelson W, DeBoy R, Kolonay J, McClarty G, Salzberg SL, Eisen J, Fraser CM (2000) Genome sequences of *Chlamydia trachomatis* MoPn and *Chlamydia pneumoniae* AR39. *Nucleic Acids Res* **15**:1397–406

Refojo PN, Teixeira M, Pereira MM (2012) The Alternative complex III: Properties and possible mechanisms for electron transfer and energy conservation. *Biochim Biophys Acta Bioenerg* **1817**:1852–9

Rochman FF, Kim J-J, Rijpstra JSS, Schumann P, Verbecke TJ, Dunfield PF (2018) *Oleiharenicola alkalitolerans* gen. nov., sp. nov., a new member of the phylum *Verrucomicrobia* isolated from an oilsands tailings pond. *Int J Syst Evol Microbiol* **68**:1078–84

Rodriguez-Contreras D, Hamilton N (2014) Gluconeogenesis is *Leishmania mexicana*: Contribution of glycerol kinase, phosphoenolpyruvate carboxykinase and pyruvate phosphate dikinase. *J Biol Chem* **289**:32989–3000

Rösel J, Radek R, Hausmann K (1996). Ultrastructure of the trichomonad flagellate *Stephanonympha nelumbium*. *J Euk Microbiol* **43**:505–11.

Saiki K, Mogi T, Anraku Y (1992) Heme O biosynthesis in Escherichia coli: the cyoE gene in the cytochrome *bo* operon encodes a protoheme IX farnesyltransferase. *Biochem Biophys Res Commun* **189**:1491–7

Salmon K, Hung S-p, Mekjian K, Baldi P, Hatfield GW, Gunsalus RP (2003) Global Gene Expression Profiling in *Escherichia coli* K12. The effects of oxygen availability and FNR. *J Biol* Chem **278**:29837–55

Sangwan PX, Chen X, Hugenholtz P, Janssen PH (2004) *Chthoniobacter flavus* gen. nov., sp. nov., the first pure-culture representative of subdivision two, Spartobacteria classis nov., of the phylum Verrucomicrobia. *Appl Environ Microbiol* **70**:5875–81

Santarella-Mellwig R, Franke J, Jaedicke A, Gorjánácz M, Bauer U, Budd A, Mattaj IW, Devos DP (2010) The compartmentalized bacteria of the Planctomycetes-Verrucomicrobia-Chlamydiae superphylum have membrane coat-like proteins. *PLoS Biol* **8**:e1000281

Sato T, Hongoh Y, Noda S, Hattori S, Ui S, Ohkuma M (2008) *Candidatus* Desulfovibrio trichonymphae, a novel intracellular symbiont of the flagellate *Trichonympha agilis* in termite gut. *Environ Microbiol* **4**:1007–15

S**ato T, Kuwahara H, Fujita K, Noda S, Kihara K, Yamada A, Ohkuma M, Hongoh Y** (2014) Intranuclear verrucomicrobial symbionts and evidence of lateral gene transfer to the host protist in the termite gut. *ISME J* **8**:1008–19

Schauer C, Thompson CL, Brune A (2012) The bacterial community in the gut of the cockroach *Shelfordella lateralis* reflects the close evolutionary relatedness of cockroaches and termites. *Appl Environ Microbiol* **78**:2758–67

Scheuermayer M, Gulder TAM, Bringmann G, Hentschel U (2006) *Rubritalea marina* gen. nov., sp. nov., a marine representative of the phylum 'Verrucomicrobia', isolated from a sponge (Porifera). *Int J Syst Evol Microbiol* **56**:2119–24

Schindelin J, Arganda-Carreras I, Frise E, Kaynig V, Longair M, Pitzsch T, Preibisch S, Rueden C, Saalfeld S, Schmid B, Tinevez J-Y, White DJ, Hartenstein V, Eliceiri K, Tomancak P, Cadona A (2012) Fiji: an open-source platform for biological-image analysis. *Nat Methods* **9**:676–82

Schlesner H (1987) *Verrucomicrobium spinosum* gen. nov, sp. nov: a fimbriated prosthecate bacterium. *Syst Appl Microbiol* **10**:54–6

Schmitz RA, Peeters SH, Versantvoort W, Picone N, Pol A, Jetten MS, Op de Camp HJM (2021) Verrucomicrobial methanotrophs: ecophysiology of metabolically versatile acidophiles. *FEMS Microbiol Rev* **45**:1–20

Schulz BE, Chan SI (1998) Thermodynamics of electron transfer in *Escherichia coli* cytochrome bo_3. *PNAS* **95**:11643–8

Schwöppe C, Winkler HH, Neuhaus HE (2002) Properties of the glucose-6-phosphate transporter from *Chlamydia pneumoniae* (HPTcp) and the glucose-6-phosphate sensor from *Escherichia coli* (UhpC). *J Bacteriol* **184**:2108–15

Seemann T (2014) Prokka: rapid prokaryotic genome annotation. *Bioinformatics* **30**:2068–9

Serra V, Gammuto L, Nitla V, Castelli M, Lanzoni O, Sassera D, Bandi C, Sandeep BV, Verni F, Modeo L, Petroni G (2020) Morphology, ultrastructure, genomics, and phylogeny of *Euplotes vanleeuwenhoeki* sp. nov. and its ultra-reduced endosymbiont "*Candidatus* Pinguicoccus supinus" sp. nov. *Sci Rep* **10**:20311

Sharma V, Wikström M (2016) The role of the K-channel and the active-site tyrosine in the catalytic mechanism of cytochrome c oxidase. *Biochim Biophys Acta Bioenerg* **1857**:1111–5

Shi L Sohaskey CD, Kana BD, Dawes S, North RJ, Mizrahi V, Gennaro ML (2005) Changes in energy metabolism of *Mycobacterium tuberculosis* in mouse lung and under in vitro conditions affecting aerobic respiration. *PNAS* **102**:15629–34

Shieh WY, Jean WD (1998) *Alterococcus agarolyticus*, gen.nov., sp.nov., a halophilic thermophilic bacterium capable of agar degradation. *Can J Microbiol* **44**:637–45

Shigenobu S, Watanabe H, Hattori M, Sakaki Y, Ishikawa H (2000) Genome sequence of the endocellular bacterial symbiont of aphids *Buchnera* sp. APS. *Nature* **407**:81–6

Silva FM, Kostygov AY, Spodareva VV, Butenko A, Tossou R, Lukeš J, Yurchenko V, Alves JMP (2018) The reduced genome of *Candidatus* Kinetoplastibacterium sorsogonicusi, the endosymbiont of *Kentomonas sorsogonicus* (*Trypanosomatidae*): loss of the haem-synthesis pathway. *Parasitology* **145**:1287–93

Slamovits CH, Keeling PJ (2006) Pyruvate-phosphate dikinase of Oxymonads and Parabasalia and the evolution of pyrophosphate-dependent glycolysis in anaerobic Eukaryotes. *Eukaryot Cell* **5**:148-54

Søndergaard D, Pedersen CNS, Greening C (2016) HydDB: A web tool for hydrogenase classification and analysis. *Sci Rep* **6**:34212

Song Y, Hervé V, Radek R, Pfeiffer F, Zheng H, Brune A (2021) Characterization and phylogenomic analysis of *Breznakiella homolactica* gen. nov. sp. nov. indicate that termite gut treponemes evolved from non-acetogenic spirochetes in cockroaches. *Environ Microbiol* **23**:4228-–45

Soo RM, Hemp J, Parks DH, Fischer WW, Hugenholtz P (2017) On the origins of oxygenic photosynthesis and aerobic respiration in Cyanobacteria. *Science* **355**:1436–40

Sousa JS, Calisto F, Langer JD, Mills DJ, Refojo PN, Teixeria M, Kühlbrandt W, Vonck J, Pereira MM (2018) Structural basis for energy transduction by respiratory alternative complex III. *Nat comm* **9**:1728

Sprenger WW, Hackstein JHP, Keltjens JT (2007) The competitive success of *Methanomicrococcus blatticola,* a dominant methylotrophic methanogen in the cockroach hindgut, is supported by high substrate affinities and favorable thermodynamics. *FEMS Microbiol Ecol* **60**:266-275

Stamatakis A (2014) RAxML version 8: A tool for phylogenetic analysis and post-analysis of large phylogenies. *Bioinformatics*, **30**:1312–3

Stevenson BS, Eichorst SA, Wertz JT, Schmid TM Breznak JA (2004) New strategies for cultivation and detection of previously uncultured microbes. *Appl Environ Microbiol* **70**:4748–55

Stingl U, Radek R, Brune A (2005) "Endomicrobia": cytoplasmic symbionts of termite gut protozoa form a separate phylum of prokaryotes. *Appl Environ Microbiol* **71**:1473–9

Strassert JFH, Köhler T, Wienemann THG, Ikeda-Ohtsubo W, Faivre N, Franckenberg S, Plarre R, Radek R, Brune A (2012) '*Candidatus* Ancillula trichonymphae', a novel lineage of endosymbiotic Actinobacteria in termite gut flagellates of the genus *Trichonympha*. *Environ Microbiol* **14**:3259–70

Strassert JFH, Mikaelyan A, Woyke T, Brune A (2016) Genome analysis of '*Candidatus* Ancillula trichonymphae', first representative of a deep-branching clade of Bifidobacteriales, strengthens evidence for convergent evolution in flagellate endosymbionts. *Environ Microbiol Rep* **8**:865–73

Swem DL, Bauer CE (2002) Coordination of ubiquinol oxidase and cytochrome cbb_3 oxidase expression by multiple regulators in *Rhodobacter capsulatus*. *J Bacteriol* **184**:2815-20

Szuróczki S, Abbaszade G, Szabó A, Bóka K, Schumann P, Tóth E (2020) *Phragmitibacter flavus* gen. nov., sp. nov. a new member of the family Verrucomicrobiaceae. *Int J Syst Evol Microbiol* **70**:2108–14

Tamames J, Gil R, Latorre A, Peretó J, Silva FJ, Moya A (2007) The frontier between cell and organelle: genome analysis of *Candidatus* Carsonella ruddii. *BMC Evol Biol* **7**:181

Tasaki E, Sakurai H, Nitao M, Matsuura K, Iuchi Y (2007) Uric acid, an important antioxidant contributing to survival in termites. *PLoS one* **12**:e0179426

Tayasu I, Abe T, Eggleton P, Bignell DE (1997) Nitrogen and carbon isotope ratios in termites: an indicator of trophic habit along the gradient from wood-feeding to soil-feeding. *Ecol Entomol* **22**:343–51

Tegtmeier D, Riese C, Geissinger O, Radek R, Brune A (2016) *Breznakia blatticola* gen. nov. sp. nov. and Breznakia pachnodae sp. nov., two fermenting bacteria isolated from insect guts, and emended description of the family Erysipelotrichaceae. *Syst Appl Microbiol* **39**:319–29

Tegtmeier D, Belitz A, Radek R, Heimerl T, Brune A (2018) *Ereboglobus luteus* gen. nov. sp. nov. from cockroach guts, and new insights into the oxygen relationship of the genera *Opitutus* and *Didymococcus* (Verrucomicrobia: *Opitutaceae*). Syst Appl Microbiol **41**:101–12

Tiedje J, Sexstone A, Parkin T, Revsbech N, Shelton D (1984) Anaerobic processes in soil. *Plant Soil* **76**:197–212

Tholen A, Brune A (2000) Impact of oxygen on metabolic fluxes and *in situ* rates of reductive acetogenesis in the hindgut of the wood-feeding termite *Reticulitermes flavipes*. *Environ Microbiol* **2**:436–49

Tholen A, Pester M, Brune A (2007) Simultaneous methanogenesis and oxygen reduction by *Methanobrevibacter cuticularis* at low oxygen fuxes. *FEMS Microl Ecol* **62**:303–12

Tokuda G, Lo N, Watanabe H, Arakawa G, Matsumoto T, Noda H (2004) Major alteration of the expression site of endogenous cellulases in members of an apical termite lineage. *Mol Ecol* **13**:3219–28

Tokura M, Ohkuma M, Kudo T (2000) Molecular phylogeny of methanogens associated with flagellated protists in the gut and with the gut epithelium of termites. *FEMS Microbiol Ecol* **33**:233–40

Trojan D. Garcia-Robledo E, Meier DV, Hausmann B, Revsbech NP, Eichorst SA, Woebken D (2021) Microaerobic lifestyle at nanomolar O_2 concentrations mediated by low-affinity terminal oxidases in abundant soil bacteria. *mSystems* **6**:e00250–21

Tseng CP, Albrecht J, Gunsalus RP (1996) Effect of microaerophilic cell growth conditions on expression of the aerobic (*cyoABCDE* and *cydAB*) and anaerobic (*narGHJI*, *frdABCD*, and *dmsABC*) respiratory pathway genes in *Escherichia coli*. *J Bacteriol* **178**:1094–8

Tyson GW, Banfield JF (2005) Cultivating the uncultivated: a community genomics perspective. *Trends Microbiol* **13**:411-5

Ueda T, Suga Y, Matsuguchi T (1995) Molecular phylogenetic analysis of a soil microbial community in a soybean field. *Eur J Soil Sci* **46**:415–21

Uehling J, Gryganskyi A, Hameed K, Tschaplinski R, Misztal PK, Wu S, Desirò A, Vande Pol N, Du Z, Zienkiewicz A, Zienkiewicz K, Morin E, Tisserant E, Splivallo R, Hainaut M, Henrissat B, Ohm R, Kuo A, Yan J, Lipzen A, Nolan M, LaButti K, Barry K, Goldstein AH, Labbé J, Schadt C, Tuskan G, Grigoriev I, Martin F, Vilgalys R, Bonito G (2017) Comparative genomics of *Mortierella elongata* and its bacterial endosymbiont *Mycoavidus cysteinexigens*. *Environ Microbiol* **19**:2964–83

Unden G, Trageser M (1991) Oxygen regulated gene expression in *Escherichia coli*: Control of anaerobic respiration by the FNR protein. *Antonie van Leeuwenhoek* **59**:65–76

Unden G, Steinmetz PA, Degreif-Dünnwald P (2014) The aerobic and anaerobic respiratory chain of *Escherichia coli* and *Salmonella enterica*: enzymes and energetics. *EcoSal Plus* **6**:2324–6200

Utami YD, Kuwahara H, Igai K, Murakami T, Sugaya K, Morikawa T, Nagura Y, Yuki M, Deevong P, Inoue T, Kihara K, Lo N, Yamada A, Ohkuma M, Hongoh Y (2019) Genome analyses of uncultured TG2/ZB3 bacteria in 'Margulisbacteria' specifically attached to ectosymbiotic spirochetes of protists in the termite gut. *ISME J* **13**:455–67

van Hellemond JJ, Opperdoes FR, Tielens AG (1998) *Trypanosomatidae* produce acetate via a mitochondrial acetate:succinate CoA transferase. *PNAS* **95**:3036–41

van Teeseling MCF, Pol A, Harhangi HR, van der Zwart S, Jetten MSM, Op den Camp HJM, van Niftrik L (2014) Expanding the verrucomicrobial methanotrophic world: description of three novel species of *Methylacidimicrobium* gen. nov. *Appl Environ Microbiol* **80**:6782–91

Veivers P, O´brien R, Slaytor M (1983) Selective defaunation of *Mastotermes darwiniensis* and its effect on cellulose and starchmetabolism. *Insect Biochem* **13**:95–101

Verkhovskaya ML, Belevich N, Euro L, Wikström M (2008) Real-time electron transfer in respiratory complex I. *PNAS* **105**:3763–7

Wagner M, Horn M (2006) The Planctomycetes, Verrucomicrobia, Chlamydiae and sister phyla comprise a superphylum with biotechnological and medical relevance. *Curr Opin Biotechnol* **17**:241–9

Ward-Rainey N, Rainey FA, Schlesner H, Stackebrandt E (1996) In Validation of the publication of new names and new combinations previously effectively published outside the IJSB. List no. 57. *Int J Syst Bacteriol* **46**:625–6

Waterworth SC, Flórez LV, Rees ER, Hertweck C, Kaltenpoth M, Kwan JC (2020) Horizontal gene transfer to a defensive symbiont with a reduced genome in a multipartite beetle microbiome. *mBio* **11**:e02430-19

Weingarten RA, Grimes JL, Olson JW (2008) Role of *Campylobacter jejuni* respiratory oxidases and reductases in host colonization. *Appl Environ Microbiol* **74**:1367–75

Wertz JT, Breznak JA (2007a) *Stenoxybacter acetivorans* gen. nov., sp. nov., an acetate-oxidizing obligate microaerophile among diverse O2-consuming bacteria from termite guts. *Appl Environ Microbiol* **73**:6819–28

Wertz JT, Breznak JA (2007b) Physiological ecology of *Stenoxybacter acetivorans*, an obligate microaerophile in termite guts. *Appl Envrion Microbiol* **73**:6829–41

Wertz JT, Kim E, Breznak JA, Schmidt TM, Rodrigues JLM (2018) Genomic and physiological characterization of the Verrucomicrobia isolate *Geminisphaera colitermitum* gen. nov., sp. nov., reveals microaerophily and nitrogen fixation genes. *Appl Environm Microbiol* **84**:e00952–18

Williams TJ, Allan MA, Ivanova N, Huntemann M, Harque S, Hancock AM, Brazendale S, Cavicchioli R (2021) Genome analysis of a verrucomicrobial endosymbiont with a tiny genome discovered in an antarctic lake. *Front Microbiol* **12**:674758

Wise MG, McArthur JV, Shimkets LJ (1996) Microbial diversity in a Carolina Bay as determined by 16S rRNA gene analysis: confirmation of novel taxa. *Appl Environ Microbiol* **63**:1505–14

Wolf PG, Biswas A, Morales SE, Greening C, Gaskins HR (2016) H_2 metabolism is widespread and diverse among human colonic microbes. *Gut Microbes* **7**:235-45

Wood HE, O´Brien W, Micheales G (1997) Properties of carboxytransphosphorylase; pyruvate, phosphate dikinase; pyrophosphate-phosphofructikinase and pyrophosphate-acetate kinase and their roles in the metabolism of inorganic pyrophosphate. *Adv Enzymol Relat Areas Mol Biol* **45**:85-155

Wood TG, Sands WA (1978) The role of termites in ecosystems. In: Brian MV (ed). Production Ecology of Ants and Termites, Cambridge University Press, Cambridge, United Kingdom 245–92

Woodcroft BJ, Singleton CM, Boyd JA, Evans PN, Emerson JB, Zayed AAF, Hoelzle RD, Lambertin TO, McCalley, Hodgkins SB, Wilson RM, Purvine SO, Nicora CD, Li C, Frolking S, Chanton JP, Crill PM, Saleska SR, Rich VI, Tyson GW (2018) Genome-centric view of carbon processing in thawing permafrost. *Nature* **560**:49–54

Xie F, Jin W, Si H, Yuan Y, Tao Y, Liu J, Wang X, Yang C, Li Q, Yan X, Lin L, Jiang Q, Zhang L, Guo C, Greening C, Heller R, Guan LL, Pope PB, Tan Z, Zhu W, Wang M, Qiu Q, Li Z, Mao S (2021) An integrated gene catalog and over 10,000 metagenome-assembled genomes from the gastrointestinal microbiome of ruminants. *Microbiome* **9**:137

Xing L, Roberts EM, Harris JD, Gingras MK, Ran H, Zhang J, Xu X, Burns ME, Dong Z (2013) Novel insect traces on a dinosaur skeleton from the Lower Jurrasic Lufeng Formation of China. *Paleogeogr Paleoclimatol, Paleoecol* **388**:58–68

Yamin A (1979) Flagellates of the orders Trichomonadida Kirby, Oxymonadida Grasse, and Hypermastigida Grassi & Foa reported from lower termites (lsoptera Families *Mastotermitidae, Kalotermitidae, Hodotermitidae, Termopsidae, Rhinotermitidae, and Serritermitidae*) and from the wood-feeding roach Cryptocercus (Dictyoptera: Cryptocercidae). In: Kistner DH (ed.). Sociobiology. California State University, USA, 5–106

Yan H, Asfahl KL, Li N, Sun F, Xiao J, Shen D, Dandekar AA, Wang M (2019) Conditional quorum-sensing induction of a cyanide-insensitive terminal oxidase stabilizes cooperating populations of *Pseudomonas aeruginosa*. *Nat Comm* **10**:4999

Yang H, Schmitt-Wagner D, Stingl U, Brune A (2005) Niche heterogeneity determines bacterial community structure in the termite gut (*Reticulitermes santonensis*). *Environ Microbiol* **7**:916–32

Yankovskaya V, Horsefield R, Tönroth S, Luna-Chavez C, Miyoshi H, Léger C, Byrne B, Cecchini G, Iwata S (2003) Architecture of succinate dehydrogenase and reactive oxygen species generation. *Science* **299**:700–4

Ye J, Coulouris G, Zaretskaja I, Cutcutache I, Rozen S, Madden T (2012) Primer-BLAST: A tool to design target-specific primers for polymerase chain reaction. *BMC Bioionform* **13**:134

Yoon J, Matsuo Y, Matsuda S, Adachi K, Kasai H, Yukota A (2007) *Cerasicoccus arenae* gen. nov., sp. nov., a carotenoid-producing marine representative of the family Puniceicoccaceae within the phylum ‘Verrucomicrobia’, isolated from marine sand. *Int J Syst Evol Microbiol* **57**:2067–72

Yoon J, Matsuo Y, Adachi K, Nozawa M, Matsuda S, Kasai H, Yukota A (2008a) Description of *Persicirhabdus sediminis* gen. nov., sp. nov., *Roseibacillus ishigakijimensis* gen. nov., sp. nov., *Roseibacillus ponti* sp. nov., *Roseibacillus persicicus* sp. nov.,

Luteolibacter pohnpeiensis gen. nov., sp. nov. and *Luteolibacter algae* sp. nov., six marine members of the phylum '*Verrucomicrobia*', and emended descriptions of the class *Verrucomicrobiae*, the order *Verrucomicrobiales* and the family *Verrucomicrobiaceae*. *Int J Syst Evol Microbiol* **58**:998–1007

Yoon J, Matsuo Y, Katsuta A, Jang J-H, Matsuda S, Adachi K, Kasai H, Yokota A (2008b) *Haloferula rosea* gen. nov., sp. nov., *Haloferula harenae* sp. nov., *Haloferula phyci* sp. nov., *Haloferula helveola* sp. nov. and *Haloferula sargassicola* sp. nov., five marine representatives of the family Verrucomicrobiaceae within the phylum 'Verrucomicrobia. *Int J Syst Evol Microbiol* **58**:2491–500

Yuki M, Kuwahara H, Shintani M, Izawa K, Sato T, Starns D, Hongoh Y, Ohkuma M (2015) Dominant ectosymbiotic bacteria of cellulolytic protists in the termite gut also have the potential to digest lignocellulose. *Environ Microbiol* **17**:4942–53

Zakharova A, Saura A, Butenko A, Podešvová L, Warmusová S, Kostygov AY, Nenarokova A, Lukeš J, Opperdoes FR, Yurchenko V (2021) A new model trypanosomatid, *Novymonas esmeraldas*: genomic perception of its "*Candidatus* Pandoraea novymonadis" endosymbiont. *mBio* **12**:e01606–21

Zheng H, Dietrich C, Thompson CL, Meuser K, Brune A (2015) Population structure of *Endomicrobia* in single host cells of termite gut flagellates (*Trichonympha* spp.). *Microbes Environ* **30**:92–8

Zheng H, Dietrich C, Brune A (2017) Genome analysis of *Endomicrobium proavitum* suggests loss and gain of relevant functions during the evolution of intracellular symbionts. *Appl Environ Microbiol* **83**:e00656–17

Zufferey R, Preisig O, Hennecke H, Thöny-Meyer L (1996) Assembly and function of the cytochrome cbb_3 oxidase subunits in *Bradyrhizobium japonicum*. *J Biol Chem* **271**:9114–9

6 LIST OF ABBREVIATIONS

AAI	Average amino acid identity
Abs	Absorption
ACIII	Alternative complex III
ADP	Adenosine diphosphate
AMP	Adenosine monophosphate
ANI	Average nucleotide identity
ASCT	Acetate succinate CoA transferase
ATP	Adenosine triphosphate
BMC	Bacterial microcompartment
Ca	Candidatus
cDNA	complementary DNA
CoA	Coenzyme A
DAPI	4′,6-diamidino-2-phenylindole
DictDb	Dictyoptera database
DNA	Deoxyribonucleic acid
ETC	Electron transport chain
FA	Formamide
FAD	Flavin adenine dinucleotide
FISH	Fluorescence *in-situ* hybrisation
GTDB	Genome taxonomy database
HATOx	High-affinity terminal oxidase
HCO	Heme-copper-oxidase
HGT	Horizontal gene transfer
HMM	Hidden Markov Model
IMG	Intergrated microbial genome server
LATOx	Low-affinity terminal oxidase
Lg	Leghemoglobin
MAG(s)	Metagenome-assembled genome(s)
Mg	Myoglobin
NAD	Nicotinamide adenine dinucleotide

NOR	Nitric oxide reductase
NTT	Nucleotide transport protein
OD	Optical density
OPA	Organosphosphate:P_i antiporter
PCR	Polymerase chain reaction
PEP	Phosphoenolpyruvate
PPDK	Pyruvate phosphate dikinase
PVC superphylum	*Planctomycetota, Verrucomicrobiota, Chlamydiota*
Q	Quinone
QH_2	Quinole
Q-loop	Mitchellian redox loop
qPCR	quantitative polymerase chain reaction
RED	Relative evolutionary distance
RNA	Ribonucleic acid
ROS	Reactive oxygen species
rRNA	Ribosomal RNA
SCS	Succinyl CoA synthetase
SDS	Sodium dodecyl sulfate
SRP	Signal recognition particle
TAT	Twin arginine translocation
TCA	Tricarboxylic acid cycle
TRIS	Tris(hydroxymethyl)aminomethane
VGT	Vertical gene transfer

7 SUPPLEMENTARY INFORMATION

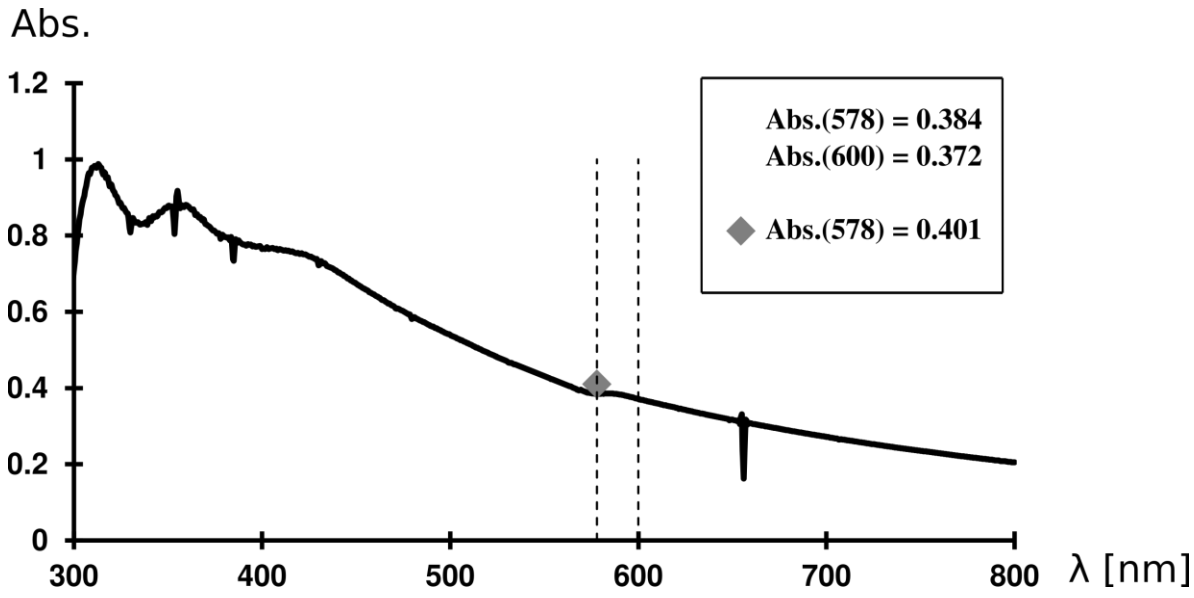

Figure S1: Spectrum of washed cells of *Ereboglobus luteus*. The figure shows a spectrum of washed cells of E. luteus measured with the speccord spectrophotometer. The dashed lines mark the absorptions at 578 nm and 600 nm. The grey diamond indicates the absorption of the same suspension measured with the tube photometer.

Table S2: List of qPCR primers and flanking primers (Fl) for *Opitutaceae* terminal oxidases

#	Primer name	Sequence (5´→3´)	organism and gene	bp
1	cydA_TAV2_82fw	ATGCCGTTCTTCATGTCAGC	TAV2- *bd* oxidase (cydA)	20
2	cydA_TAV2_421rv	AAATCCCCGACGTAAACCCC	TAV2- *bd* oxidase (cydA)	20
3	cyoE_TAV2_81fw	GTTGGGCGATTACCTGGAGT	TAV2- bo_3 oxidase (cyoE)	20
4	cyoE_TAV2_576rv	CAGGATGCCAAACAACACCC	TAV2- bo_3 oxidase (cyoE)	20
7	ccoN_TAV2_137fw	TCGGAACACTCTTCGCACTC	ccoN_cbb_3 oxidase	20
8	ccoN_TAV2_1126rv	TCGGAACACTCTTCGCACTC	ccoN_cbb_3 oxidase	20
9	Ho45_cydA_385fw	GGATTTGACTGGGTGGAGGG	Ho45- *bd* oxidase (cydA)	20
10	Ho45_cydA_633rv	GAAGTGTCCCGAGAAAGGCA	Ho45- *bd* oxidase (cydA)	20
11	*O. terrae*_cydA_295fw	GGCATCTTCGCCTTCTTCCT	*O.terrae*- *bd* oxidase (cydA)	20
12	*O. terrae*_cydA_550rv	GGTCCATCGAGGAAGGGTTG	*O.terrae*- *bd* oxidase (cydA)	20
13	*O. terrae*_ccoN_543fw	CAACGTCTACCACCCGATCA	*O.terrae*- cbb_3 oxidase ccoN)	20
14	*O. terrae*_ccoN_752rv	ACGTGATGCGAAATGTTGCC	*O.terrae*- cbb_3 oxidase (ccoN)	20
15	*O. terrae*_cyoE_314fw	TGTTTTTGCTCTACGCGCTG	*O.terrae*- bo_3 oxidase (cyoE)	20
16	*O. terrae*_cyoE_593rv	TGGACGGCAGAGTAGTCCTT	*O.terrae*- bo_3 oxidase (cyoE)	20
17	Ho45_cydA_Fl_171fw	CTTCATGAAACACGCGGGAC	Ho45- *bd* oxidase (cydA)	20
18	Ho45_cydA_Fl_747rv	CGTTTCCACGTCAGGAATGC	Ho45- *bd* oxidase (cydA)	20
19	TAV2_cydA_Fl_150fw	GACCAGAATGTGGCTCAAGG	TAV2- *bd* oxidase (cydA)	20
20	TAV2_cydA_Fl_651rv	CGCCAAACGTCATCGAAATC	TAV2- *bd* oxidase (cydA)	20
21	TAV2_cyoE_qP_240rv	CAACCAGTGGATGGAGAGC	TAV2- bo_3 oxidase (cyoE)	19
22	TAV2_cyoE_Fl_709rv	CATTGACGAGCGACCAACC	TAV2- bo_3 oxidase (cyoE)	19
23	TAV2_ccoN_qP_357fw	CCGTCCATCTGAATACCGTC	TAV2_cbb_3 oxidase (ccoN)	20
24	TAV2_ccoN_qP_599rv	GGGAGAGGTAGTAGCTGTGT	TAV2_cbb_3 oxidase (ccoN)	20
25	*O. terrae*_cydA_Fl_130fw	AACCCGCTCTATCACCAGATG	*O.terrae*- *bd* oxidase (cydA)	21
26	*O. terrae*_cydA_Fl_789rv	GGTTTCCCAATGCCCTTCG	*O.terrae*- *bd* oxidase (cydA)	19
27	*O. terrae*_ccoN_Fl_396fw	GCTGGCCATGATCTTCCTTT	*O.terrae*- cbb_3 oxidase (ccoN)	20
28	*O. terrae*_ccoN_Fl_914rv	GGGAGAAACGAGATCCAACC	*O.terrae*- cbb_3 oxidase (ccoN)	20
29	*O. terrae*_cyoE_Fl_124fw	GATCCGATCCAACTCGCGCT	*O.terrae*- bo_3 oxidase (cyoE)	20
30	*O. terrae*_cyoE_Fl_771rv	CTTGATCGCCTGCCACAGAA	*O.terrae*- bo_3 oxidase (cyoE)	20
31	TAV2_rpoA_Fl_203fw	ACGAGTTTCAGAGCATCGAC	TAV2 RNA-Pol (rpoA)	20
32	TAV2_rpoA_Fl_839rv	GTGATGTTGGCGTTGTTGAG	TAV2 RNA-Pol (rpoA)	20
33	Ho45_rpoA_Fl_203fw	ACGAATTCCAGAGCATCGAC	Ho45 RNA-Pol (rpoA)	20

34	Ho45_rpoA_Fl_839rv	GTGATGTTCGCGTTGTTGAG	Ho45 RNA-Pol (rpoA)	20
35	O. terrae_rpoA_Fl_143fw	TTCTCCTCAGCTCCATCGAA	*O.terrae* RNA-Pol (rpoA)	20
36	*O. terrae*_rpoA_Fl_733rv	CGGACTGCTGGTTCTCAAAT	*O.terrae* RNA-Pol (rpoA)	20
37	TAV2_rpoA_qP_476fw	AACGCCGAGATCGAAATCAA	TAV2 RNA-Pol (rpoA)	20
38	TAV2_rpoA_qP_656rv	CGAGGTTGAGCTTGTCGTAG	TAV2 RNA-Pol (rpoA)	20
39	Ho45_rpoA_qP_431fw	AGATCGAAATCAAGACCGGC	Ho45 RNA-Pol (rpoA)	20
40	Ho45_rpoA_qP_617fw	TCGGTCCAGACTTCAAGGAT	Ho45 RNA-Pol (rpoA)	20
41	*O. terrae*_rpoA_qP_367fw	ATCCAGGTCATCAATCCCGA	*O. terrae* RNA-Pol (rpoA)	20
42	*O. terrae*_rpoA_qP_602fw	AGCACGAGCTTGTCGTAATC	*O. terrae* RNA-Pol (rpoA)	20

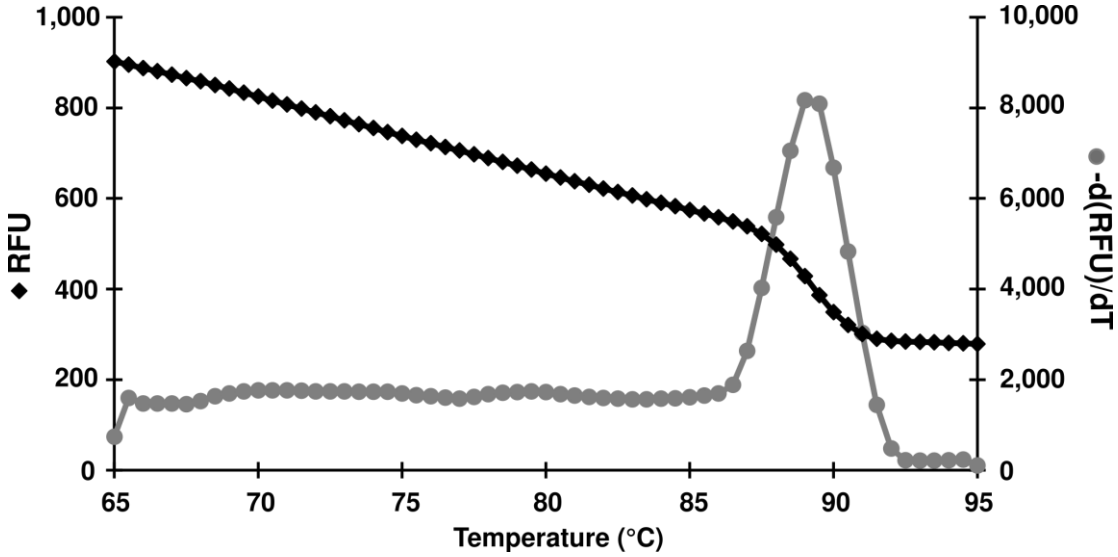

Figure S3: qPCR melting curve example. The figure shows the melting curve of the qPCR experiments. The chose example was the amplification of the *bd* oxidase gene (*cydA*) of *Opitutus terrae*. Both the relative fluorescence of the qPCR product (RFU, black diamonds) and the derivation (-d(RFU)/dT, grey circles) are depicted between 65°C and 95°C. More than one peek in the derivation of the fluorescence would indicate multiple qPCR products of differential size and therefore unspecific amplification.

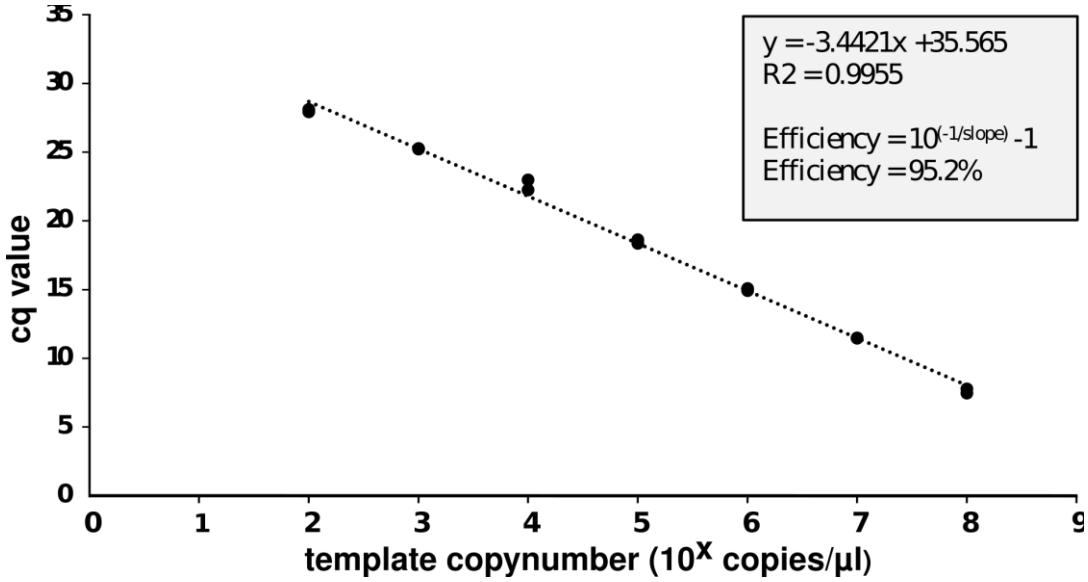

Figure S4: qPCR standard curve. The figure shows the cycle in which the qPCR amplification overcomes the threshold (cq value = C_T value) dependent on the inserted gene copy number of the standard. This example shows the standard for the 16S rRNA gene of *Geminispahera colitermitum*. The primer efficiency was calculated based on the slope of the curve.

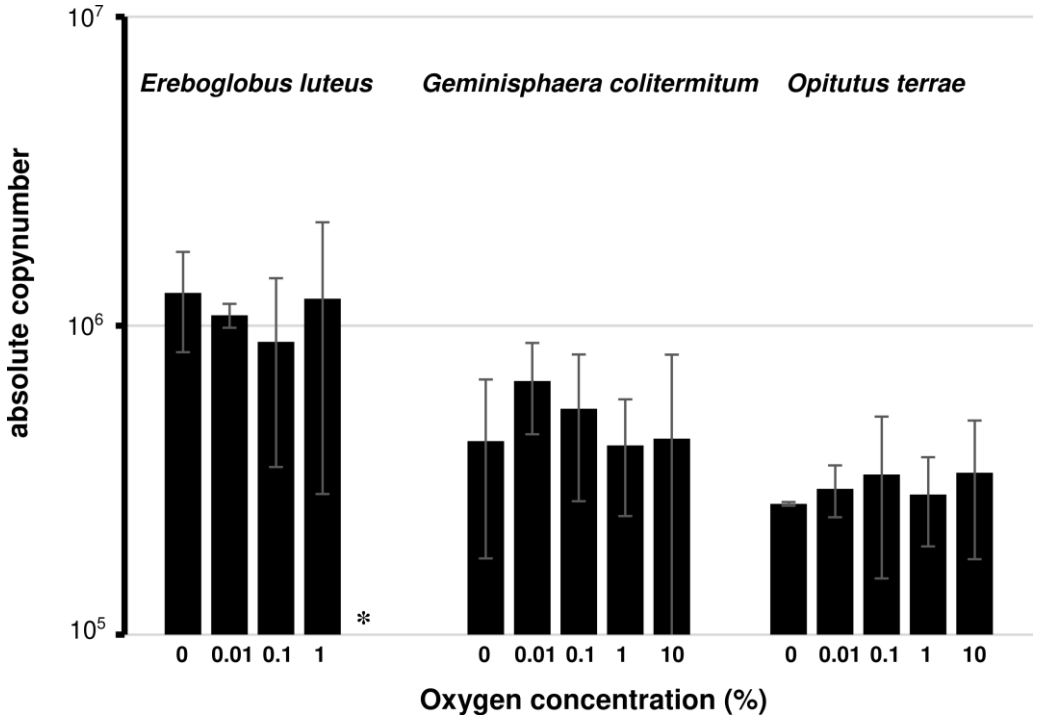

Figure S5: Transcription level of the 16S rRNA gene of *Opitutaceae*. The figure shows the absolute copynumber / ng RNA of *Ereboglobus luteus* (black), *Geminisphaera colitermitum* (grey/black) and *Opitutus terrae* (grey) under different oxygen precultivation conditions. The asterix indicates the missing value for 10% O_2 for *E. luteus*, which is not growing at O_2 concentrations above 4%.

Table S6: Composition of Fahräeus medium

Component	Concentration (g/l)
$CaCl_2$	0.132
$MgSO_4 \times 7\ H_2O$	0.125
KH_2PO_4	0.1
$Na_2HPO_4 \times 2\ H_2O$	0.075
Fe-citrate	0.005
1 M TRIS-EDTA solution	1 ml/l

Table S7: Characteristics of the MAGs and reference genomes

Verrucomicrobiota MAGs and Reference genomes	Complete-ness (%)	Contami-nation (%)	Genome size (Mbp)	Compl.-corrected genomes size	GC content (%)	Quality
Cc175_bin.120	73.31	3.38	0.94	1.28	41.5	MQ
Cc175_bin.121	76.86	1.72	1.02	1.33	41.5	MQ
Cc175_bin.33	71.62	0.9	1.15	1.60	43.2	MQ
Cc175_bin.37	60.34	0.86	0.62	1.02	61.8	MQ
Cc175_bin.40	52.54	3.04	0.61	1.17	43.4	MQ
Cc175_bin.47	62.78	0	0.84	1.34	50.8	MQ
Cc175_bin.8	72.37	0.23	0.85	1.17	56.3	MQ
Cc175_bin.98	67.19	0.68	0.78	1.16	44.2	MQ
Cd354_bin.103	60.64	0.68	0.76	1.26	43.7	MQ
Cd354_bin.116	79.56	0	1.02	1.28	42.1	MQ
Cd354_bin.81	78	0.68	0.91	1.16	43.2	MQ
Cd354_bin.92	74.1	1.58	0.82	1.11	48.1	MQ
Cf509_bin.39	82.39	1.35	2.43	2.95	61.8	MQ
Cf509_bin.41	85.77	3.04	2.76	3.21	54.9	MQ
Ct408_bin.116	52.1	0	0.43	0.82	46.3	MQ
Ct408_bin.121	75.01	0.34	0.83	1.10	47.0	MQ
Ct408_bin.149	75	0.17	0.92	1.23	40.6	MQ
Ct408_bin.56	91.38	8.62	1.02	1.12	40.2	MQ
Ct408_bin.77	75.97	0	0.86	1.14	39.8	MQ
Ct408_bin.80	73.29	0.82	3.58	4.89	64.0	MQ
Ct408_bin.89	64.57	1.35	0.74	1.14	55.9	MQ
Gsp477_bin.122	73.59	0	0.95	1.29	47.6	MQ
Gsp477_bin.14	72.92	0.68	1.05	1.44	54.5	MQ
Gsp477_bin.142	67.04	0	0.67	0.99	41.4	MQ
Gsp477_bin.153	64.53	2.03	0.72	1.11	42.2	MQ
Gsp477_bin.156	73.42	0	1.39	1.89	44.5	MQ
Gsp477_bin.160	76.01	7.94	0.93	1.22	44.0	MQ
Gsp477_bin.174	78.04	0	0.88	1.13	50.1	MQ
Gsp477_bin.23	75	0.68	0.92	1.23	43.2	MQ
Gsp477_bin.29	68.07	0	0.79	1.16	44.9	MQ
Gsp477_bin.70	63.51	0	0.90	1.42	42.5	MQ
Gx481_bin.174	78.78	5.14	6.37	8.08	62.5	MQ
Gx481_bin.184	78.55	0	1.02	1.30	41.3	MQ
Gx481_bin.188	76.69	1.01	0.96	1.25	48.1	MQ
Gx481_bin.192	86.52	5.07	2.77	3.20	61.2	MQ
Gx481_bin.202	63.61	2.48	0.65	1.02	49.9	MQ
Gx481_bin.23	78.04	1.35	0.93	1.20	42.5	MQ
Gx481_bin.94	85.72	0.68	2.76	3.22	60.3	MQ
Gx485_bin.11	58.42	0.81	0.65	1.11	42.4	MQ
Gx485_bin.111	93.2	3.04	3.00	3.21	60.9	HQ
Gx485_bin.97	64.91	0	3.92	6.04	61.0	MQ
Hm464_bin.137	83.04	0.37	1.98	2.39	58.8	MQ
Hm464_bin.66	89.35	1.35	2.38	2.66	49.5	MQ
Hs463_bin.103	55.56	0.68	2.31	4.15	64.4	MQ
Im510_bin.18	66.99	1.69	0.66	0.98	45.8	MQ
Iy174_bin.61	75.75	0	0.94	1.24	55.1	MQ
Kf353_bin.141	56.7	3.41	0.71	1.26	43.1	MQ
Kf353_bin.47	74.66	2.36	0.84	1.13	41.4	MQ
Md513_bin.100	83.51	0.68	3.12	3.73	66.1	MQ
Md513_bin.46	67.62	0	1.46	2.16	66.7	MQ
Nc350_bin.13	56.88	3.07	0.62	1.09	50.9	MQ

Nc350_bin.186	76.49	0.68	0.97	1.27	43.1	MQ
Nc350_bin.191	67.09	0	0.87	1.30	44.8	MQ
Nc350_bin.44	77.36	1.35	0.92	1.19	42.5	MQ
Nc350_bin.88	91.89	1.35	2.50	2.72	56.0	HQ
Ncb351_bin.30	72.71	0.68	0.96	1.31	43.6	MQ
Ncb351_bin.42	74.88	2.03	1.00	1.33	41.3	MQ
Ncb351_bin.52	75.34	2.03	0.92	1.22	39.8	MQ
Ncb351_bin.56	78.21	0.68	0.99	1.27	40.6	MQ
Ncb351_bin.8	74.66	0.68	0.78	1.05	40.8	MQ
Ncb351_bin.90	75.64	0	0.82	1.08	42.0	MQ
Ncb351_bin.92	70.05	4.45	1.06	1.51	48.2	MQ
Ncb351_bin.93	51.72	0	0.57	1.10	43.6	MQ
Nm470_bin.100	72.92	0.68	1.04	1.43	51.1	MQ
Nm470_bin.120	72.95	0.68	4.46	6.11	65.2	MQ
Nm470_bin.121	65.68	0	0.85	1.29	57.7	MQ
Nm470_bin.13	68.52	0	1.04	1.51	51.7	MQ
Nm470_bin.68	75.34	1.35	0.85	1.12	41.2	MQ
Nm470_bin.74	67.57	4.65	0.88	1.31	42.2	MQ
Nm470_bin.87	70.93	0	0.87	1.23	49.4	MQ
Pal332_bin.2	87.84	0.68	1.30	1.48	36.1	MQ
Pc512_bin.4	83.11	0	1.76	2.12	57.3	MQ
Pc512_bin.95	71.36	2.03	1.78	2.50	58.6	MQ
Pc512_bin.99	71.49	0	1.57	2.20	61.3	MQ
Pcl387_bin.12	72.27	0.68	0.87	1.20	41.4	MQ
Pcl387_bin.134	76.01	6.08	0.81	1.07	48.7	MQ
Pcl387_bin.136	79.39	0.68	0.89	1.12	46.4	MQ
Pcl387_bin.165	78.89	0	1.00	1.27	40.7	MQ
Pcl387_bin.18	71.26	1.35	1.02	1.43	43.9	MQ
Pcl387_bin.38	71.82	0	0.85	1.19	59.5	MQ
Pcl387_bin.45	66.84	2.36	0.86	1.29	48.4	MQ
Po218_bin.25	55.17	0	0.70	1.27	38.3	MQ
Po218_bin.38	68.02	0	0.86	1.26	52.9	MQ
Po218_bin.73	73.99	1.56	0.70	0.95	46.0	MQ
Pq454_bin.37	80.23	0.03	2.70	3.37	59.3	MQ
Roe453_bin.126	76.86	0	0.78	1.02	57.3	MQ
Roe453_bin.18	73.07	1.35	0.85	1.17	50.3	MQ
Roe453_bin.74	71.68	0	0.97	1.35	62.5	MQ
TD116_bin.50	91.89	0.68	2.96	3.23	52.0	HQ
Zx50_bin.34	63.54	4.55	1.22	1.92	60.7	MQ
Zx50_bin.46	86.82	4.45	2.05	2.37	57.5	MQ
Zx50_bin.6	58.68	0.34	1.79	3.05	66.6	MQ
Akkermansia_glycaniphila	91.84	0	3.16	3.44	57.9	HQ
Akkermansia_muciniphila	97.96	0	2.66	2.72	55.8	HQ
Ca._Didemnitutus_mandela	80.12	0	2.17	2.71	51.9	MQ
Ca._Xiphinematobacter_sp	89.86	0	0.92	1.02	47.7	MQ
Cephaloticoccus_capnophilus	97.95	0	2.09	2.14	60.5	HQ
Cephaloticoccus_primus	97.26	0	2.36	2.42	63.0	HQ
Chlamydia_muridarum	99.19	0	1.08	1.09	40.3	HQ
Coraliomargarita_akajimensis	100.00	0	3.75	3.75	53.6	HQ
Coraliomargarita_sp_CAG312	92.23	0	2.44	2.65	46.3	HQ
Ereboglobus_luteus	93.81	0	4.18	4.45	59.7	HQ
Estrella_lausannensis	96.28	0	2.83	2.94	48.2	HQ
Geminisphaera_colitermitum	98.06	0	5.67	5.78	60.9	HQ
Kiritimatiella_glycovorans	100	0	2.95	2.95	63.3	HQ
Lacunisphaera_limnophila	99.32	0	4.20	4.23	66.5	HQ
Lentisphaera_araneosa	97.12	0	6.02	6.20	41.0	HQ
Lenti._bact._GWF2_44_16	95.41	0	5.16	5.41	44.0	HQ
Methylacidiphilum_fumariolicum	100.00	0	2.48	2.48	41.5	HQ

Methylacidiphilum_infernorum	100.00	0	2.29	2.29	45.5	HQ
Methylacidiphilum_kamchatkense	100.00	0	2.21	2.21	40.4	HQ
Oleiharenicola_alkalitolerans	100.00	0	4.72	4.72	66.1	HQ
Opitutaceae_bacterium_TSB47	100.00	0	7.82	7.82	62.8	HQ
Opitutae_bacterium_UBA1116	90.54	0	1.94	2.15	46.8	HQ
Opitutae_bacterium_UBA3534	97.14	0	1.85	1.90	46.2	HQ
Opitutae_bacterium_UBA4506	98.42	0	4.03	4.09	54.3	HQ
Opitutae_bacterium_UBA7350	92.60	0	1.35	1.46	55.0	HQ
Opitutus_sp	100.00	0	2.09	2.09	60.5	HQ
Opitutus_terrae	99.32	0	5.96	6.00	65.3	HQ
Parachlamydia_acanthamoebae	100	0	3.00	3.00	38.9	HQ
Pedosphaera_parvula	99.32	0	7.41	7.46	53.6	HQ
Prosthecobacter_debontii	100.00	0	6.29	6.29	56.5	HQ
Puniceicoccales_bact._Verruco_01	92.58	0	2.50	2.71	63.0	HQ
Rariglobus_hedericola	100.00	0	4.10	4.10	60.8	HQ
TAV1	98.93	0	7.07	7.15	63.3	HQ
TAV3	94.10	0	5.62	5.98	60.8	HQ
TAV4	92.98	0	5.61	6.03	60.8	HQ
TAV5	100.00	0	7.42	7.42	63.5	HQ
Verr. bact._CG_4_10_14	91.89	0	1.75	1.90	43.4	HQ
Verr._bact._GWC2_42_7	67.27	0	1.30	1.93	41.8	MQ
Verr._bact._GWF2_51_19	78.21	0	1.26	1.61	50.6	MQ
Verr._bact._Opi_OSU_00C	78.57	0	2.05	2.61	39.0	MQ
Verr._bact._UBA1183	78.21	0	1.06	1.35	41.6	MQ
Verr._bact._UBA3636	87.21	0	4.77	5.47	64.6	MQ
Verr._bact._UBA6015	90.03	0	4.23	4.70	58.3	HQ
Verr._bact._UBA6458	86.91	0	1.61	1.86	62.7	MQ
Verrucomicrobium_spinosum	100.00	0	8.22	8.22	60.3	HQ
Victivallis_vadensis	93.92	0	5.20	5.54	59.6	HQ
Waddlia_chondrophila	97.47	0	2.13	2.19	43.7	HQ

Table S8: GTDBtk classification of the *Verrucomicrobiota* MAGs

MAG ID	GTDBtk classification: **p**hylum_**c**lass_**o**rder_**f**amily_**g**enus_**s**pecies
Cc175_bin.120	p__Verrucomicrobiota;c__Verrucomicrobiae;o__Opitutales;f__;g__;s__
Cc175_bin.121	p__Verrucomicrobiota;c__Verrucomicrobiae;o__Opitutales;f__UBA9783;g__;s__
Cc175_bin.33	p__Verrucomicrobiota;c__Verrucomicrobiae;o__Opitutales;f__;g__;s__
Cc175_bin.37	p__Verrucomicrobiota;c__Verrucomicrobiae;o__Opitutales;f__;g__;s__
Cc175_bin.40	p__Verrucomicrobiota;c__Verrucomicrobiae;o__Opitutales;f__;g__;s__
Cc175_bin.47	p__Verrucomicrobiota;c__Verrucomicrobiae;o__Opitutales;f__;g__;s__
Cc175_bin.8	p__Verrucomicrobiota;c__Verrucomicrobiae;o__Opitutales;f__;g__;s__
Cc175_bin.98	p__Verrucomicrobiota;c__Verrucomicrobiae;o__Opitutales;f__;g__;s__
Cd354_bin.103	p__Verrucomicrobiota;c__Verrucomicrobiae;o__Opitutales;f__;g__;s__
Cd354_bin.116	p__Verrucomicrobiota;c__Verrucomicrobiae;o__Opitutales;f__UBA9783;g__;s__
Cd354_bin.81	p__Verrucomicrobiota;c__Verrucomicrobiae;o__Opitutales;f__;g__;s__
Cd354_bin.92	p__Verrucomicrobiota;c__Verrucomicrobiae;o__Opitutales;f__;g__;s__
Cf509_bin.39	p__Verrucomicrobiota;c__Verrucomicrobiae;o__Opitutales;f__UBA953;g__;s__
Cf509_bin.41	p__Verrucomicrobiota;c__Verrucomicrobiae;o__Methylacidiphilales;f__;g__;s__
Ct408_bin.116	p__Verrucomicrobiota;c__Verrucomicrobiae;o__Opitutales;f__;g__;s__
Ct408_bin.121	p__Verrucomicrobiota;c__Verrucomicrobiae;o__Opitutales;f__;g__;s__
Ct408_bin.149	p__Verrucomicrobiota;c__Verrucomicrobiae;o__Opitutales;f__;g__;s__
Ct408_bin.56	p__Verrucomicrobiota;c__Verrucomicrobiae;o__Opitutales;f__UBA9783;g__;s__
Ct408_bin.77	p__Verrucomicrobiota;c__Verrucomicrobiae;o__Opitutales;f__;g__;s__
Ct408_bin.80	p__Verrucomicrobiota;c__Verrucomicrobiae;o__Opitutales;f__Opitutaceae;g__Ereboglobus;s__
Ct408_bin.89	p__Verrucomicrobiota;c__Verrucomicrobiae;o__Opitutales;f__;g__;s__
Gsp477_bin.122	p__Verrucomicrobiota;c__Verrucomicrobiae;o__Opitutales;f__;g__;s__
Gsp477_bin.14	p__Verrucomicrobiota;c__Verrucomicrobiae;o__Opitutales;f__;g__;s__
Gsp477_bin.142	p__Verrucomicrobiota;c__Verrucomicrobiae;o__Opitutales;f__;g__;s__
Gsp477_bin.153	p__Verrucomicrobiota;c__Verrucomicrobiae;o__Opitutales;f__;g__;s__
Gsp477_bin.156	p__Verrucomicrobiota;c__Verrucomicrobiae;o__Opitutales;f__;g__;s__
Gsp477_bin.160	p__Verrucomicrobiota;c__Verrucomicrobiae;o__Opitutales;f__;g__;s__
Gsp477_bin.174	p__Verrucomicrobiota;c__Verrucomicrobiae;o__Opitutales;f__;g__;s__
Gsp477_bin.23	p__Verrucomicrobiota;c__Verrucomicrobiae;o__Opitutales;f__;g__;s__
Gsp477_bin.29	p__Verrucomicrobiota;c__Verrucomicrobiae;o__Opitutales;f__;g__;s__
Gsp477_bin.70	p__Verrucomicrobiota;c__Verrucomicrobiae;o__Opitutales;f__;g__;s__
Gx481_bin.174	p__Verrucomicrobiota;c__Verrucomicrobiae;o__Opitutales;f__Opitutaceae;g__Geminisphaera;s__
Gx481_bin.184	p__Verrucomicrobiota;c__Verrucomicrobiae;o__Opitutales;f__UBA9783;g__;s__
Gx481_bin.188	p__Verrucomicrobiota;c__Verrucomicrobiae;o__Opitutales;f__;g__;s__
Gx481_bin.192	p__Verrucomicrobiota;c__Verrucomicrobiae;o__Methylacidiphilales;f__;g__;s__
Gx481_bin.202	p__Verrucomicrobiota;c__Verrucomicrobiae;o__Opitutales;f__;g__;s__
Gx481_bin.23	p__Verrucomicrobiota;c__Verrucomicrobiae;o__Opitutales;f__;g__;s__
Gx481_bin.94	p__Verrucomicrobiota;c__Verrucomicrobiae;o__Methylacidiphilales;f__;g__;s__
Gx485_bin.11	p__Verrucomicrobiota;c__Verrucomicrobiae;o__Opitutales;f__;g__;s__
Gx485_bin.111	p__Verrucomicrobiota;c__Verrucomicrobiae;o__Methylacidiphilales;f__;g__;s__
Gx485_bin.97	p__Verrucomicrobiota;c__Verrucomicrobiae;o__Opitutales;f__Opitutaceae;g__Ereboglobus;s__
Hm464_bin.137	p__Verrucomicrobiota;c__Kiritimatiellae;o__LD1-PB3;f__Lenti-01;g__Lenti-01;s__
Hm464_bin.66	p__Verrucomicrobiota;c__Lentisphaeria;o__Victivallales;f__Victivallaceae;g__Victivallis;s__
Hs463_bin.103	p__Verrucomicrobiota;c__Verrucomicrobiae;o__Opitutales;f__Opitutaceae;g__Ereboglobus;s__
Im510_bin.18	p__Verrucomicrobiota;c__Verrucomicrobiae;o__Opitutales;f__;g__;s__
Iy174_bin.61	p__Verrucomicrobiota;c__Verrucomicrobiae;o__Opitutales;f__;g__;s__
Kf353_bin.141	p__Verrucomicrobiota;c__Verrucomicrobiae;o__Opitutales;f__;g__;s__
Kf353_bin.47	p__Verrucomicrobiota;c__Verrucomicrobiae;o__Opitutales;f__;g__;s__
Md513_bin.100	p__Verrucomicrobiota;c__Verrucomicrobiae;o__Opitutales;f__UBA953;g__;s__
Md513_bin.46	p__Verrucomicrobiota;c__Verrucomicrobiae;o__Opitutales;f__Opitutaceae;g__Geminisphaera;s__
Nc350_bin.13	p__Verrucomicrobiota;c__Verrucomicrobiae;o__Opitutales;f__;g__;s__
Nc350_bin.186	p__Verrucomicrobiota;c__Verrucomicrobiae;o__Opitutales;f__;g__;s__
Nc350_bin.191	p__Verrucomicrobiota;c__Verrucomicrobiae;o__Opitutales;f__;g__;s__
Nc350_bin.44	p__Verrucomicrobiota;c__Verrucomicrobiae;o__Opitutales;f__;g__;s__
Nc350_bin.88	p__Verrucomicrobiota;c__Verrucomicrobiae;o__Opitutales;f__UBA953;g__;s__
Ncb351_bin.30	p__Verrucomicrobiota;c__Verrucomicrobiae;o__Opitutales;f__;g__;s__
Ncb351_bin.42	p__Verrucomicrobiota;c__Verrucomicrobiae;o__Opitutales;f__;g__;s__
Ncb351_bin.52	p__Verrucomicrobiota;c__Verrucomicrobiae;o__Opitutales;f__;g__;s__
Ncb351_bin.56	p__Verrucomicrobiota;c__Verrucomicrobiae;o__Opitutales;f__UBA9783;g__;s__
Ncb351_bin.8	p__Verrucomicrobiota;c__Verrucomicrobiae;o__Opitutales;f__;g__;s__

Ncb351_bin.90	p__Verrucomicrobiota;c__Verrucomicrobiae;o__Opitutales;f__;g__;s__
Ncb351_bin.92	p__Verrucomicrobiota;c__Verrucomicrobiae;o__Opitutales;f__;g__;s__
Ncb351_bin.93	p__Verrucomicrobiota;c__Verrucomicrobiae;o__Opitutales;f__;g__;s__
Nm470_bin.100	p__Verrucomicrobiota;c__Verrucomicrobiae;o__Opitutales;f__;g__;s__
Nm470_bin.120	p__Verrucomicrobiota;c__Verrucomicrobiae;o__Opitutales;f__Opitutaceae;g__Ereboglobus;s__
Nm470_bin.121	p__Verrucomicrobiota;c__Verrucomicrobiae;o__Opitutales;f__;g__;s__
Nm470_bin.13	p__Verrucomicrobiota;c__Verrucomicrobiae;o__Opitutales;f__;g__;s__
Nm470_bin.68	p__Verrucomicrobiota;c__Verrucomicrobiae;o__Opitutales;f__;g__;s__
Nm470_bin.74	p__Verrucomicrobiota;c__Verrucomicrobiae;o__Opitutales;f__;g__;s__
Nm470_bin.87	p__Verrucomicrobiota;c__Verrucomicrobiae;o__Opitutales;f__;g__;s__
Pal332_bin.2	p__Verrucomicrobiota_A;c__Chlamydiia;o__Parachlamydiales;f__Ga0074140;g__PSRO01;s__
Pc512_bin.4	p__Verrucomicrobiota;c__Verrucomicrobiae;o__Opitutales;f__UBA953;g__;s__
Pc512_bin.95	p__Verrucomicrobiota;c__Verrucomicrobiae;o__Methylacidiphilales;f__;g__;s__
Pc512_bin.99	p__Verrucomicrobiota;c__Verrucomicrobiae;o__Opitutales;f__UBA953;g__;s__
Pcl387_bin.12	p__Verrucomicrobiota;c__Verrucomicrobiae;o__Opitutales;f__;g__;s__
Pcl387_bin.134	p__Verrucomicrobiota;c__Verrucomicrobiae;o__Opitutales;f__;g__;s__
Pcl387_bin.136	p__Verrucomicrobiota;c__Verrucomicrobiae;o__Opitutales;f__;g__;s__
Pcl387_bin.165	p__Verrucomicrobiota;c__Verrucomicrobiae;o__Opitutales;f__UBA9783;g__;s__
Pcl387_bin.18	p__Verrucomicrobiota;c__Verrucomicrobiae;o__Opitutales;f__;g__;s__
Pcl387_bin.38	p__Verrucomicrobiota;c__Verrucomicrobiae;o__Opitutales;f__;g__;s__
Pcl387_bin.45	p__Verrucomicrobiota;c__Verrucomicrobiae;o__Opitutales;f__;g__;s__
Po218_bin.25	p__Verrucomicrobiota;c__Verrucomicrobiae;o__Opitutales;f__UBA12508;g__;s__
Po218_bin.38	p__Verrucomicrobiota;c__Verrucomicrobiae;o__Opitutales;f__;g__;s__
Po218_bin.73	p__Verrucomicrobiota;c__Verrucomicrobiae;o__Opitutales;f__;g__;s__
Pq454_bin.37	p__Verrucomicrobiota;c__Verrucomicrobiae;o__Opitutales;f__UBA953;g__;s__
Roe453_bin.126	p__Verrucomicrobiota;c__Verrucomicrobiae;o__Opitutales;f__;g__;s__
Roe453_bin.18	p__Verrucomicrobiota;c__Verrucomicrobiae;o__Opitutales;f__;g__;s__
Roe453_bin.74	p__Verrucomicrobiota;c__Verrucomicrobiae;o__Opitutales;f__;g__;s__
TD116_bin.50	p__Verrucomicrobiota;c__Verrucomicrobiae;o__Opitutales;f__UBA953;g__;s__
Zx50_bin.34	p__Verrucomicrobiota;c__Verrucomicrobiae;o__Opitutales;f__UBA953;g__;s__
Zx50_bin.46	p__Verrucomicrobiota;c__Verrucomicrobiae;o__Opitutales;f__UBA953;g__;s__
Zx50_bin.6	p__Verrucomicrobiota;c__Kiritimatiellae;o__RFP12;f__UBA1067;g__;s__

Table S9: List of Hidden Markov Models

HMM target	gene / abbrev.	database	model
Oxydative phosphorylation			
Complex 1			
NADH oxidoreductase			
NADH-Ox.Red. Subunit C	*nuoC*	PFAM	PF00329
		TIGRFAM	TIGR01961
NADH-Ox.Red. Subunit B	*nuoB*	PFAM	PF01058
		TIGRFAM	TIGR01957
NADH-Ox.Red. Subunit E	*nuoE*	TIGERFAM	TIGR1958
NADH-Ox.Red. Subunit F	*nuoF*	PFAM	PF10589
		TIGRFAM	TIGR01959
NADH-Ox.Red. Subunit G	*nuoG*	PFAM	PF01568
		TIGRFAM	TIGR01973
NADH-Ox.Red. Subunit K	*nuoK*	PFAM	PF00420
		PANTHER	PTHR11434
NADH-Ox.Red. Subunit L	*nuoL*	PFAM	PF00361
		TIGRFAM	TIGR01974
NADH-Ox.Red. Subunit M	*nuoM*	PFAM	PF00361
		TIGRFAM	TIGR01972
NADH-Ox.Red. Subunit N	*nuoN*	TIGRFAM	TIGR01770
NADH dehydrogenase	*ndh*	PFAM	PF07992
Complex 2			
Succinate dehydrogenase (SDH)			
SDH subunit C	*sdhC*	TIGRFAM	TIGR02046
SDH subunit A	*sdhA*	TIGRFAM	TIGR01811
SDH subunit B	*sdhB*	TIGRFAM	TIGR00384
Complex 3			
Cytochrome c reductase	*cytC*	PFAM	PF02921
Terminal oxidases			
bd oxidase			
bd oxidase subunit 1 (cat)	*cydA*	PFAM	PF01654
		PANTHER	PTHR30365
bd oxidase subunit 2	*cydB*	PFAM	PF02322
		PANTHER	PTHR43141
Heme copper oxidases			
cbb3 oxidase			
cbb3 oxidase subunit 1 (cat)	*ccoN / fixN*	PANTHER	PTHR10422_SF29
		TIGRFAM	TIGR00780
cbb3 oxidase subunit 2	*ccoO / fixO*	TIGRFAM	TIGR00781
		PFAM	PF02433
bo3 oxidase			
bo3 oxidase subunit 1 (cat)	*cyoB*	TIGRFAM	TIGR02843
		PANTHER	PTHR10422_SF39
bo3 oxidase subunit 2	*cyoA*	TIGRFAM	TIGR01433
		PANTHER	PTHR2288_SF18
Central carbon metabolism			
Glycolysis			

Glucose PTS system	PTS EIIA	PFAM	PF00358
Glucose MFT	MFS1	PFAM	PF07690
Hexokinase	HK	PFAM	PF02689
		PFAM	PF00480
Glucose-6-P-Isomerase	GPI	PFAM	PF00342
Phosphofructokinase	PFK	PFAM	PF00365
Fructose-1,6-bis-P aldolase	ALDOA	TIGRFAM	TIGR00167
Triose isomerase	TIM	PFAM	PF00121
Glyceraldehyde-3P dehydrogenase	GAPDH	PFAM	PF00044
Phosphoglycerate kinase	PGK	PFAM	PF00162
Phosphoglycerate mutase	PGM	PFAM	PF06415
Enolase	Eno1	PFAM	PF03952
Pyruvate kinase	PyrK	PFAM	PF02887
Pyruvate-Ferredoxin oxidoreductase	POR	PFAM	PF01558
Further PEP /Pyruvate metabolism			
PEP mutase	PEPM	TIGRFAM	TIGR02320
PEP carboxylase	PEPC	PFAM	PF00311
PEP carboxykinase	PEPCK	TIGRFAM	TIGR00224
Pyruvate phosphate dikinase	PPDK	PFAM	PF01326
Acetyl CoA metabolism			
Acetate CoA ligase	ACL	TIGRFAM	TIGR02188
Acetate kinase	ACK	TIGRFAM	TIGR00016
Acetate Succinate CoA transferase	ASCT	TIGRFAM	TIGR03458
Succinyl CoA synthetase	SCS	PFAM	PF02629
Acetyl CoA carboxylase	ACACA	TIGRFAM	TIGR00515
Phosphate acyl transferase	PAT	PFAM	PF00198
TCA cycle			
Citrate synthase	CS	PFAM	PF00285
Aconitase	ACO	PFAM	PF00330
2-oxoglutarate dehydroganse	OGDC	PFAM	PF00676
Succinyl CoA synthetase	SCS	PFAM	PF02629
Succinate dehydrogase	*sdhC*	TIGRFAM	TIGR02046
Fumarase	FH	PFAM	PF00206
Malate dehydrogenase	MDH	PFAM	PF00056
NTTs			
ATP translocase	NTT	TIGRFAM	TIGR00769
		PFAM	PF03219
Sugar phosphate uptake			
Sugar phosphate transporter	glpT/uhpC	TIGRFAM	TIGR00172
Lactate metabolism			
Lactate permease	*LctP*	PFAM	PF02652
Lactate dehydrogenas	*ldh*	PFAM	PF01070
Glycogen metabolism			
Nucleotide transferase	*glgC*	PFAM	PF00483
Glycogen synthase	*glgA*	PFAM	PF00534
Glucanotransferase	*glgB*	PFAM	PF00128
Phosphorylase	*glgP*	PFAM	PF00343
Glucohydrolase	*glgX*	PFAM	PF13980
Maltotriose glucosidase	*malZ*	PFAM	PF00128
Amylomaltase	*malQ*	PFAM	PF02446
Glucokinase	*glk*	PFAM	PF02685

Phosphoglucomutase	*pgm*	PFAM	PF02878
Pentose Phosphate pathway			
Phosphogluconate dehydrogenase	*gnd*	TIGRFAM	TIGR00873
Ribulose-5-phosphate dehydrogenase	*rpiB*	TIGRFAM	TIGR01120
Ribulose-5-phosphate epimerase	*rpe*	TIGRFAM	TIGR01163
Transketolase	*trk*	PFAM	PF02779
Lactonase	*ahlL*	PFAM	PF10282
Purin metabolism			
Adenosin deaminase	*ADA*	TIGRFAM	TIGR01410
purin nucleoside phosphorylase	*PNP*	PFAM	PF01028
Ribokinase	*rbk*	TIGRFAM	TIGR02152
Pyrophosphatase	*HAD_2*	PFAM	PF13419
Fatty acid biosynthesis			
Acetyl CoA carboxylase	*ACACA*	TIGRFAM	TIGR00515
Acyl-Carrier Protein	*acp*	TIGRFAM	TIGR00517
Acetyl CoA:ACP transacylase	*fabD*	TIGRFAM	TIGR00128
3-keto-acyl-reductase	*fabG*	TIGRFAM	TIGR01829
3-hydroxy-acyl hydratase	*fabZ*	TIGRFAM	TIGR01750
Enoyl-ACP reductase	*fabI*	PANTHER	PTRH42359_SF2
Glycerol-3P-acyltransferase	*fslY*	TIGRFAM	TIGR00023
3-keto-acyl-synthetase	*fabH*	TIGRFAM	TIGR00747
Peptidoglycan metabolism			
EPSP synthetase	*murA*	PFAM	PF00275
N-acetyl-muramate dehydrogenase	*murB*	PFAM	PF01565
Acetyl-muramate alanine ligase	*murC*	PFAM	PF01225
Acetylmuramoyl-Glu-ligase	*murD*	PFAM	PF02875
muramine ligase	*murEF*	PFAM	PF08245
Lipid II flipase	*murJ*	PFAM	PF03023
D-ALA, D-ALA ligase	*dalA*	PFAM	PF07478
Penicilin-insensitve transglycolase	*mrcA*	PFAM	PF00912
Transpeptidase	*mrcA*	PFAM	PF00905
Transferase hexapeptide	*glmU*	PFAM	PF00132
Phosphoglucoisomerase SIS domain	*glmS*	PFAM	PF01380
Phophosugar mutase	*glmM*	PFAM	PF02878
Glycosyltransferase	*murG*	PFAM	PF04101
Reactive oxygen species ROS			
Peroxidase	*gpxX*	TIGRFAM	TIGR00198
Catalase	*cat*	PFAM	PF00141
Superoxide dismutase CuZn	*SOD_CuZn*	PFAM	PF00080
Superoxide dismutase FeMn	*SOD_FeMn*	PFAM	PF02777
Rubredoxin	*rubR*	PFAM	PF00258
Phosphosugar uptake			
Glycerol-3P transporter	*glpT*	TIGRFAM	TIGR00712
Glucose-6-Phosphate transporter	*uhpC*	custom_UM	custom_UM
Bacterial Microcompartments BMC			
BMC Shell BMC-P	*BMCP*	PFAM	PF03319
BMC Shell BMC-H	*BMCH*	PFAM	PF00936
Nitrogen-related metabolism			
Urea metabolsim			
Urea transporter	*ureT*	PFAM	PF03253
Urease	*urea*	PFAM	PF00449

uric acid permase	*PucJ*	TIGRFAM	TIGR03173
uricase	*UOXP*	PFAM	PF001014
NH_4 transporter	*AmtB*	PFAM	PF00909
Protein segregation			
SRP rezeptor	*ftsY*	TIGRFAM	TIGR00064
SecA binding protein	*secA*	TIGRFAM	TIGR00963
SecB binding protein	*secB*	TIGRFAM	TIGR00809
Translocase subunit Y	*secB*	TIGRFAM	TIGR00967
Translocase subunit E	*secE*	TIGRFAM	TIGR00964
Translocase subunit G	*secG*	TIGRFAM	TIGR00810
TAT system subunit A	*tatA*	TIGRFAM	TIGR01411
TAT system subunit B	*tatB*	TIGRFAM	TIGR01410
TAT system subunit C	*tatC*	TIGRFAM	TIGR00945
Aminoacid biosynthesis (key genes)	***Amino acid***		
2-oxo-glutarate derived amino acids			
Glutamate synthase	Glutamate; E	PFAM	PF04898
Glutamine synthetase	Glutamine, Q	TIGRFAM	TIGR03105
Arginosuccinate lyase	Arginine, R	TIGRFAM	TIGR00838
Pyroline carboxylate reductase	Proline, P	TIGRFAM	TIGR00112
Oxaloacetate derived amino acids			
ASP aminotransferase	Aspartate, D	PFAM	PF00155
Asparagine synthase	Asparagine, N	TIGRFAM	TIGR01536
Methionine synthase	Methionine, M	TIGRFAM	TIGR02082
Threonine synthase	Threonine, T	PFAM	PF14821
Diaminipimelate decarboxylase	Lysine, K	TIGRFAM	TIGR01048
Pentose phosphate pathway derived			
Histidinole dehydrogenase	Histidine, H	PFAM	PF00069
3-phosphoglycerate derived			
Phosphoserine phosphotransferase	Serine, S	TIGRFAM	TIGR02137
Serine hydroxymethyltransferase	Glycine, G	PFAM	PF00464
Cysteine synthase	Cysteine, C	TIGRFAM	TIGR01139
Pyruvate derived amino acids			
Alanine glyoxylate transaminase	Alanine, A	PFAM	PF00266
BC amino acid transaminase	Valin, V	PFAM	PF01603
Isopropyl-malate dehydrogenase	Leucin, L	TIGRFAM	TIGR00169
BC amino acid transaminase	Isoleucin, I	PFAM	PF01603
PEP derived amino acids			
Tryptophane synthase	Tryptophane, W	TIGRFAM	TIGR00263
Prephenate dehydratase	Phenylalanine, F	PFAM	PF01817
Prephenate dehydrogenase	Tyrosine, Y	PFAM	PF02153
Amino acid transporters	**Details**		
Amino acid permease	unspecific	PFAM	PF01490
Amino acid transporter	substrate binding	TIGRFAM	TIGR01096
Amino acid permease	His, Glu, Gln, Arg	TIGRFAM	TIGR01726
Aminoacid permease 2	unspecific	PFAM	PF13520
BC amino acid permease	Branched chained	PFAM	PF02653
Amino acid permease	unspecific	PANTHER	PTHR11616_SF101
Hydrogenases			
[FeFe] hydrogenase	*hydA*	TIGRFAM	TIGR02512
[Fe] hydrogenase	*hydA*	PFAM	PF02256
[NiFe] hydrogenase	*hydA*	TIGRFAM	TIGR00391

Cofactor biosynthesis			
Biotin biosynthesis			
Ad.-8-amino-7-oxinonanoate transaminase	*bioA*	TIGRFAM	TIGR00508
8-amino-7-oxononanoate synthase	*bioF*	TIGRFAM	TIGR00858
6-carboxyhexanoate-CoA ligase	*bioW*	TIGRFAM	TIGR01204
Pimeloyl-methyl ester esterase	*bioH*	TIGRFAM	TIGR01738
Dethiobiotin synthetase	*bioD*	TIGRFAM	TIGR00347
Bioin synthetase	*bioB*	TIGRFAM	TIGR00433
Folic acid biosynthesis			
Cyclohydrolase	*folE*	TIGRFAM	TIGR00063
Dihydroneopterin aldolase	*folB*	TIGRFAM	TIGR00525
Para-aminobenzoate synthase	*pabB*	TIGRFAM	TIGR00553
Methylenetetrahydrofolate reductase	*fadH*	TIGRFAM	TIGR00667
Dihydropteroate synthase	*folP*	TIGRFAM	TIGR01496
2-am.-4-hy.-6-h. diphosphokinase	*folK*	TIGRFAM	TIGR01498
Dihydrofolate synthetase	*folC*	TIGRFAM	TIGR01499
Aminodeoxychorismate lyase	*pabC*	TIGRFAM	TIGR03461


Glyptotermes
Procryptotermes
Cryptotermes
Neotermes
MAG groups
Ia
Ib
Ic
IIa
IIb
IIc
IIIa
IIIb
IV
V
Opitutaceae
'Gx481 bin.23'
'Gx485 bin.11'
'Nm470 bin.74'
'Cc175 bin.120'
'Nc350 bin.44'
'Cd354 bin.103'
'Gsp477 bin.153'
'Pcl387 bin.12'
'Nm470 bin.68'
'Ncb351 bin.8'
'Ncb351 bin.52'
'Kf353 bin.47'
'Gsp477 bin.29'
'Gsp477 bin.160'
'Gsp477 bin.174'
'Nc350 bin.191'
'Ncb351 bin.92'
'Roe453 bin.18'
'Ncb351 bin.93'
'Pcl387 bin.134'
'Gx481 bin.188'
'Po218 bin.73'
'Cc175 bin.40'
'Cc175 bin.98'
'Cd354 bin.81'
'Pcl387 bin.18'
'Cc175 bin.33'
'Nc350 bin.186'
'Ncb351 bin.30'
'Ct408 bin.149'
'Gsp477 bin.70'
'Kf353 bin.141'
'Gsp477 bin.23'
'Im510 bin.18'
'Ncb351 bin.42'
'Po218 bin.25'
'Cd354 bin.92'
'Gx481 bin.202'
'Gsp477 bin.142'
'Ct408 bin.77'
'Ncb351 bin.90'
'Pcl387 bin.38'
'Cc175 bin.37'
'Roe453 bin.126'
'Ct408 bin.121'
'Pcl387 bin.136'
'Ct408 bin.89'
'Cc175 bin.8'
'Nm470 bin.121'
'Nm470 bin.13'
'Gsp477 bin.14'
'Nm470 bin.87'
'Po218 bin.38'
'Iy174 bin.61'
'Roe453 bin.74'
'Cc175 bin.47'
'Pcl387 bin.45'
'Nm470 bin.100'
'Gsp477 bin.122'
'Ct408 bin.116'
'Gsp477 bin.156'
'Gx481 bin.184'
'Cc175 bin.121'
'Cd354 bin.116'
'Pcl387 bin.165'
'Ncb351 bin.56'
'Ct408 bin.56'
Verrucomicrobia bacterium UBA1183
'Nc350 bin.13'
Verrucomicrobia bacterium GWC2 42 7
Verrucomicrobia bacterium GWF2 51 19
Opitutae bacterium UBA3534
Verrucomicrobia bacterium CG 4 10 14
Opitutae bacterium UBA1116
'Pq454 bin.37'
'Md513 bin.100'
'Cf509 bin.39'
'Nc350 bin.88'
'Pc512 bin.4'
'Zx50 bin.34'
'Zx50 bin.46'
'Pc512 bin.99'
'TD116 bin.50'
Opitutae bacterium UBA7397
Coraliomargarita sp CAG312
Coraliomargarita akajimensis
Opitutae bacterium UBA7350
Opitutae bacterium UBA4506
Opitutae bacterium isolate IN42
Verrucomicrobia bacterium Opi OSU 00C
Puniceicoccales bacterium Verruco 01
Opitutaceae bacterium isolate SP4023
TAV4
TAV3
Geminisphaera colitermitum
TAV5
TAV1
'Gx481 bin.174'
Rariglobus hedericola
Opitutaceae bacterium TSB47
'Ct408 bin.80'
'Nm470 bin.120'
'Hs463 bin.103'
'Gx485 bin.97'
Ereboglobus luteus
'Md513 bin.46'
Opitutus terrae
Opitutus sp
Cephaloticoccus capnophilus
Cephaloticoccus primus
Lacunisphaera limnophila
Oleiharenicola alkalitolerans
Candidatus Didemnitutus mandela
Tree scale: 1

Figure S10: Distribution of the Opitutales MAGs host termites. The figure visualizes the distribution of MAGs from the same termite host to the different MAG groups. Highlighted are the most abundant termite hosts *Cryptotermes sp.* (yellow), *Glyptotermes sp.* (orange), *Neotermes sp.* (red) and *Procryptotermes sp*. (green). No clear pattern can be identified.

Danksagung

Ich danke …

… an erster Stelle meinem Doktorvater und Mentor **Prof. Dr. Andreas Brune**, der mich bereits zu meinem Bachelorstudium in seiner Arbeitsgruppe aufgenommen hat und mir in all den Jahren sowohl auf wissenschaftlicher, als auch persönlicher Ebene viel beigebracht hat. Besonders der große Freiraum zur persönlichen Entwicklung, aber auch die ständige Bereitschaft zum Gespräch haben mir sehr geholfen und sind nicht selbstverständlich.

… **Dr. Werner Liesack** und **Prof. Dr. Johann Heider** für die wissenschaftlichen Diskussionen und Hilfestellungen während meiner Promotion und das Mitwirken in meinem *Thesis Advisory Committee*.

… den Mitgliedern meiner Prüfungskommission **Prof. Dr. Uwe G. Maier**, **Prof. Dr. Robert R. Junker** und insbesondere **Prof. Dr. Johann Heider** für die Übernahme des Zweitgutachtens.

… allen aktuellen und ehemaligen Mitgliedern der ***Termite group***, die immer ein produktives Arbeiten in einer angenehmen und freundschaftlichen Atmosphäre ermöglicht haben. Der persönliche Austausch auf dem Weg zur Mensa oder in der *Coffee corner* war oft eine willkommene Ablenkung. Ich werde mich an viele schöne Zeiten im Labor, beim *Lab Retreat* oder im privaten Rahmen erinnern.

… **Dr. Vincent Hervé**, der durch seine bioinformatische Expertise einen Teil dieser Arbeit erst möglich gemacht hat und ein guter Lehrer für den Umgang mit metagenomischen Daten war.

… **Katja Platt**, die mich vom ersten Tag an begleitet hat, mir viele Techniken beigebracht hat und mir oft mit Ihrer Erfahrung weiterhelfen konnte.

… den Mitgliedern der **Arbeitsgruppe Liesack** für den langjährigen Austausch im Joint Seminar.

… den Mitgliedern der **Arbeitsgruppe Shima**, die mir vorallem im Umgang mit Proteinen und dem anaeroben Zelt geholfen haben.

… der ***International Max Planck Research School*** in Marburg für das Organisieren von zahlreichen Seminarreihen, Workshops und Veranstaltungen, bei denen ich durch den Austausch mit anderen Doktoranden und Wissenschaftlern viel lernen konnte.

… **meiner Partnerin**, **meiner Familie** und **meinen Freunden**, die in guten und schlechten Zeiten zu mir gestanden haben und mich immer auf meinem Weg unterstützt haben. Insbesondere **meine Eltern** haben es mir ermöglicht meinen eigenen Weg zu verfolgen und haben es mir verziehen, wenn ich länger nicht zu Besuch kommen konnte.

Erklärung

Ich versichere, dass ich meine Dissertation mit dem Titel „Diversity, function and oxygen relationship of free-living and flagellate-associated *Opitutales* (phylum *Verrucomicrobiota*) in the termite gut“ selbstständig ohne unerlaubte Hilfe angefertigt und mich dabei keiner anderen als der von mir ausdrücklich bezeichneten Quellen und Hilfsmittel bedient habe.

Diese Dissertation wurde in der jetzigen oder einer ähnlichen Form noch bei keiner anderen Hochschule eingereicht und hat noch keinen sonstigen Prüfungszwecken gedient.

Marburg, den 07.06.2022

Christopher Feldewert